OPTIMAL HANDLING AND FAULT-TOLERANT SPEED REGULATION OF HEAVY HAUL TRAINS

by

Xiangtao Zhuan

Submitted in partial fulfilment of the requirements for the degree

Philosophae Doctoral (Electronic Engineering)

in the Faculty of

Engineering, Built Environment and Information Technology

University of Pretoria, Pretoria

October, 2006

Optimal Handling and Fault-tolerant Speed Regulation of Heavy Haul Trains

by

Xiangtao Zhuan

Promotor: **Prof. Xiaohua Xia**

Department: **Electrical, Electronic and Computer Engineering**

Faculty of Engineering, Built Environment and Information Technology

Degree: **PhD (Electronic Engineering)**

Keywords: output regulation, measurement feedback, nonlinear system, train control, ECP braking system, distributed power control, optimal control, LQR, FDI, FTC

Summary

Heavy haul trains are used to transport mineral resources from inland mines to harbours in South Africa. It is believed that the cost is less with a larger load per car or per train. This has resulted in the use of long heavy haul trains. The increase in train length has posed unprecedented technical challenges. For heavy haul trains, energy consumption, running time and in-train forces between neighbouring cars are of much concern to transportation corporations.

The objective of the study is to find optimal driving methodologies for the implementation of a desired speed profile with energy consumption and in-train forces considered.

Firstly, three control strategies are proposed in this study for train handling. In view of the characteristics of traditional pneumatic braking systems and the new Electronically Controlled Pneumatic (ECP) braking systems, a simulation study of optimal open loop controllers was undertaken. The result shows that the ECP braking systems demonstrate superb performance compared with pneumatic braking systems, especially together with independent distributed power (iDP) control.

Thus, the main focus of the study was the control of heavy haul trains equipped with

ECP braking systems. It is shown that there are redundancies in designing an open loop controller. An optimization procedure is applied to schedule cruise control by taking the in-train forces into initial design consideration. Optimal open loop scheduling presents a better starting point for a closed-loop controller design. A type of linear quadratic regulator (LQR) controller with state feedback is simulated to verify the above result.

However, the closed-loop control law is designed based on full state feedback, which is not practical since not all the states can be measured.

An observer could be designed to supplement the LQR controller if partial states are measured. This is, however, not the approach taken in this study. Instead, the application of output regulation of nonlinear systems with measured output feedback to the control of heavy haul trains is considered. This approach to design is practically feasible and manageable, and by its nature, is also easily integrable with human drivers. In this study, the existing result of output regulation of nonlinear systems is extended. The output regulation problem of nonlinear systems with measured output feedback is formulated in this study and solved for the local version and global version. For its application to train control, some application issues are discussed. Based on the proposed theory, a speed regulator for train control is designed. Simulation results show its applicability.

Lastly, this study concentrates on the fault-tolerant capacity of the speed regulator. Two kinds of fault modes are considered. Fault detection and isolation for the sensor fault and braking system fault are exploited. Controller redesign is also given. Simulation results show that such a speed regulator has a fault-tolerant capacity to the corresponding faults.

Acknowledgement

No words could express my feeling about the past years I have spent on my doctoral study at the University of Pretoria. It is there I met Professor Xiaohua Xia, who has had and will continue to have a significant impact on my life. He is not just a professional advisor, but also a good friend. His ideas and points of view have been a constant source of inspiration, and our endless discussions have taught me to be more inquisitive. From him, I have also learned how to enjoy the job and living. I would like to express my deepest gratitude to him for his support, encouragement and guidance. Thanks for widening my views and helping me achieving my goals.

I would also like to thank all the members in the train project at the University of Pretoria. They are Mingshan Chou, Jerry Wang, Herry Mizero and Martin Strempel. Their excellent work contributes much to my study. The discussions among us give me a lot of inspiration.

I am very grateful to my former advisor, Professor Guilin Zheng at Wuhan University, China during my master's study. His moral support and advice give me much encouragement and motivation.

Thanks to all the friends I met here in Pretoria: Dr. G. Ma, Miss Y. Li, Mr. M. Chen, Mr. D. Wei, Dr. J. Zhang and many others. In particular, I want to mention Mr. Xiyin Liang in our control group, who gives me a lot of help in my study. Their moral support has helped me in difficult moments: from them I learned a great deal.

I am in debt to my family in China, my parents and my sister. It has been hard to spend this time far from them, but the distance strengthens our connection even more. I would like to thank my beloved wife, Qi Li, for her love, patience and encouragement, and our little son, Yi Zhuan. To them and their smiles I owe everything I attained.

Publications

The following list contains publications that are based on the work presented in the thesis.

X. Zhuan and X. Xia, "Cruise control scheduling of heavy haul trains," *IEEE Transactions on Control System Technology*, Vol. 14, No. 4, 2006, pp. 757–766.

X. Zhuan and X. Xia, "Optimal scheduling and control of heavy haul trains equipped with electronically controlled pneumatic braking systems," *IEEE Transactions on Control System Technology*, 2006 (accepted).

X. Zhuan and X. Xia, "Speed regulation with measured output feedback in the control of heavy haul trains," *Automatica*, 2006 (submitted).

X. Zhuan and X. Xia, "Output regulation of nonlinear systems by using measurement feedback," *IEEE Transactions on Automatic Control*, 2006 (submitted).

X. Xia and X. Zhuan, "Model-based handling of ECP heavy haul trains," *SA Journal of Science*, 2005 (accepted).

X. Zhuan and X. Xia, "Optimal scheduling and control of heavy haul trains equipped with electronically controlled pneumatic braking systems," *Proceedings of the 6th World Congress on Intelligent Control and Automation*, 21–23 June, 2006, Dalian, China, pp. 8168–8172.

X. Zhuan and X. Xia, "Output regulation of nonlinear systems in the form of measured output feedback," *Proceedings of South African Control Conference*, July 2006, Durban, South Africa, pp. 33–38.

X. Zhuan and X. Xia, "Speed regulation with measurement feedback of heavy haul trains," *Proceedings of the 4th IFAC–Symposium on Mechatronic Systems*, 12–14 September 2006, Heidelberg, Germany, pp. 794–798.

Contents

List of Figures

List of Tables

Chapter 1

Introduction

1.1 Background

The railway is believed to be the most economical among all transportation means, especially for the transportation of mineral resources. In South Africa, most mines are situated inland, so heavy haul trains are required to transport these resources to harbours. It is presumed that the cost is less with a larger quantity of load per car or per train in terms of the schedule and the number of people involved. This has resulted in the use of long trains with multi-locomotives.

Traditionally, the operation of such multi-locomotive trains with pneumatic braking systems is in essence a simple one. The brake control signal is transmitted throughout the train wagons, which results in the same effort command of all the wagons. All the locomotives also have to make the same efforts, for the remote locomotives (groups) are operated in tandem with the leading one. In this operation there are only two control signals, one for locomotives, and the other for wagons. There are two prominent drawbacks with such an operation method.

1) The locomotives are distributed, but the power is not distributed independently.

2) The wagons' braking system is pneumatic and the braking control signal is propagated to each wagon through the air pressure change along the air pipe running throughout the train, which leads to different time delays in braking the wagons.

These drawbacks result in slow running speed, the possibility of derailment and a limit on the train length.

The first disadvantage is eliminated through the employment of the (independent) distributed power (DP, iDP) traction operation, in which the traction powers of the

locomotives are different.

The second one was also provisionally solved with the application of new technology in the 1990s. To improve the train performance (the second of the above disadvantages), the Association of American Railroads developed a new braking system – the Electronically Controlled Pneumatic (ECP) braking system, in which the brake command signals are electronic and are received by all the wagons simultaneously although pneumatics are still used to supply the brake power. Spoornet, one of the train operators in South Africa, is the first railway in the world to roll out the ECP braking system (on its COALink line) on a large scale. The introduction of ECP braking systems can be seen in [1, 2]. Operational advantages follow the application of ECP braking systems [1].

1) Wheel and brake shoe wear can be reduced with an appropriate distribution of braking and pressure control;

2) Energy-efficient operation can be reached with the use of graduated release capability to eliminate power braking;

3) The safety level can be increased with the accurate control of the whole train and decreased stopping distance;

4) The in-train forces can be reduced owing to the complete brake control of every car of the train.

At present, such a heavy haul train in South Africa is composed of about 200 wagons and it is about 2.5 km long. A train running on the COALink line of Spoornet is shown in Fig. 1.1. It is exactly because of the above advantages that extremely long trains (up to 10 km in length) are considered in the business plan of Spoornet of South Africa on its COALink. This increase in train length has posed unprecedented technical challenges.

According to [3], train handling includes the start phase of the train, the speed maintenance phase, and the stop phase of the train. Since the railway track is long and the train is running in the speed maintenance phase during most of the running time, the train scheduling of the speed maintenance phase is the focus of this study. In realizing optimal management of in-train forces, it is justifiable to assume that a steady state of train motion is reached and held. In this study, the term "scheduling" is borrowed from the railway industry for train operation and handling, where it refers to the decision of a driving sequence in terms on locomotives' power notches and wagons' braking pressure along a specific railway track. In the context of control systems, this "scheduling" activity is interpreted as an open loop control design, which brings the train to an expected motion trajectory.

For heavy haul trains, energy consumption, running time and in-train forces between the neighbouring cars are of much concern to transportation corporations. The

Figure 1.1: A heavy haul train of Spoornet, South Africa

energy consumption is related to the direct economic profit while the running time determines the quality of the service. In-train force control contributes to the safe running of the train and to limiting maintenance cost. The larger the in-train force is, the higher the maintenance cost. For long trains, this is even more important. It is also more difficult to control the in-train forces of a long heavy haul train. It is noticed that the in-train forces depend both on the driving speed and on the power/brake distribution along the train. This is why the independent Distributed Power (iDP) operation and ECP braking systems have been introduced into practice.

1.2 Literature review of train handling

A frame for train handling is shown in Fig. 1.2. In train handling, various studies have tried to achieve different objectives.

For energy consumption, some studies have been done in [4, 5, 6, 7, 8, 9] for a train to travel from one station to the next one in a given time. In most of these papers, the locomotives are supposed to have three discrete control settings: power, coast and

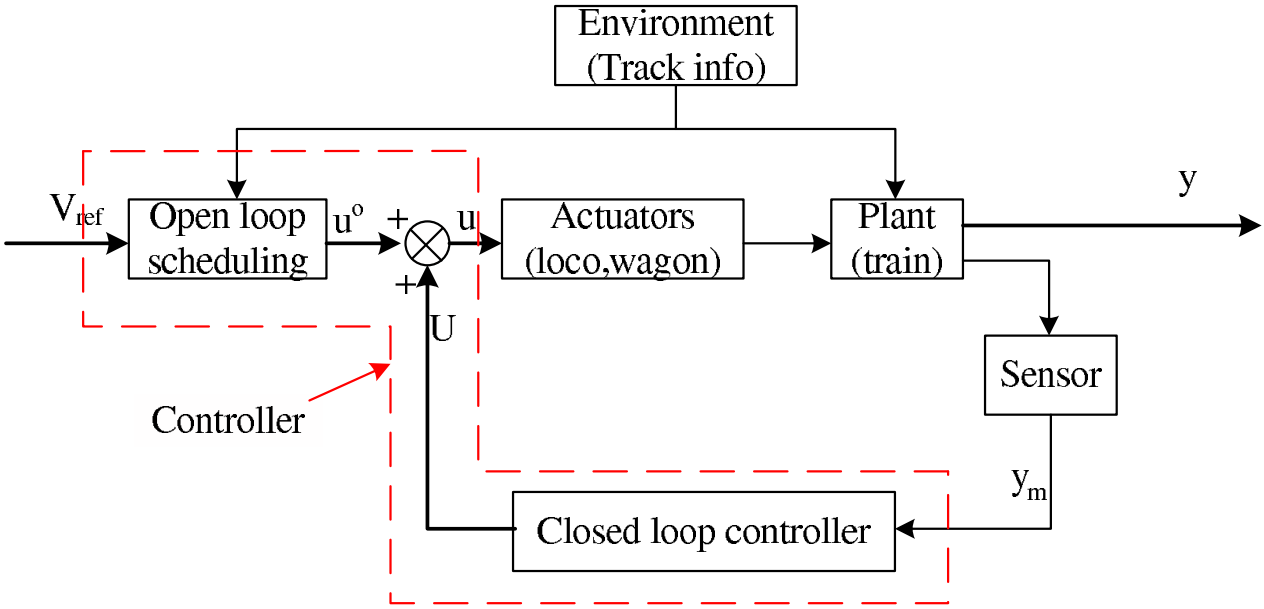

Figure 1.2: Train handling

brake. A finite sequence of the locomotive settings is arbitrarily predetermined and then the optimal algorithms are to determine the switching points where the control setting changes. Recently, an analytical approach has been proposed in [10] to find the control switching point. A train is modelled as a mass point in these papers. It is shown in [6] that a train with distributed mass can be treated as a point mass with actual gradient profile replaced by an *effective gradient acceleration*. In these papers, the dynamics within a train are ignored and speed tracking and in-train forces are not investigated.

The other models a train as a cascade of mass points connected with couplers, for example in [11, 12, 13, 14, 15]. This model is more accurate than a mass-point model for a train 2.5 km long. In these papers, a desired speed profile along a given track is assumed first. The subject of the studies is to design controllers to maintain the desired speed with some objectives considered.

For high speed (passenger) trains, speed tracking is the most important. The studies can be seen in [12, 13, 14]. In [12] [13], the H_2/H_∞ method with full state feedback is employed to deal with the cruising of high speed trains. The objective is to maintain the train speed as expected. Cruise control is proposed for two types of high speed trains, distributed driving with each car having its own driving force, and push-pull driving only with driving forces at the first and the last car. A calculation method to determine equilibrium point for distributed driving is given. Even though the push-pull driving is also taken as a way to operate heavy haul trains, again, this paper does not present optimal scheduling of equilibrium points. In [14], similar to [12], different input/output decoupling problems for high speed trains are studied. To get the equilibrium point, it is assumed that one of the in-train forces is zero or the driving force is equally distributed to the locomotives. This assumption leads to a heuristic

trim point. In these papers, a train is considered as a cascade of mass points connected with nonlinear couplers. This model can be used to study the dynamics within a train. However, the in-train forces are not emphasized in these papers because they are not particularly important for such short trains. Without ECP technology, the application of these control approaches to heavy haul trains is hindered by the control signal transmission delay.

An early study of in-train forces can be seen in [11], where an LQR optimal algorithm is employed to minimize the coupler forces and/or velocity deviations from the reference values. It is assumed that at the nominal point, the nominal input vector consisting of throttling and braking forces to maintain the nominal speed, is equal to the sum of the resistance and gravity forces. Then a linearized model is used to calculate the control law. Considering the large number and the constraints of the variables, the train model is simplified. This paper offers an excellent setup to deal with the in-train forces and various calculations of optimal closed-loop control. While closed-loop control is used to optimize the interplay between in-train forces and speed holding, the scheduling of the desired holding speed is typically determined through an open loop controller design. It is noted, however, that the off-line open loop scheduling in [11] is a rather heuristic one, without making optimal use of the control redundancies. The closed-loop control is designed based on full state feedback, and with two crude assumptions for the insufficiency of the measurement of the states, the closed-loop controller is simplified to full speed feedback. Even for speed, it replaces all cars' speeds with the limited number of locomotives' speeds.

It is quite interesting to note that the early study of [11] takes into consideration some practical aspects of ECP and iDP even though the ECP/iDP technology is not implemented in practice on a visible scale. However, the model in this paper is largely simplified by taking variations due to track slope and curvature changes as model disturbances. New technologies, such as the Global Position System (GPS), make the information readily available.

In [15] and [16], based on a cascade point mass model, which is validated in [17] with the operational data from Spoornet, an LQR approach is employed to optimize the in-train forces, energy consumption and velocity tracking of a heavy haul train equipped with an ECP braking system. Considering the constraints of control input channel number, a concept of fencing is proposed. In off-line scheduling, the equilibria are calculated under the assumption that the driving force is equally distributed to the locomotives while all the braking forces of wagons are zeros and the braking force is equally distributed to the locomotives and wagons. This open loop scheduling is heuristic, too. With the discrete quantities of the locomotives' efforts considered, the efforts of the locomotives are almost always equal.

In [18], flatness-based methods in [19] are used to design the open loop control schemes for a heavy haul train, where a train is taken as an infinite dimensional linear model.

The off-line scheduling for the equilibria in the above papers is based on some heuristic assumptions without considering the optimization of the equilibrium. The difference among the different equilibria is of course not discussed.

The heuristic scheduling way may lead to irrational power distribution, especially when one locomotive group is climbing uphill and the other one is driving downhill. Assuming a train composed of some wagons with one locomotive at the front and one at the rear is running over a hill (the front part is driving downhill while the rear part is climbing uphill), it is expected that the front locomotive is braking and the rear one is powering and thus the in-train forces are small. However, with the above heuristic scheduling, the efforts of the front locomotive and the rear one are always the same, which may lead to irrational power distribution. An extreme example is shown in Fig. 1.3.

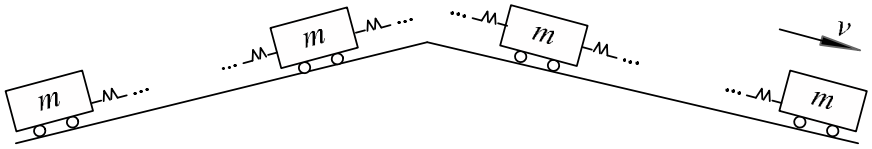

Figure 1.3: Irrational power distribution

With open loop scheduling, the running error always exists and it sometimes leads to oscillation, which should be avoided in train handling.

The methods to design closed-loop controllers in the above-mentioned papers are all within linear system theories and based on linearized models. The closed-loop controllers are in the form of state feedback or in the form of measurement feedback with some crude assumptions. In train handling, only some speeds of the cars are practically measurable. A closed-loop controller based on speed measurement feedback is necessary.

In the above papers on train handling, all the controllers are designed on the assumption that the train is well set up and all the actuators (traction efforts and braking efforts of locomotives and wagons) and sensors (speed sensors) work as designed, which is an ideal condition. In practice, some of the actuators and/or sensors may be faulty, and even worse, the train structure may be changed. For example, the speed sensor has a constant bias, or the amplifier in the sensor circuit has a fault, which leads to a gain fault in the sensor. The locomotive may fail during the running, which happened in the ECP trial run to collect data to validate the cascade-mass-point model in [17] on 18 November 2003. In the stop distance calculation of the collision mentioned in chapter 2, one locomotive was not functional during the running. The air pressure in the braking pipe may be different from the expected one because of the pressure sensor fault in the pressure recharge system or the air leakage, which makes the braking forces acting on the wheels less than expected.

When this happens, the controller, designed on the basis of the faultless train model, cannot work as well as expected, and sometimes it even leads to unsafe running, such

as train-breaking and derailment. The safe running of trains cannot be promised, so some safe running methods need to be applied in train handling.

1.3 Motivation

From the above, it is evident that there are some problems in train handling.

1) Optimal scheduling in the calculation of the equilibria of the nominal model. According to the literature, there are several scheduling methods. However, there is no comparison among them and it is not known which one is the best or if there is another better one. This step is very important because it is hoped that good open loop scheduling will present a good starting point and it can improve the performance of the closed-loop controller.

2) The design of a closed-loop controller with speed measurement feedback.

3) The fault-tolerant control problem of the designed controller.

It is assumed that there are redundancies in designing an open loop controller. An optimization procedure is applied in this thesis to schedule cruise control by taking the in-train forces into initial design consideration. It is hoped that an optimal open loop controller design will present a better starting point for a closed-loop controller design. A type of LQR controller with state feedback is simulated to justify the above redundancies.

However, the closed-loop control law is designed based on full state feedback, which is not practical since not all the states can be measured.

An observer could be designed to supplement the LQR controller if partial states are measured. This is, however, not the approach taken in this study. Instead, the application of output regulation of nonlinear systems with measured output feedback to the control of heavy haul trains is considered. The optimal scheduling of the open loop controller is still based on "trading off" the equilibria. Thus the precise balance between energy consumption and in-train forces is still maintained by the choice of weight factors in the optimal scheduling. For closed-loop control, the speed regulation is imposed. This approach to design is practically feasible and manageable, and by its nature, is also easily integrable with human drivers, if it works as expected. Instead of the linear system theory, a nonlinear system theory is adopted, implying without a linear approximation philosophy, the control is closer to reality. Another advantage of the approach is the assumption that only the locomotives' speeds are available for measurement.

For the last problem above, model-based fault detection and isolation (FDI) is employed in this thesis for sensor faults and braking system faults. Based on the fault signals of the FDIs, the controller designed with output regulation can be redesigned to make it fault-tolerant.

The above indicates that this study is undertaken to find a driving methodology for the implementation of a given speed profile for the train. In the controller, the energy consumption, in-train forces and speed tracking are taken into account. Considering the possibility of failures of sensors and actuators, the controller should be fault-tolerant.

1.4 Contributions of thesis

In this study, the contributions are as follows,

1) One first assumes and validates that the optimal open loop scheduling can improve the performance of the closed-loop controller compared with the existing heuristic scheduling.

2) The output regulation problem of nonlinear systems with measured output feedback is formulated and solved for the global version and local version. This has extended the existing theory of the output regulation problem and it is applied to train control.

3) The result of output regulation of nonlinear systems with measured output feedback is applied to train handling. Some necessary designs for the application are undertaken.

4) Taking into consideration the possibilities of the failures of the sensors and actuators, fault detection and isolations for the gain faults of the sensors and the braking systems are designed. Based on the fault signals from FDIs, the speed regulator can be redesigned. Thus, the controller is fault-tolerant.

1.5 Layout of thesis

This thesis includes six chapters. In this chapter, the background of train handling is described first and followed by a literature review on train handling. Based on the literature review, the problems in train handling are identified and some approaches are proposed for them. The contributions of this thesis are presented last.

A train model is described in chapter 2, where the longitudinal dynamics of a heavy haul train is modelled as a cascade of mass points connected with couplers. The

mathematical model is given, as well as the state constraints and input constraints. The second part is about the calculation of the emergency stop distance in a collision. A mass-point model and a cascade-mass-point model are used respectively. From a comparison of the calculation result, it can be seen that the cascade-mass-point model is more accurate for a train longer than 1.8 km.

In chapter 3, three control strategies are proposed first. Then optimal scheduling taking the in-train force into consideration is developed and simulated for trains equipped with a traditional pneumatic braking system and an ECP braking system, respectively. This is followed by a comparison of optimal scheduling and heuristic scheduling. The simulation result shows that optimal scheduling presents a better starting point for closed-loop control, which is confirmed with an LQR controller.

A speed regulator (closed-loop control) with measurement feedback is proposed in chapter 4 for train handling. The output regulation problem of nonlinear systems with measurement feedback is formulated and solved in the global version and the local version in the first part of this chapter. In the second part, some application issues of the result of the local version to train handling are discussed.

The fault-tolerant control of heavy haul trains is investigated in chapter 5. Firstly, the fault detectability algorithm is quoted from [61]. Based on this, the fault detection and isolation of the sensor gain faults are designed. The fault detection and isolation for the braking system faults are designed based on an analysis of the steady-state speeds. The fault signals for locomotives are assumed to be given. With these fault signals, the speed regulator is redesigned. Finally, the simulation for different kinds of faults proceeded.

Chapter 6 is the summary of this thesis and presents some discussion of further studies in train handling.

Chapter 2

Train model

2.1 Introduction

According to the literature, there are two models in the study of train handling: a mass-point model and a cascade-mass-point model. For the study of in-train forces, it is natural to choose the cascade-mass-point model in this thesis.

In section 2.2 of this chapter, the longitudinal dynamics of a heavy haul train is modelled as a cascade of mass points connected with nonlinear couplers. Considering the practical application in COALink line trains, the states and input constraints are given. This model is used throughout the thesis.

The second part of this chapter describes the calculation of the emergency stop distance for a collision. A mass-point model and a cascade-mass-point model are employed respectively. The result can be used to compare the difference between the two models.

2.2 Cascade mass-point model

A heavy haul train, composed of locomotives and wagons (both referred to as cars), can be modelled as a cascade of mass points connected with couplers. In the following model, only the longitudinal dynamics of the train is analyzed.

2.2.1 Car model

A car is running on the track while it is subjected to aerodynamic force, the adjoining cars' internal forces, the gravity force and its own traction or brake force. The forces experienced by a car in the longitudinal direction are shown in Fig. 2.1.

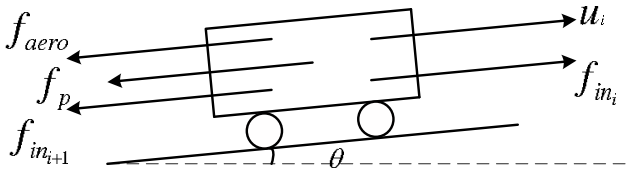

Figure 2.1: Longitudinal model of car

The aerodynamics of a train can be divided into two parts [22] [23]: mechanical drag and aerodynamic drag. The former includes the sliding forces between the train's wheels and the track and the rolling forces of wheels. Aerodynamic drag is dependent on the cross-sectional area of train body, train length, shape of train fore- and after-bodies, surface roughness of the train body, and geographical conditions around the proceeding train.

It has been reasonably assumed that the aerodynamic drag is proportional to the square of the speed, while the mechanical drag is proportional to the speed. Compared with the mechanical drag, the portion of the aerodynamic drag becomes larger as the train speed and length increase (see details from [22] and [23]).

In the open air without any crosswind effects, the total drag on a travelling car can be expressed by the sum of the aerodynamic and mechanical ones:

$$f = D_M + D_A = mc_0 + mc_1 v + mc_2 v^2, \tag{2.1}$$

where D_A and D_M are the aerodynamic and mechanical drags, respectively, c_0, c_1 and c_2 are constants determined by experiments, v is the car speed and m is the car mass under discussion.

The variables f_{in_i} and $f_{in_{i+1}}$ are the in-train forces between the neighbouring cars. Only one in-train force is experienced by the front and rear car. The variable u_i is the car's traction or brake force. For a wagon it refers to the brake force, which must be no more than zero, while for a locomotive it refers to traction force or brake force, whose quantity depends on the locomotive's power notch and speed and its dynamic brake capacity.

In Fig. 2.1, the resistance force $f_p = f_g + f_c$, a function of the position, is composed of the gravity force $f_g = mg\sin\theta \approx mg\theta$ in longitudinal direction and the curvature resistance force f_c [24]. Generally, the track information is known, so it is convenient to yield the function of f_p. In the following simulation study, the curvature resistance force is ignored, which will not affect the simulation result.

2.2.2 Coupler model

The coupler between two cars is modelled as Fig. 2.2. When the draft gear is in its natural length, the in-train force is zero. Considering the coupler's slack length, the coupler can be regarded as a composition of the two gears plus the slack length. Assuming the sum of the length of two gears is $L_0 - \frac{1}{2}L_{slack}$ while the in-train force is zero, the displacement of the coupler is defined as $x = L - L_0$ in which L is the coupler length. The variable f_{in_i} is the in-train force between the ith and $(i+1)$th cars, which is a function of x_i, the relative displacement between the two neighbouring cars, and the difference of the neighbouring cars' velocities (damping effect). A typical relationship between the static in-train force f_{in} (without damping) and x is depicted in Fig. 2.3, which is simplified from the data of Spoornet.

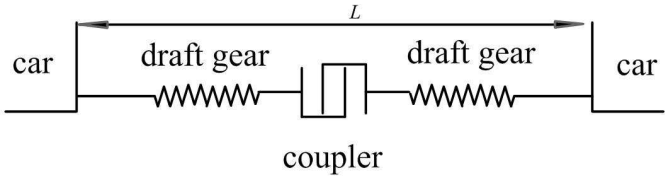

Figure 2.2: Longitudinal model of coupler

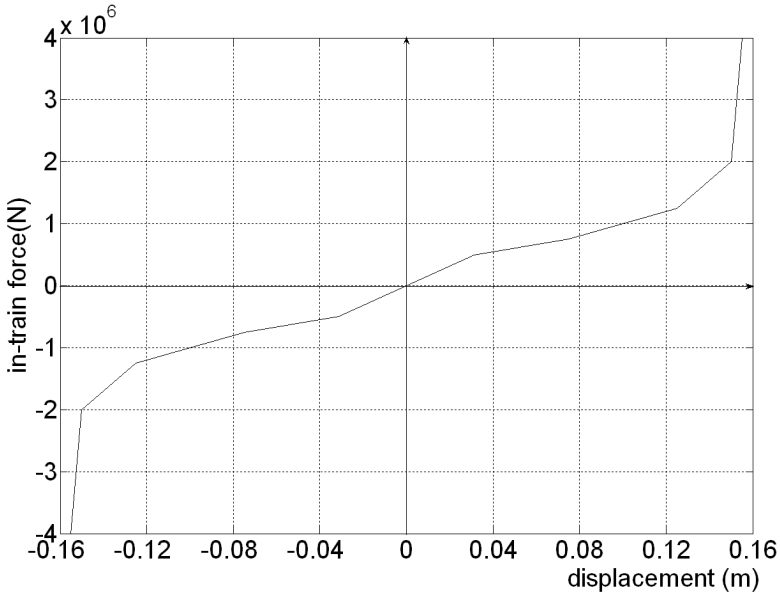

Figure 2.3: Coupler force vs. displacement

2.2.3 Train model of a cascade of mass points

Fig. 2.4 is a sketch of the longitudinal motion of a train. Assuming the train consists of n cars and the locomotives are located at positions l_i, $i = 1, 2, \cdots, k$, where k is the

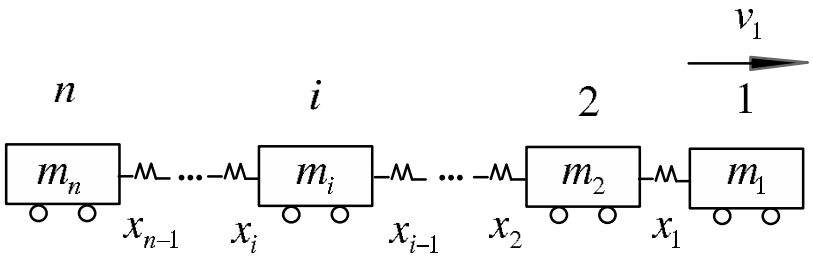

Figure 2.4: Longitudinal model of train

number of locomotives, the train model is described by the following equations.

$$m_s\dot{v}_s = u_s + f_{in_{s-1}} - f_{in_s} - f_{a_s}, \quad s = 1, 2, \cdots, n, \tag{2.2}$$

$$\dot{x}_j = v_j - v_{j+1}, \quad j = 1, 2, \cdots, n-1, \tag{2.3}$$

where the variable m_i is the ith car's mass; the variable v_i is the speed of the ith car; the variables $f_{a_i} = f_{aero_i} + f_{p_i}$, $i = 1, 2, \cdots, n$; the variable $f_{aero_i} = m_i(c_{0_i} + c_{1_i}v_i + c_{2_i}v_i^2)$ is the cars' aerodynamic force; the variable $f_{p_i} = f_{g_i} + f_{c_i}$ is the force due to the tracking slope and curvature where the ith car is running; and the variable f_{in_i} is the in-train force between the ith and $(i+1)$th cars. In (2.2), one has $f_{in_0} = 0, f_{in_n} = 0$.

This model is the same in nature as that in [16], which is validated in [17] with the data from Spoornet.

2.2.4 Input constraint

For a heavy haul train, the control inputs are the efforts of the locomotives and the wagons. The efforts of locomotives can be traction forces or dynamic braking forces, and the efforts of wagons are braking forces. The dynamic brake power is also called regenerative brake power, which can be fed back to the system and could conceivably be saved. All these inputs are constrained. For a locomotive, the effort is governed by the current velocity and the current notch setting, which is depicted in Fig. 2.5 for the 7E1 locomotive used in the COALink trains. The locomotives in this study are assumed to be electric and it is also convenient to formulate the problem of a train with diesel–electric locomotives in a similar way.

In the practical operation of 7E1 locomotives, any notch change requires an interval delay for the field changes. When it changes from dynamic braking to traction or the other way round, the time delay requires a longer interval.

The braking forces of the wagons are also limited by the braking capacities of the wagons.

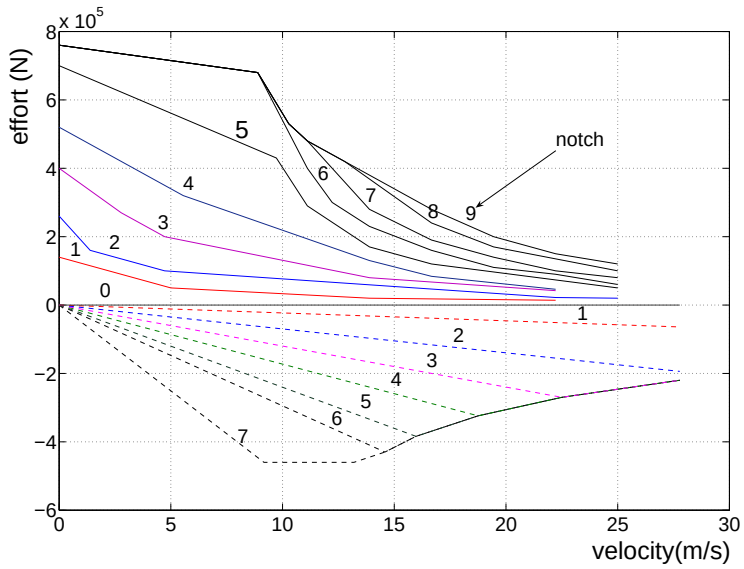

Figure 2.5: Locomotive group effort vs. notch and velocity

2.2.5 In-train force constraints

The quantity of the in-train forces is related to the safe running of the train. In practice, the safety range of the in-train forces for COALink trains is $\pm$ 2,000 kN.

2.3 Stop distance calculation – a model-comparison

During the study, the (emergency) stop distance of a train in a collision is requested to be calculated. The stop distance is calculated with a mass-point model and a cascade-mass-point model, respectively. From the calculation, the difference between the two models can be seen. As indicated in chapter 1, the iDP (DP) operation cannot be considered in a mass point model as well as the internal dynamics in the train. Even without considering the iDP operation, the cascade-mass-point model is still more accurate in modelling a train longer than 1.8 km. To demonstrate this, the calculation procedure is reported in the following.

2.3.1 Information on the collision

When a stop distance is to be calculated, the following data are required:

1) Train composition: locomotive type, wagon type, mass and length of the locomotives and wagons, characteristics of the couplers connecting the locomotives

and wagons, braking system characteristics (pneumatic braking system or ECP braking system, and its parameters).

2) Track data.

3) Operation code.

4) The initial speed of the train before brake is applied.

Limited information is known from the collision report:

1) The train locomotive was numbered E 7092.

2) There were 40 wagons pulled by two locomotives, one at the front and one at the rear. The weight of the locomotive is unknown; the wagons and their load weighed 66 ton each, but the wagon type is unknown.

3) One of the locomotives was not functional.

4) During the collision, the maximum sight distance from the approaching path of the train was 728 m. The departure path shows the end position of the train at 250 m from the area of impact.

5) The initial speed of the train before applying brake is unknown.

2.3.2 Calculation of stop distance

The emergency stop distance is considered. So the control sequence of the train is assumed to be in the emergency operation. From the collision report, this assumption is justified. As is known from [3], the emergency application of freight equipment provides an extremely rapid transmission of the application throughout the train, as well as developing higher brake cylinder pressure than is obtained during service braking. By the movement of the brake valve on the locomotive to the emergency position, the brake pipe is vented unrestricted to the atmosphere, which results in a rapid drop in brake pressure, causing the succeeding valves to go to emergencies and vent brake pipe pressure to the atmosphere at the location. The transmission rate of an emergency is about 930 feet per second or 635 miles per hour. During the emergency, the AB or ABD control valves will apply rapidly causing approximate 15psi brake cylinder pressure to occur on each car within 1.5 seconds after the car brake valve is at the emergency position. This action applies the brake shoes to the wheel quickly and minimizes severe slack changes. During an emergency application, the locomotive throttle should be reduced to idle [3].

From the above description, it is clear that there are time delays for the wagons to start braking after the application of the emergency brake. The time delays are different

from wagon to wagon. The longer the distance from the wagon to the locomotive from where the emergency command originates, the longer the time delay. However, the time delays are limited, since the train is composed of only 40 wagons with one locomotive at the front and one locomotive at the rear. The length of the train is about 524 m and the longest time delay is about 2 seconds. From the collision report, the wagon type is unknown and the locomotive type, from the number plate, could be 7E. The calculation of the braking distance can be done by two methods respectively employing a simple mass-point model and a cascade-mass-point model. The simple mass-point model takes the whole train as a single mass point, while the cascade-mass-point model take it as mass points connected by couplers. The cascade-mass-point model is a more accurate model that takes into consideration the couplers' energy consumption. It could be seen from the results that the braking distances are different from two different calculations. Because of lack of information, the calculation of the braking distance is done on the basis of the following set of technical assumptions:

(1) The locomotives are idle when the emergency operation is initiated.

(2) The track is flat.

(3) The train is running in its steady state with a velocity that is unknown. However, calculation is done with a number of initial speeds of worst case scenarios.

(4) The train is equipped with a pneumatic braking system. All the brake equipment works as designed.

(5) The air dynamics is ignored.

(6) In the analysis using a simple model, the in-train dynamics is ignored, too.

(7) The locomotive is thought to be of the 7E1 type, whose length is 20.47 m and whose mass is 126 tons.

(8) The loaded mass of the wagon is known to be 66 tons.

(9) The wagon types are unknown. Spoornet has a number of different wagon types in operation: CCL1, CCL2, CCL3, CCL5–9 and CCR1, CCR2, CCR3 and CCR5-9. Calculations are done for all these wagon types.

The characteristics of the wagon types in emergency application are indicated in Table 2.1, where BBF is the brake block force, EBCP is the emergency brake cylinder pressure and COF BB is the coefficient of friction. All these terms of the railway are referred to [3] or [25].

In the following calculation, the simple model is used to estimate the possible velocities and the cascade-mass-point model is used to simulate the emergency operation of the train.

Table 2.1: Wagon types and parameters

	CCL1&3	CCL2	CCL5–9	CCR1&3	CCR2	CCR5–9
EBCP (kpa)	472	472	472	240	240	240
COF BB	0.25	0.25	0.33	0.25	0.25	0.33
BBF(N)	218,951	220,921	215,205	266,782	220,921	215,205

2.3.3 Simple model

In this model, a train is simplified to a mass point. The train mass is

$$M = (126 \times 2 + 66 \times 40) \times 1,000 = 2,892,000kg.$$

When the wagon's type is CCL1&3

The brake force acting on the train is

$$F = 40 \times COF\ BB \times BBF = 40 \times 0.25 \times 218,951 = 2,189,510 \text{ N}.$$

The deceleration velocity of the train is

$$a = \frac{F}{M} = \frac{2,189,510}{2,892,000} = 0.7571 \text{ m/s}^2.$$

The first point from where the train driver is able to see to the collision point is 728 m. The first simple calculation is the maximum initial speed of the train that the collision could have been avoided.

For the maximum possible braking distance $s_1 = 728$ m, the admitted maximum initial velocity is

$$v_0 = \sqrt{2as_1} = \sqrt{2 \times 0.7571 \times 728} = 33.2 \text{ m/s} = 119.5 \text{ km/hour}.$$

The distance from the point (where the train driver is able to see the collision point) to its full stop is 978 m. The next simple calculation is the maximum initial speed of the train if the driver had applied the emergency brake immediately at this point. For the real braking distance $s_1 = 978$ m, the velocity before the application of emergency braking is

$$v_0 = \sqrt{2as_1} = \sqrt{2 \times 0.7571 \times 978} = 38.48 \text{ m/s} = 138.54 \text{ km/hour}.$$

This calculation is done without considering the time delay of the application of the emergency. If one considers the worst case, considering the longest time delay for each wagon and the operational time between the emergency operation of the brake valve and

the full application of the emergency brake, one allows 2 seconds for transmission delay and 2 seconds for the application delay. This yields $T_d = 4$ s and $s_1 = T_d v_0 + v_0^2/(2a)$. The solution is $v_0 = 30.31$ m/s $= 109.12$ km/hour for $s_1 = 728$ m. When $s_1 = 978$ m, the initial velocity is $v_0 = 35.57$ m/s $= 128.06$ km/hour. That is, if the train's velocity before emergency is no more than 109.12 km/hour (128.06 km/hour), the train can be stopped within the braking distance 728 m (978 m).

It is normal that a reaction time is needed for the train driver to apply the emergency brake. A normal reaction time is 5 seconds. When 5 seconds is accepted for the decision of the operation of the emergency brake, then $T_d = 9$ s. The initial velocity is solved with $v_0 = 27.08$ m/s $= 97.5$ km/hour and $v_0 = 32.27$ m/s $= 116.16$ km/hour for $s_1 = 728$ m and $s_1 = 978$ m, respectively.

The similar calculation steps are applied in other wagon types.

When the wagon's type is CCL2

The brake force acting on the train is

$$F = 40 \times COF\ BB \times BBF = 2,209,210 \text{ N}.$$

The deceleration velocity of the train is $a = 0.7639$ m/s^2.

For the maximum possible braking distance $s_1 = 728$ m, the admitted maximum initial velocity is $v_0 = 33.35$ m/s $= 120.1$ km/hour.

For the real braking distance $s_1 = 978$ m, the velocity before the application of emergency braking is$v_0 = 38.65$ m/s $= 139.16$ km/hour.

Considering 2 seconds for transmission delay and 2 seconds for the application delay, one has $T_d = 4s$ and the solution is $v_0 = 30.43$ m/s $= 109.56$ km/hour for $s_1 = 728$ m while $v_0 = 35.72$ m/s $= 128.59$ km/hour for $s_1 = 978$ m.

When 5 seconds is considered for the decision of the operation of the emergency brake, $T_d = 9s$. The initial velocity is solved with $v_0 = 27.18$ m/s $= 97.84$ km/hour and $v_0 = 32.39$ m/s $= 116.59$ km/hour for $s_1 = 728$ m and $s = 978$ m, respectively.

When the wagon's type is CCL5–9

The brake force acting on the train is

$$F = 40 \times COF\ BB \times BBF = 2,840,700 \text{ N}.$$

The deceleration velocity of the train is $a = 0.9827$ m/s^2.

For the maximum possible braking distance $s_1 = 728$ m, the admitted maximum initial velocity is $v_0 = 37.8$ m/s = 136.2 km/hour. . For the real braking distance $s_1 = 978$ m, the velocity before the application of emergency braking is$v_0 = 43.84$ m/s = 157.83 km/hour.

Considering 2 seconds for transmission delay and 2 seconds for the application delay, the solution is $v_0 = 34.01$ m/s = 122.76 km/hour for $s_1 = 728$ m while $v_0 = 40.09$ m/s = 144.32 km/hour for $s_1 = 978$ m.

When 5 seconds is considered for the decision of the operation of the emergency brake, $T_d = 9s$. The initial velocity is solved with $v_0 = 30.00$ m/s = 108.01 km/hour and $v_0 = 35.88$ m/s = 129.17 km/hour for $s_1 = 728$ m and $s = 978$ m, respectively.

When the wagon's type is CCL1&3

The brake force acting on the train is $F = 2,667,820$ N. The deceleration velocity of the train is $a = 0.9225$ m/s^2.

For the maximum possible braking distance $s_1 = 728$ m, the admitted maximum initial velocity is $v_0 = 36.65$ m/s = 131.9 km/hour.

For the real braking distance $s_1 = 978$ m, the velocity before the application of emergency braking is$v_0 = 42.48$ m/s = 152.92 km/hour.

Considering 2 seconds for transmission delay and 2 seconds for the application delay, the solution is $v_0 = 33.14$ m/s = 119.32 km/hour for $s_1 = 728$ m while $v_0 = 38.95$ m/s = 140.21 km/hour for $s_1 = 978$ m.

When 5 seconds is considered for the decision of the operation of the emergency brake, $T_d = 9$ s. The initial velocity is solved with $v_0 = 29.28$ m/s = 105.39 km/hour and $v_0 = 34.98$ m/s = 125.93 km/hour for $s_1 = 728$ m and $s = 978$ m, respectively.

When the wagon's type is CCR2

The result is the same as that of CCL2.

When the wagon's type is CCR5-9

The result is the same as that of CCL5-9.

2.3.4 Cascade mass-point model

The simple model is used to estimate the initial velocity of the train. Here a cascade-mass-point model connected with nonlinear couplers is used to simulate the running of the train. In this model, the locomotive is thought to be 7E1 and the wagons are thought to be the above different types of wagons. The coupler characteristic is as indicated in Fig. 2.5.

The operational procedure of the emergency brake is thought to be as follows.

First the train driver notices the environment and makes a decision to initiate the emergency brake operation. In the following simulation, the time is denoted as T_1. The train driver begins to move the brake valve to the emergency position. During this operation, the braking pipe needs time to release its air pressure. This time is denoted as T_2. Actually there is another time delay mixed in this time delay, which is the transmission delay of the braking signal. In simulation, the transmission velocity of the emergency brake is about 300 m/s.

The following tables show the simulation results. In these tables, S_1 is the braking distance without any time delays considered; S_2 is the braking distance with the transmission delays (part of T_2) considered; S_3 is the braking distance with the transmission delays and another 2-second delay for the application delay considered and S_4 is the braking distance with the transmission delay, 2-second application delay (T_2) and 5-second decision time delay (T_1) considered.

Table 2.2: Wagon type CCL1&3

V_0 (km/hour)	S_1 (m)	S_2 (m)	S_3 (m)	S_4 (m)
138.54		986.62	1,063.58	1,256.00
128.05		844.83	915.97	1,093.82
119.52	712.9	738.00	814.40	
117.29	686.5	711.12	776.28	
116.17		697.83	762.37	923.72
109.12		616.89	677.51	
108.00	582.1	604.50	664.50	
97.49		494.52	548.68	684.08

Some explanations of the above tables follow.

In Table 2.2, the wagon type of the train is CCL1&3 and the BBF is 54, 738 N. If the driver applied emergency braking once the train reached the point of sight distance (728 m from the cross) and the train's velocity was no more than 109.12 km/hour, the braking distance would not be more than 677.51 m. If the driver applied emergency braking 5 seconds after the train passed the point of sight and the train's velocity was no more than 116.17 km/hour, the braking distance would not be more than 923.72 m. Even if the couplers connecting the locomotives and wagons were rigid, the above

Table 2.3: Wagon type CCL2(CCR2)

V_0 (km/hour)	S_1 (m)	S_2 (m)	S_3 (m)	S_4 (m)
139.16		986.75	1,064.50	1,257.33
128.59		844.48	915.92	1,094.52
120.06	712.95	738.15	804.85	
117.28	686.67	711.37	776.83	
116.59		696.71	761.49	923.42
109.55		616.27	677.10	
108.00	576.90	599.50	659.50	
97.84		493.62	547.98	683.86

Table 2.4: Wagon type CCL5–9(CCR5–9)

V_0 (km/hour)	S_1 (m)	S_2 (m)	S_3 (m)	S_4 (m)
157.77		990.48	1,078.12	1,297.25
144.32		830.91	911.09	1,111.53
136.08		740.90	816.50	
133.38		712.35	786.45	
129.17		668.72	740.48	919.89
122.76		605.00	673.20	
108.00		471.00	531.00	
108.01		471.10	531.10	681.11

Table 2.5: Wagon type CCR1&3

V_0 (km/hour)	S_1 (m)	S_2 (m)	S_3 (m)	S_4 (m)
152.92		989.42	1,074.38	1,286.77
140.21		834.45	912.35	1,107.09
131.94		710.45	813.75	
129.28		711.59	783.41	
125.93		676.02	745.98	920.88
119.32		607.86	674.14	
108.00		500.50	560.50	
105.39		477.12	535.68	682.05

two distances would not be more than 728 m and 978 m, respectively.

In Table 2.3, the wagon type of the train is CCL2 or CCR2 and the BBF is 55, 230 N. If the driver applied emergency braking once the train reached the point of sight distance (728 m from the cross) and the train's velocity was no more than 122.76 km/hour, the braking distance would not be more than 673.20 m. If the driver applied emergency braking 5 seconds after the train passed the point of sight and the train's velocity was no more than 116.59 km/hour, the braking distance would not be more than 923.42 m. Even if the couplers connecting the locomotives and wagons were rigid, the above two distances would not be more than 728 m and 978 m, respectively.

In Table 2.4, the wagon type of the train is CCL5-9 or CCR5-9 and the BBF is 71, 018 N. If the driver applied emergency braking once the train reached the point of sight distance (728 m from the cross) and the train's velocity was no more than 109.55 km/hour, the braking distance would not be more than 677.10 m. If the driver applied emergency braking 5 seconds after the train passed the point of sight and the train's velocity was no more than 129.17 km/hour, the braking distance would not be more than 919.89 m. Even if the couplers connecting the locomotives and wagons were rigid, the above two distances would not be more than 728 m and 978 m, respectively.

In Table 2.5, the wagon type of the train is CCR1&3 and the BBF is 66, 696 N. If the driver applied emergency braking once the train reached the point of sight distance (728 m from the cross) and the train's velocity was no more than 119.32 km/hour, the braking distance would not be more than 674.14 m. If the driver applied emergency braking 5 seconds after the train passed the point of sight and the train's velocity was no more than 125.93 km/hour, the braking distance would not be more than 920.88 m. Even if the couplers connecting the locomotives and wagons were rigid, the above two distances would not be more than 728 m and 978 m, respectively.

2.3.5 Conclusions of the calculation

Although some information is unknown about the train and the track, some conclusions can be drawn based upon the aforementioned assumptions and calculations:

1) The faster the train, the longer the braking distance.
2) For different braking systems, the braking distances are different.
3) The smaller the COF BB of the wagons is, the longer the braking distance is.
4) The later the driver initiated emergency operation, the longer the braking distance was.
5) If the braking equipment worked as designed, and the driver initiated the emergency operation once the train was at the point of sight distance from the cross,

the braking distance would not be more than 728 m if the velocity of the train was no more than 110 km/hour. Even if the driver applied emergency operation 5 seconds after the train passed the sight point, the braking distance would not be more than 728 m if the velocity of the train was no more than 97 km/hour.

6) If the braking equipment worked as designed, and the driver initiated the emergency operation once the train was at the point of sight distance from the cross, the braking distance would not be more than 978 m if the velocity of the train was no more than 128 km/hour. Even if the driver initiated the emergency operation 5 seconds after the train passed the sight point, the braking distance would not be more than 978 m if the velocity of the train was no than 116 km/hour.

From this calculation, it is also seen that at the same initial speed, the stop distance calculated with the cascade-mass-point model is shorter than that in the case of the mass-point model (simple model). This is because with a cascade-mass-point model, part of the kinetic energy is consumed by the couplers, which is ignored in the mass-point model. From this point of view, the cascade-mass-point model is more accurate when a train is longer than 1.8 km, which is the case in this study.

2.4 Conclusion

In this chapter, a cascade of mass points connected with nonlinear couplers is described as a model for a long heavy haul train. This model has been validated in [17] with data from Spoornet.

A stop distance calculation is also given in this chapter with a mass-point model and a cascade-mass-point model, respectively. The calculation result shows that the latter is more accurate when a train is longer than 1.8 km, which is the case in this study.

Chapter 3

Optimal scheduling

3.1 Introduction

In train handling, different kinds of scheduling approaches are proposed in the literature. However, the differences among them are not discussed. It is assumed that there are redundancies in optimization of scheduling. Optimal scheduling may improve the performance of a train. It is said in chapter 1 that the ECP braking system can improve train performance. In this chapter, the difference between trains equipped with a pneumatic braking system and an ECP braking system is first compared and then the difference between optimal scheduling and heuristic scheduling is discussed.

In the first part of this chapter, three control strategies are proposed for train handling. In the second part, the performances reached with optimal scheduling with in-train forces taken into initial consideration on trains equipped with a tradition pneumatic braking system and an ECP braking system are compared. ECP braking systems show superb performance compared with pneumatic braking systems. Thus, in the rest of this thesis, the handling of trains equipped with ECP braking systems is studied.

It is hoped that optimal scheduling can improve the performance of train handling. Optimal scheduling, taking in-train forces and energy consumption into consideration, is compared with the heuristic scheduling proposed in [15] in the third part of this chapter. It is shown that optimal scheduling presents a better start for closed-loop controllers. The work of this part is seen in [20].

In the last part, a closed-loop controller combining the optimal scheduling and LQR controller in [15], employing a linear system theory, is adopted to compare with the closed-loop controller in [15]. Optimal scheduling is used to calculate the equilibria, while a closed-loop controller based on LQR is employed to bring the trajectory of the train to the equilibria. It is confirmed from the simulation that Optimal scheduling

actually improves the performance of the closed-loop controllers and that the 2-2 strategy, ECP/iDP-only strategy yields the best performance of all strategies. The work of this part can be seen in [21].

3.2 Control strategies

A traditional heavy haul train with a pneumatic controlled braking system is controlled by drivers in the leading locomotive. A single air pipe runs throughout the whole train and is responsible for supplying pressure to the braking system in each wagon as well as transmitting braking control signals. The driver controls the leading locomotive's effort while other locomotives' efforts follow that of the leading one. Because of the pressure wave propagation speed, the front wagons are responsible for most of the braking owing to the signal propagation delay and the pressure gradient. From a control point of view, there are only two control signals in this kind of strategy, one for locomotive effort and the other one for wagon brake.

When the locomotives' efforts are controlled independently and separately, this is referred to as multi-powered [11] or distributed powered. In this strategy, every locomotive or every locomotive group (some locomotives connected with rigid drawbar) has an independent control signal.

While the train is equipped with an ECP braking system, the braking control signal is transmitted electronically. There is nearly no time delay for the braking signal transmission. When the above two control strategies are implemented with an ECP system, the braking signals are not delayed.

An ECP braking system adds a new dimension to control strategy: it allows individual wagon braking. So in a fully ECP/iDP mode, every car, including locomotives and wagons, has its own independent control signal.

Summarizing the above, three major types of control are discussed in this study:

- 1-1 strategy
  One control signal is for all locomotives and one braking control signal for all wagons. Currently, this control strategy is still in use on the heavy haul trains of Spoornet equipped with ECP braking systems, for this control strategy was in use before the application of ECP braking systems and was well designed for short heavy haul trains. However, this strategy hinders the expansion of the train's length.

- 2-1 strategy
  Different control signals are for different locomotives while the same braking control signals server for all wagons. This is an iDP-only strategy.

- 2-2 strategy
  Every car has its own control signal. This is an ECP/iDP-only strategy.

3.3 Optimal scheduling on trains equipped with different braking systems

In chapter 1, it is said that a train equipped with an ECP braking system performs better compared with the traditional pneumatic braking system. The main difference between these two braking systems is the braking command signals. In a pneumatic braking system, the braking signals for all the wagons are the same and there are different time delays for the wagons to receive them. In an ECP braking system, the signal for all wagons may be different and it is received by all wagons simultaneously. In this chapter optimal scheduling on the trains equipped with these two braking systems will respectively be simulated and the difference between them will be compared. Here only the result of in-train forces is compared, while other advantages of the application of an ECP braking system are not shown. From the simulation, the ECP braking system shows superb performance compared to the pneumatic braking system on the one hand. On the other hand, the application of an ECP braking system enriches the control strategy of train handling.

An optimization procedure is applied to schedule cruise control by taking the in-train forces into initial design consideration. It is hoped that an optimal open loop controller design will present a better starting point for a closed-loop controller design. To demonstrate the open loop control design, the throttling and braking are constrained and three different operational strategies of heavy haul trains are distinguished.

3.3.1 Formulation of the optimal problem

Transient control

The inputs in (2.2) are insensitive to the change in the reference speed. To get a rapid response to the reference speed change, transient control is designed through an acceleration profile in the following open loop scheduling. When a closed-loop controller is considered, this step is unnecessary. An acceleration profile is calculated according to the velocity profile with a parameter, the acceleration limit, a_{rr}. For example, at the travel distance $dis = 1,000$ m, the reference velocity is changed from 12 m/s to 15 m/s

and at the distance $dis = 5,000$ m, it is changed to 10 m/s, then the acceleration profile is as in Table 3.1, where s_1, s_2 are calculated as $s_1 = 1,000 + (15^2 - 12^2)/(2a_{rr})$, $s_2 = 5,000 + (15^2 - 10^2)/(2a_{rr})$. Thus from the point 1,000 m to the point s_1 and from

Table 3.1: Acceleration profile

distance	$\cdots$	1,000	s_1	5,000	s_2	$\cdots$
a	0	a_{rr}	0	$-a_{rr}$	0	$\cdots$

the point 5,000 m to the point s_2, the open loop scheduling should maintain the accelerations.

Performance function of optimal control

The objectives of a train control project are that with optimal control, 1) the train can travel a given distance within a given period; 2) energy consumption is reduced; and 3) the range of in-train forces is in the admission range of the train couplers. At the equilibrium point, where the speeds of the cars and the displacements of couplers are constant, that is, $\dot{v}_i = 0, \dot{x}_j = 0, i = 1, 2, \cdots n, j = 1, 2, \cdots, n-1$, the energy consumption of all control strategies is nearly equal, for most of the energy is used to conquer the resistance of drag forces, which are determined by the speed profile, track profile and the train. So the second objective can be ignored in scheduling the open loop controller. The first objective is more closely related to the speed profile and speed holding. In scheduling the open loop controller, it is assumed that the desired speed is reached and held. In this chapter, the objective, therefore, is taken as

$$J = \sum_{i=0}^{n-1} f_{in_i}^2, \tag{3.1}$$

where n is the number of cars in the train. That is, the purpose of the scheduling is to minimize the in-train forces.

In the following analysis, the train is assumed to consist of n cars, in which there are k locomotives. The cars are numbered from the front to the back with 1 to n. The locomotives' numbers are from l_1 to l_k.

Constraints of the optimal problem

For open loop control, the dynamic process in the train is ignored and the reference velocity is reached or the acceleration is maintained, that is,

$$\begin{aligned} \frac{dv_i}{dt} &= a, \qquad i = 1, 2, \cdots, n \\ \frac{dx_j}{dt} &= 0, \qquad j = 1, 2, \cdots, n-1, \end{aligned} \tag{3.2}$$

where a is the acceleration, which is zero when the train is cruising and is $a_r(-a_r)$ when the train is running within a scheduled acceleration (deceleration) period.

Applying (3.2) to equations (2.2) and (2.3), one has

$$u_s + f_{in_{s-1}} - f_{in_s} - f_{a_s} - m_s a = 0, \quad s = 1, 2, \cdots, n. \tag{3.3}$$

From the first $(n-1)$ equations of (3.3), the in-train forces can be calculated as

$$f_{in_s} = \sum_{i=1}^{s} u_i - \sum_{i=1}^{s} (f_{a_i} + m_i a), \quad s = 1, 2, \cdots, n-1. \tag{3.4}$$

From the last equation of (3.3), one has

$$\sum_{i=1}^{n} u_i - \sum_{i=1}^{n} (f_{a_i} + m_i a) = 0. \tag{3.5}$$

In train operations, the inputs and the in-train forces have some constraints:

$$\begin{aligned} \underline{U}_i \le u_i \le \overline{U}_i, &\qquad i = 1, 2, \cdots, n; \\ \underline{F}_{in_j} \le f_{in_j} \le \overline{F}_{in_j}, &\qquad j = 1, 2, \cdots, n-1, \end{aligned} \tag{3.6}$$

where $\underline{U}_i, \overline{U}_i$ are the upper and lower constraints for the ith input, and $\underline{F}_{in_j}, \overline{F}_{in_j}$ are the up and lower constraints for the jth in-train force, respectively. For a wagon, $\overline{U}_i = 0$ and the value of $\underline{U}_i$ depends on the capacity of the wagon's brake. For a locomotive, the constraints $\underline{U}_i, \overline{U}_i$ depend on the locomotive's capacity in traction effort. The notch should be changed step by step, and every notch should be kept for longer than a fixed time interval before it is changed. The constraints $\underline{F}_{in_j}, \overline{F}_{in_j}$ are limited because of the requirement of safe operation and limiting of maintenance cost.

Thus open loop scheduling is an optimization problem of the objective function (3.1) with equality constraints (3.3) and inequality constraints (3.6).

3.3.2 Optimization algorithm

In the following, the optimization algorithm of the 1-1 strategy is given as an example. The other two are similar and are omitted.

With the 1-1 strategy, all the locomotives share the drag forces equally and the brake forces of all the wagons are equal. This imposes additional constraints on the optimization problem.

$$\begin{aligned} u_{l_1} = u_{l_2} = \cdots = u_{l_{m-1}} = \cdots = u_{l_k} &\triangleq u_t, \\ u_i &\triangleq u_b, \qquad i = 1, \cdots, n; i \neq l_j, j = 1, \cdots, k. \end{aligned} \tag{3.7}$$

It is distinguished between two cases.

1) The last locomotive is not at the rear of the train. In this case, $l_k < n$. Combining (3.7) with (3.4), one has

$$f_{in_i} = \begin{cases} iu_b - \sum_{j=1}^{i}(f_{a_j} + m_j a), & 1 \leq i < l_1, \\ (i-1)u_b + u_t - \sum_{j=1}^{i}(f_{a_j} + m_j a), & l_1 \leq i < l_2, \\ \cdots \\ (i-k)u_b + ku_t - \sum_{j=1}^{i}(f_{a_j} + m_j a), & l_k \leq i < n, \end{cases}$$

and

$$ku_t + (n-k)u_b = \sum_{i=1}^{n}(f_{a_i} + m_i a).$$

The objective function is rewritten as

$$\begin{aligned} J = \sum_{i=1}^{n-1} f_{in_i}^2 = &\sum_{i=1}^{l_1-1}\left(iu_b - \sum_{j=1}^{i}(f_{a_j} + m_j a)\right)^2 + \cdots + \\ &+ \sum_{i=l_{k-1}}^{l_k-1}\left((i-k+1)u_b + (k-1)u_t - \sum_{j=1}^{i}(f_{a_j} + m_j a)\right)^2 \\ &+ \sum_{i=l_k}^{n-1}\left((i-k)u_b + ku_t - \sum_{j=1}^{i}(f_{a_j} + m_j a)\right)^2. \end{aligned}$$

The optimization with equality and inequality constraints can be solved with the Lagrange multiplier approach [26]. The equality constraints can be taken care of with

the following extended objective function with a Lagrange multiplier:

$$\bar{J} = J + 2\lambda \left(ku_t + (n-k)u_b - \sum_{j=1}^{n} (f_{a_j} + m_j a) \right). \tag{3.8}$$

First, one calculates

$$\begin{aligned} \frac{1}{2}\frac{\partial J}{\partial u_t} &= \sum_{j=1}^{k} \left(\sum_{i=l_j}^{l_{j+1}-1} jQ_{i,j} \right), \\ \frac{1}{2}\frac{\partial J}{\partial u_b} &= \sum_{j=0}^{k} \left(\sum_{i=l_j}^{l_{j+1}-1} (i-j)Q_{i,j} \right), \end{aligned} \tag{3.9}$$

where $Q_{i,s} = (i-s)u_b + su_t - \sum_{j=1}^{i} (f_{a_j} + m_j a), s = 0, \cdots, k, l_0 = 1, l_{k+1} = n$ and, denotes them as

$$\begin{aligned} \frac{1}{2}\frac{\partial J}{\partial u_t} &= T_b u_b + T_t u_t + \sum_{i=1}^{n-1} T_i (f_{a_i} + m_i a), \\ \frac{1}{2}\frac{\partial J}{\partial u_b} &= B_b u_b + B_t u_t + \sum_{i=1}^{n-1} B_i (f_{a_i} + m_i a). \end{aligned} \tag{3.10}$$

The necessary condition for extremality of $\bar{J}$ is:

$$\begin{aligned} \frac{1}{2}\frac{\partial \bar{J}}{\partial u_t} &= \frac{1}{2}\frac{\partial J}{\partial u_t} + \lambda k = 0, \\ \frac{1}{2}\frac{\partial \bar{J}}{\partial u_b} &= \frac{1}{2}\frac{\partial J}{\partial u_b} + \lambda (n-k) = 0, \\ ku_t + (n-k)u_b - \sum_{i=1}^{n} (f_{a_i} + m_i a) &= 0. \end{aligned} \tag{3.11}$$

From them, one can get the following equations:

$$\begin{aligned} P_{bb} u_b + P_{tt} u_t &= \sum_{i=1}^{n-1} \left(kB_i - (n-k)T_i \right) F_i, \\ P_{bb} &= (n-k)T_b - kB_b, \\ P_{tt} &= (n-k)T_t - kB_t, \\ (n-k)u_b + ku_t &= \sum_{i=1}^{n} F_i, \end{aligned} \tag{3.12}$$

where $F_i = f_{a_i} + m_i a$ and from which one can get the solutions of u_b, u_t. In applying this solution to (3.6), if no constraint is violated, this solution is the optimal value. If some constraints are violated, then one takes these violated inequality constraints as

equality constraints, and re-solves the optimization problem. For example, one may wish to minimize $J(x)$ subject to $f(y) \leq 0$, where f, J and x are vectors of different dimensions. Suppose that x has p components and that n components of the inequality constraints are violated, that is, $f_i(x) > 0, \quad i = 1, 2, \cdots, n$. The other constraints, $f_i(x) \leq 0, \quad i = n+1, \cdots$, may be disregarded. Define a new function, $\bar{J} = J + \lambda^T F$, where $\lambda^T = [\lambda_1 \quad \cdots \quad \lambda_n]$, $F = [f_1(x) \quad \cdots \quad f_n(x)]^T$ to replace J. Solving this minimization problem, one can get a new solution which is more admissible. The above process is repeated if necessary. This procedure of solving a constrained optimization problem is described in detail in [26].

2) The last locomotive is at the rear of the train. In this case, $l_k = n$.

In the above calculation ($l_k < n$), one could consider $l_{k+1} = n$. So one can replace k in the above case with $k-1$ in this case.

$$f_{in_i} = \begin{cases} iu_b - \sum_{j=1}^{i}(f_{a_j} + m_j a), & 1 \leq i < l_1, \\ (i-1)u_b + u_t - \sum_{j=1}^{i}(f_{a_j} + m_j a), & l_1 \leq i < l_2, \\ \cdots \\ (i-k+1)u_b + (k-1)u_t - \sum_{j=1}^{i}(f_{a_j} + m_j a), & l_{k-1} \leq i < n, \end{cases}$$

and

$$ku_t + (n-k)u_b = \sum_{i=1}^{n}(f_{a_i} + m_i a).$$

One can get similar results.

For instance, $n = 52$, $l_1 = 1$, $l_2 = 52$, then

$$\begin{aligned} u_t &= \frac{1}{2262}\sum_{i=1}^{52}\frac{-3888 - 25i + 5i^2}{2}(f_{a_i} + m_i a), \\ u_b &= \frac{1}{2262}\sum_{i=1}^{52}\frac{1230 + 5i - i^2}{10}(f_{a_i} + m_i a). \end{aligned} \tag{3.13}$$

The mathematic developments for the other two control strategies are similar to the above one.

3.3.3 Simulation of different braking systems

In simulation, one assumes that the train consists of 200 wagons. Every four wagons (a rake) are linked with rigid drawbars of which the in-train forces are not considered and

are regarded as one unit. There are two locomotives at the front and two at the rear. The neighbouring locomotives are linked with rigid drawbars and regarded as one unit too. So the train can be regarded as consisting of 50 wagons between two locomotives.

The parameters of the train are given in the following tables [15].

Table 3.2: Locomotive group parameters

m(ton)	c_0(m/s^2)	c_1(1/s)	c_2(1/m)	L(m)
252	7.6685e-3	1.08e-4	2.06e-5	40.94

Table 3.3: Wagon group parameters

m(ton)	c_0(m/s^2)	c_1(1/s)	c_2(1/m)	L (m)	F_b(kN)
417	6.3625e-3	1.08e-4	1.492e-5	48.28	720

In the tables, F_b represents the capacity of brake force, and L is the longitudinal length of a locomotive or wagon group. Fig. 2.5 shows the locomotive (group) effort (7E1) corresponding to a particular notch level and velocity. These data, including the track profile, are based on the COALink trains operated in South Africa by Spoornet. The relation between the displacement and the static force (without damping) of the coupler is shown in Fig. 2.3. The damping coefficient is notoriously difficult to estimate because the train speed is limited by dominant quadratic resistance term. According to [11] it can be as high as $\frac{1}{34}$ of the spring coefficient. Since the damping coefficient is not available in this study, it is taken as $\frac{1}{100}$ of the spring coefficient in the train model, and ignored in the control design.

In (3.6), $\overline{F_{in_i}} = -F_{in_i} = 1600$ kN. There are some constraints with the locomotive notch operation. Firstly, the notch could only be changed stepwise; secondly, the locomotive engine should stay at a notch for at least 10 seconds, and when the locomotive's effort changes from traction to dynamic braking or the other way round, the first notch should last at least 20 seconds. The acceleration limit a_r is 0.07 m/s^2. The reference velocity is 36 km/h from the simulation starting point -2 km to 3 km and then it is 43.2 km/h. At the point 6 km, it is changed to 54 km/h, while it is changed to 43.2 km/h again at the point 8 km. Some distances are negative because the reference point is chosen in the middle of the track and the distance values are relative.

The initial state is that the train is in its steady state with all the cars' velocities 10.5 m/s and all the in-train forces zeros. For a traditional train, the time delay for a wagon's braking force is calculated with the wagon's distance to the first locomotives divided by the velocity of sound.

The simulation is processed with MATLAB. The train model runs continuously and the control signal is updated every second.

The track profile is shown in Fig. 3.1. All simulations in this study, without special description, are processed on this track profile and the track profile in the rest is omitted.

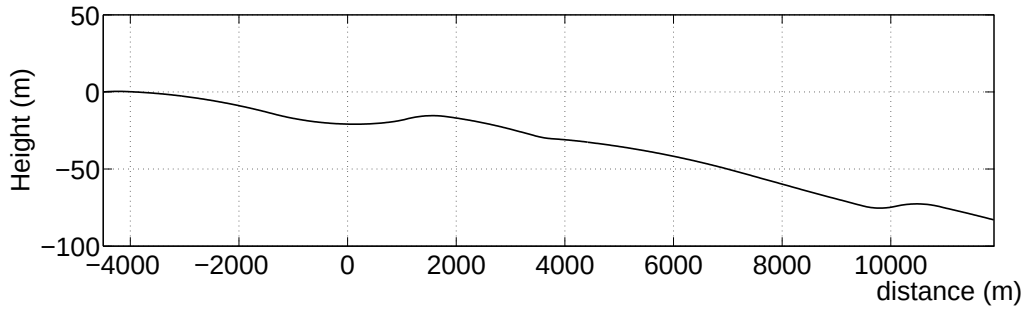

Figure 3.1: Track profile

Simulation results are shown in the following figures.

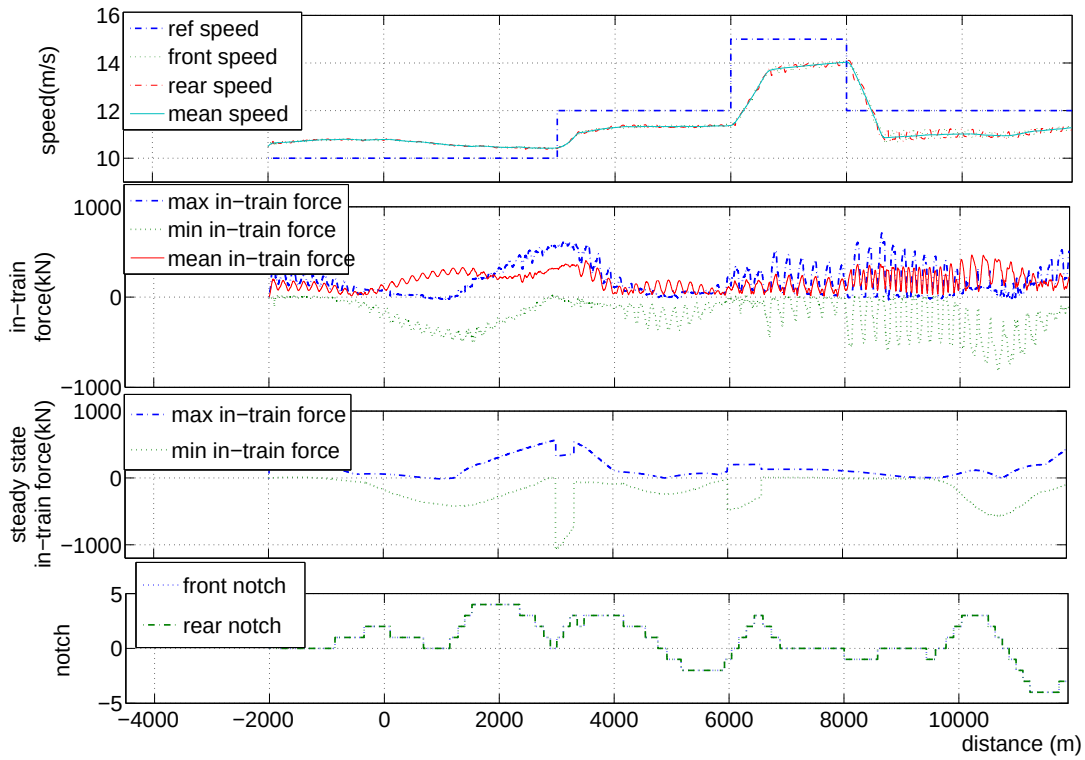

Figure 3.2: 1-1 strategy without ECP

Fig. 3.2 and Fig. 3.3 show the applications to traditional heavy haul trains (with pneumatic braking system) of 1-1 strategy controller and 2-1 strategy controller, respectively. The train is not equipped with an ECP braking system and therefore there are time delays for the wagons' control signal transmission.

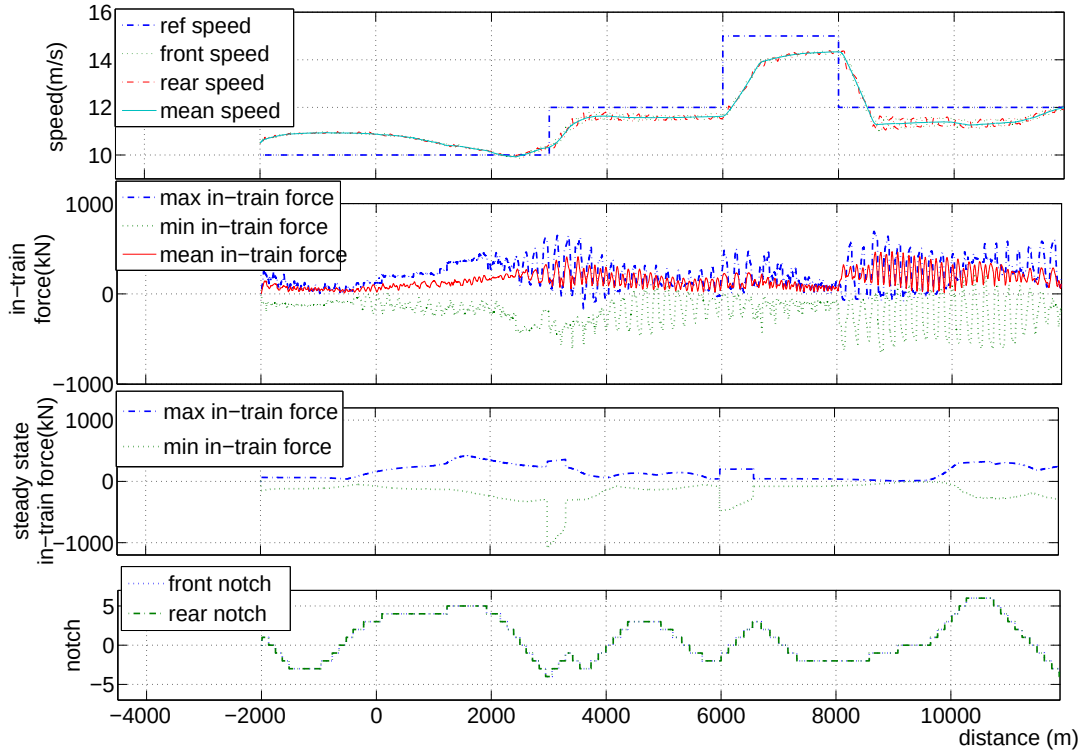

Figure 3.3: 2-1 strategy without ECP

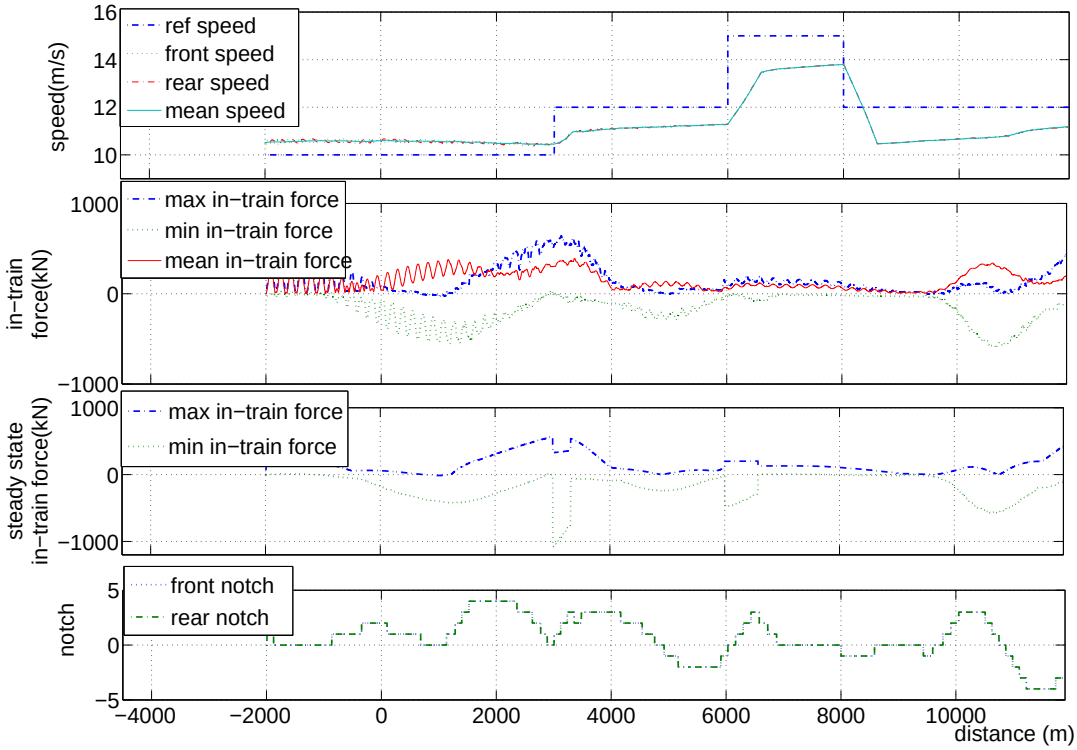

Figure 3.4: 1-1 strategy with ECP

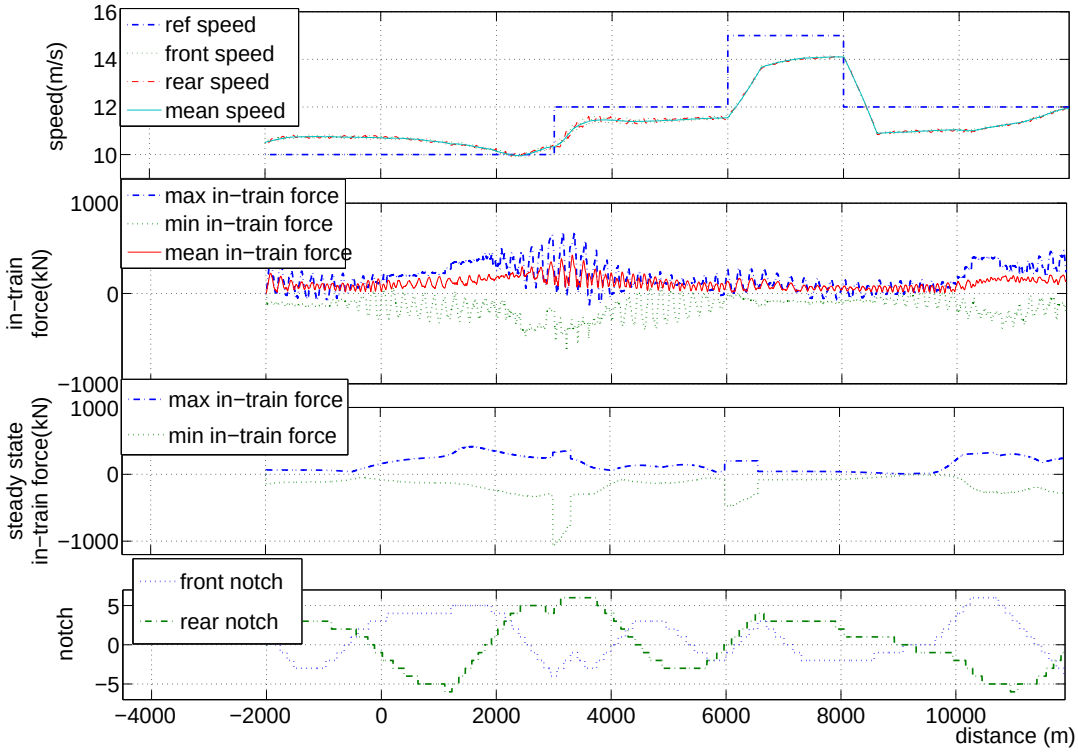

Figure 3.5: 2-1 strategy with ECP

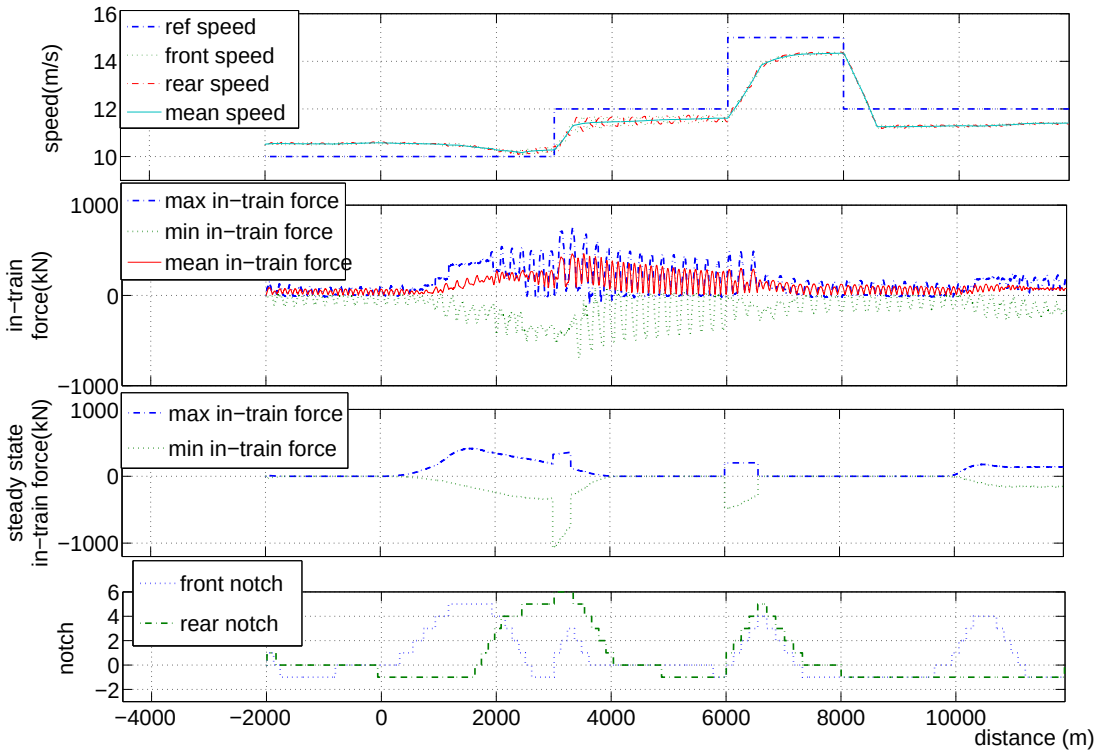

Figure 3.6: 2-2 strategy with ECP/iDP

The applications to a heavy haul train with an ECP braking system installed of 1-1 strategy controller, 2-1 strategy controller and 2-2 strategy controller are shown in Fig. 3.4, Fig. 3.5 and Fig. 3.6, respectively. The control inputs in Fig. 3.4 are the same as in Fig. 3.2 and those in Fig. 3.5 are the same as in Fig. 3.3. However, because of the installation of an ECP braking system, there is no time delay for the wagon control signal transmission.

In these figures, the first subplot is the front locomotive group speed, rear locomotive group speed and the mean speed of all the cars with respect to the distance from the starting point. The second subplot is maximum and minimum in-train forces and mean in-train force (the mean value of the absolute values of all the in-train forces at a specific time with respect to the distance). The third is the steady in-train forces, which are calculated by applying the efforts of the cars to the train model, with the reference speed (and the acceleration) maintained and the dynamic process ignored.

Table 3.4 is the performance comparison of Fig.s from 3.2 to 3.6. The variable $|\delta\bar{v}|$ is the absolute value of the difference between the reference velocity and the mean value of all the cars' velocities at a specific point. $\overline{|f_{in}|}$ is the mean value of the absolute values of all the couplers' in-train forces at a specific point. Item E is the energy consumed during travel. The items max, mean and std are the maximum value, mean value and standard deviation of the statistical variable, respectively.

Table 3.4: Comparison of braking systems: pneumatics vs. ECP

	$\|\delta\bar{v}\|$(m/s)			$\overline{\|f_{in}\|}$(kN)			E
	max	mean	std	max	mean	std	(MJ)
Fig. 3.2	3.6225	0.9179	0.51	466.46	173.17	96.61	1,170
Fig. 3.4	3.7063	0.9650	0.53	391.82	146.70	101.79	1,180
Fig. 3.3	3.3715	0.7032	0.54	467.16	151.20	88.26	2,110
Fig. 3.5	3.4530	0.7401	0.50	424.50	113.51	63.05	2,130
Fig. 3.6	3.3901	0.6510	0.42	461.86	111.18	90.95	1,370

When comparing Fig. 3.2 with Fig. 3.3, it can be seen that the locomotive speed error is smaller in the 2-1 strategy than in the 1-1 strategy. The absolute values of the maximum and the minimum in-train forces are smaller with the 2-1 strategy when it comes to steady running. However, the energy consumption with the 1-1 strategy is a little less than with the 2-1 strategy. This is because some energy is used to overcome the in-train forces' fluctuation and larger brake forces are applied. The same result can be seen when comparing Fig. 3.4 with Fig. 3.5.

When comparing Fig. 3.5 with Fig. 3.6, the locomotive speed fluctuation and error with the 2-2 strategy are smaller than those with the 2-1 strategy. The absolute values of maximum and minimum in-train forces with the 2-2 strategy are also a little lower than with the 2-1 strategy. The energy consumption with the 2-1 strategy is a little higher than with the 2-2 strategy. The steady in-train forces with the 2-2 strategy are nearly zero when the train is running in its steady state without velocity accelerations

or decelerations.

When comparing Fig. 3.2 with Fig. 3.4, both with the 1-1 strategy, the former train is equipped with a pneumatic braking system and the latter is equipped with an ECP braking system. The speed fluctuation in Fig. 3.2 is greater than in Fig. 3.4. The absolute values of maximum and minimum in-train forces and the mean in-train forces are greater in Fig. 3.2 than in Fig. 3.4. The energy consumption is almost equal in both figures.

When comparing Fig. 3.3 with Fig. 3.5, one can reach similar conclusions than when comparing Fig. 3.2 with Fig. 3.4.

It can be seen that the velocity error exists in all the results when open loop scheduling is used. When comparing the steady in-train forces, which represent the reference value for closed-loop control, the performance of the 2-2 strategy is the best among the three control strategies and the performance of the train equipped with an ECP braking system is better than that of a traditional train. With the introduction of the acceleration profile, the speed variations lead to larger in-train forces, especially within the speed acceleration periods. However, the accelerations decrease the speed tracking error. The transient control is a "trade-off" between the two aspects.

From the simulation results, the following conclusions can be drawn:

1) The scheduling with the averagely distributed power among the locomotives is not optimal for train performance.

2) The higher the number of controllable inputs is, the better the train performance.

3) The ECP braking system has demonstrated superb performance compared with a pneumatic braking system.

4) The 2-2 strategy is the best among the strategies for heavy haul trains equipped with ECP braking systems.

5) Open loop scheduling cannot yield satisfactory performance, but may be a good reference for closed-loop control, which is the purpose of this chapter.

3.4 Scheduling

An open loop controller is used to calculate the inputs when a train is running in its steady state with the reference velocity and acceleration maintained.

In [11], the off-line schedule for the throttling and braking inputs is chosen in such a way that the train is in its steady state with the reference velocity maintained. The

settings do not contribute to additional accelerations/decelerations of the train. The schedule determines the sequencing and the amplitudes of the inputs in case there are continuous input variations and no power limits. The applied inputs ${}^{o}u(t)$ are nonlinear functions of the schedule parameters p (grade of the track, velocity profile and train data) and the travelled distance z of the train: ${}^{o}u = f_u(z, p)$. The inputs are approximated by step functions of variable amplitudes. Such an optimal problem can be solved with MISER developed Toe in [74]. The sequence of the steps is predetermined and tuned, and the time instants of the step functions at which the steps are applied are decided on line. It is obvious that this off-line schedule is heuristic and subject to the pre-determined control sequence, so it will not be discussed further in this study.

The transient control is the same as in section 3.3.1.

3.4.1 Heuristic scheduling

According to [15], open loop control is chosen as follows, with $Beq = \sum_{i=0}^{n}(f_{a_i} + m_i a)$,

$$\begin{array}{lll} u_l = Beq/k, & u_b = 0 & Beq \geq 0, \\ u_l = Beq/n, & u_b = Beq/n & Beq < 0, \end{array} \tag{3.14}$$

where u_l is the locomotives' effort and u_b is the wagons' effort, and the variables k and n are the respective total numbers of locomotives and cars. The acceleration $a = 0$ in the cruising period while $a = \pm a_{rr}$ in the scheduled acceleration/decelertation periods. The power distribution is heuristic, so one calls it heuristic scheduling.

3.4.2 Optimal scheduling

According to the three operational strategies described in Section 3.2, there are three corresponding optimal open loop controllers for the train. In the following, the performance is a function of the in-train forces and the energy, which can be written as

$$J = \sum_{i=0}^{n-1} K_f f_{in_i}^2 + \sum_{i=0}^{n} K_e u_i^2, \tag{3.15}$$

where the weights of the in-train force and energy consumption are K_f and K_e, respectively. Optimal power distribution is characteristic of this scheduling, so one calls it optimal scheduling.

The energy cost is not proportional to u^2, but items proportional to u^2 are also evaluations of energy. From the energy point of view, it is not rational to include the minus input in the energy consumption function. However, considering the braking application for the cost of maintenance of the rail track and the train wheels, it is

retained in the performance function although it is not suitable to be classified into energy. On the other hand, if necessary, it is not difficult to separate the positive inputs and negative inputs in the performance function. In this study the energy consumption and the cost of braking are processed in a simple way.

For open loop control, the dynamic process in the train is ignored and the system is assumed to be in its steady state with acceleration maintained, that is,

$$\frac{dv_i}{dt} = a, \frac{dx_j}{dt} \quad = 0, \quad i = 1, \cdots, n, \quad j = 1, \cdots, n-1. \tag{3.16}$$

Applying (3.16) to (2.2), and assuming $f_{in_0} = 0$, one has

$$u_s + f_{in_{s-1}} - f_{in_s} - f_{a_s} - m_s a = 0, \qquad s = 1, \cdots, n. \tag{3.17}$$

In train operations, the inputs, $u_i, i = 1, \cdots, n$ and the in-train forces f_{in_i} have some constraints.

$$\begin{aligned} \underline{U}_i \le u_i \le \overline{U}_i, \qquad & i = 1, \cdots, n; \\ \underline{F}_{in_j} \le f_{in_j} \le \overline{F}_{in_j}, \qquad & j = 1, \cdots, n-1, \end{aligned} \tag{3.18}$$

where $\underline{U}_i, \overline{U}_i$ are the upper and lower constraints for the ith input, and $\underline{F}_{in_j}, \overline{F}_{in_j}$ are the upper and lower constraints for the jth in-train force, respectively. For wagons, $\overline{U_i} = 0$ and the values of $\underline{U_i}$ depend on the braking capacities of the wagons. For locomotives, the constraints $\underline{U}_i, \overline{U}_i$ depend on the locomotives' capacities in traction efforts and the running states. The constraints $\underline{F}_{in_j}, \overline{F}_{in_j}$ are limited because of the requirement of safe operation and maintenance cost.

Thus optimal scheduling is a standard quadratic programming (QP) problem with objective function (3.15), equality constraints (3.17), inequality constraints (3.18) and some additional equality constraints.

With the 1-1 strategy, the additional constraints imposed on the optimization problem are

$$u_{l_j} \triangleq u_t, \qquad u_i \triangleq u_b, \quad i = 1, \cdots, n; \quad i \neq l_j, j = 1, \cdots, k. \tag{3.19}$$

With the 2-1 strategy, the additional constraints are the following

$$u_i \triangleq u_b, \qquad i = 1, \cdots, n; \quad i \neq l_j, j = 1, \cdots, k. \tag{3.20}$$

With the 2-2 strategy, there is no additional constraint.

3.4.3 Simulation of heuristic scheduling vs. optimal scheduling

There is only one open loop operational strategy for heuristic scheduling, as shown in Fig. 3.7. Figs. 3.8, 3.9 and 3.10 are the optimal scheduling of 1-1 strategy, 2-1 strategy

and 2-2 strategy respectively, with $K_e = 1,\ K_f = 1$.

In these figures, the first subplot is the front locomotive group speed, rear locomotive group speed and the mean speed of all the cars with respect to the distance from the starting point. The second subplot is maximum and minimum in-train forces and the mean value of the absolute values of all the in-train forces in a specific time with respect to the distance.The third is the steady in-train forces, which are calculated by applying the efforts of the cars to the train model with the reference speed (and the acceleration) maintained and the dynamic process ignored. As can be seen there are dips in the third subplots of these figures when the reference speed changes. This is because the steady-state in-train forces in the third subplots are the calculation results of the algebraic equations. When the reference speed has a step-type change in the algebraic equations, the other variables, such as in-train forces, unavoidably have step-type changes, which results in the dips.

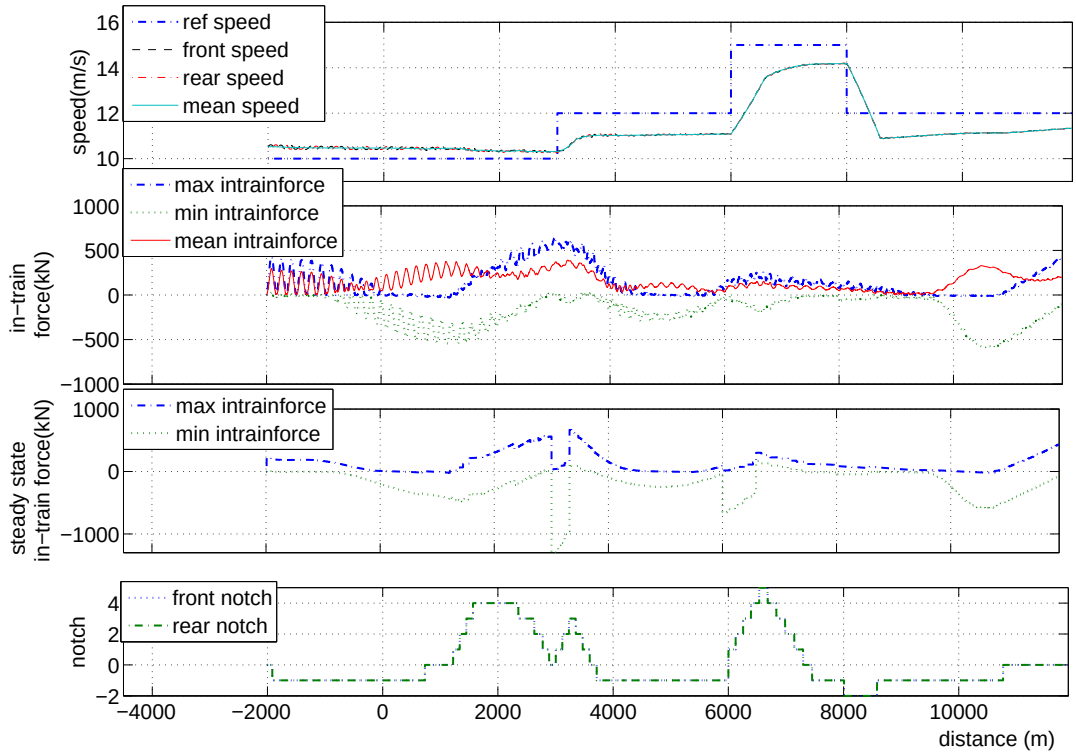

Figure 3.7: Heuristic scheduling

Table 3.5 is the performance comparison of Fig. 3.7 to Fig. 3.10. The variable $|\delta\bar{v}|$ is the absolute value of the difference between the reference velocity and the mean value of all the cars' velocities at a specific point. $\overline{|f_{in}|}$ is the mean value of the absolute values of all the couplers' in-train forces at a specific point. The item E is the energy consumed during travel. The items max, mean and std are the maximum value, mean value and standard deviation of the statistical variable, respectively.

The running results of the open loop scheduling show that the velocity tracking

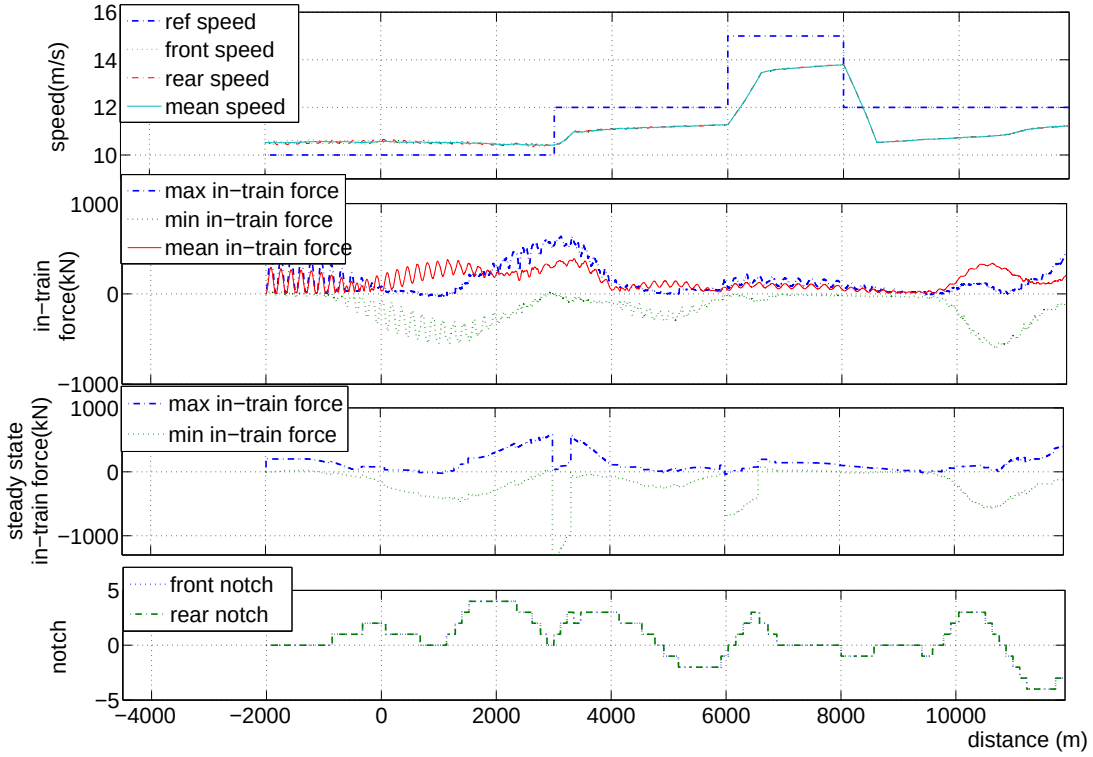

Figure 3.8: 1-1 strategy optimal scheduling

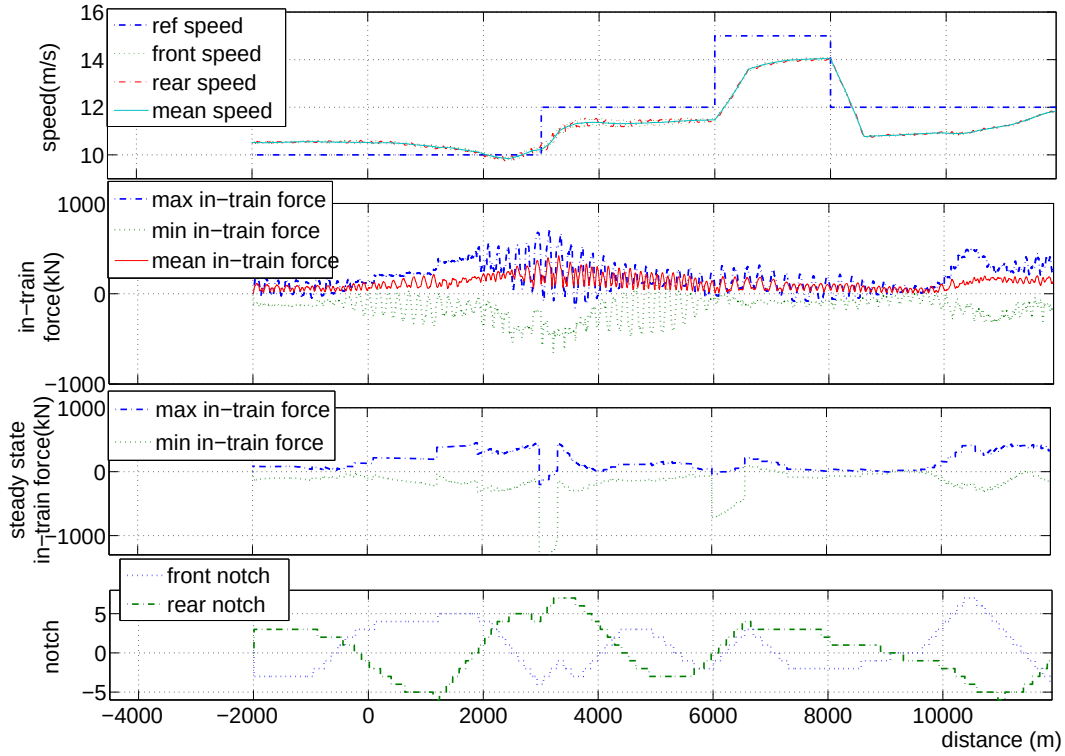

Figure 3.9: 2-1 strategy optimal scheduling

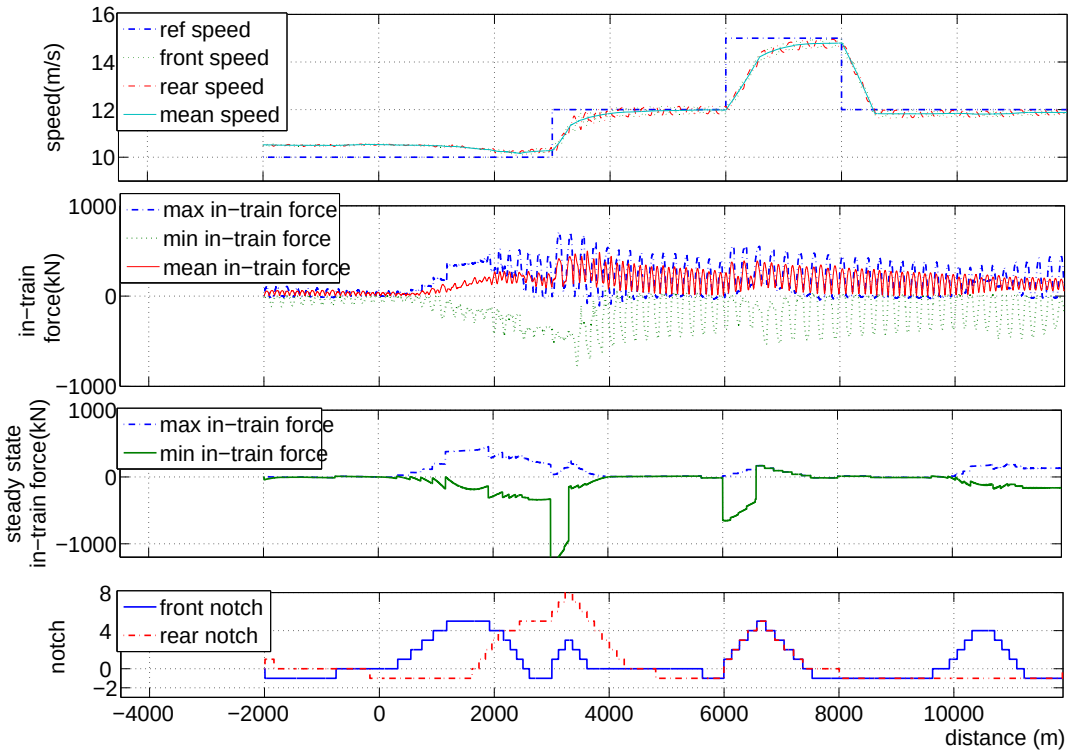

Figure 3.10: 2-2 strategy optimal scheduling

Table 3.5: Comparison of optimal scheduling vs. heuristic scheduling

	$\lvert\delta\bar{v}\rvert$(m/s)			$\overline{\lvert f_{in}\rvert}$(kN)			E
	max	mean	std	max	mean	std	(MJ)
Fig. 3.7	3.9179	0.8225	0.53	390.23	143.85	98.86	8,520
Fig. 3.8	3.7187	0.9410	0.54	392.13	144.81	101.83	11,400
Fig. 3.9	3.5277	0.7460	0.54	420.31	118.51	70.42	23,300
Fig. 3.10	3.0195	0.4152	0.46	498.59	141.43	103.73	16,400

error exists in all the scheduling. The performance of the heuristic scheduling and 1-1 strategy optimal scheduling are similar. The performance of in-train force of 2-2 strategy optimal scheduling is the worst because of oscillation, while its speed tracking error is the smallest. The velocity tracking error and the possibility of oscillation are the drawbacks of an open loop controller.

However, the performance of the steady-state in-train force of the 2-2 strategy optimal scheduling is best. The performance of the steady-state in-train force of 1-1 strategy optimal scheduling is similar to that of heuristic scheduling. The performance of the steady-state in-train force of 2-1 strategy optimal scheduling is also better than that of 1-1 strategy optimal scheduling, except within the acceleration/deceleration periods, where the states of the train change abruptly. Actually, the entire state of the train should change continuously, which leads to smoother change. The open loop scheduling does not consider the real running state, and it is difficult to say which scheduling is best. However, the open loop scheduling provides a reference to the closed-loop controller, so the steady state calculated by the scheduling is more important than the real running result. From this point of view, one can see that the performance of the 1-1 strategy optimal scheduling is similar to that based on heuristic scheduling, and the performance of 2-2 strategy optimal scheduling is best.

3.5 LQR controller

3.5.1 LQR closed-loop controller

With the calculation of open loop scheduling (optimal scheduling or heuristic scheduling), the steady state and input of the train can be denoted as $f^0_{in_j}(x^0_j), v^0_i(v_r), u^0_i, j = 1, \cdots, n-1, i = 1, \cdots, n$, which are the in-train forces (static displacement of coupler), the velocities and the traction forces or braking forces of the cars. The static displacement x^0_j is interpolated from $f^0_{in_j}$. Then one can rewrite the train model with the following equations.

$$\begin{aligned} \delta\dot{v}_s &= (\delta u_s + \delta f_{in_{s-1}} - \delta f_{in_s} - \delta f a_s)/m_s, \qquad s = 1, \cdots, n, \\ \delta\dot{x}_j &= \delta v_j - \delta v_{j+1}, j = 1, \cdots, n-1, \end{aligned} \tag{3.21}$$

where $\delta v_s = v_s - v^0_s = v_s - v_r, \delta u_s = u_s - u^0_s, \delta f_{in_s} = f_{in_s} - f^0_{in_s}, \delta x_j = x_j - x^0_j$. The variable v_r is the reference speed. When the damping of the coupler is ignored, this model can be linearized as follows:

$$\begin{aligned} \delta\dot{v}_s &= (\delta u_s + k_{s-1}\delta x_{s-1} - k_s\delta x_s)/m_s - (c_{1_s} + 2c_{2_s}v_r)\delta v_s, \quad s = 1, \cdots, n, \\ \delta\dot{x}_j &= \delta v_j - \delta v_{j+1}, \quad j = 1, \cdots, n-1, \end{aligned} \tag{3.22}$$

where k_s is the linearized coefficient of the coupler with the assumption $k_0 = 0$. The model can be written as

$$\dot{X} = AX + BU,$$

where $X = [\delta v_1, \cdots, \delta v_n, \delta x_1, \cdots, \delta x_{n-1}]^T$, $U = [\delta u_1, \cdots, \delta u_n]^T$, $A = \begin{bmatrix} A_{11} & A_{12} \\ A_{21} & A_{22} \end{bmatrix}$, $A_{11} = -\text{diag}(c_{1_1} + 2c_{2_1}v_r, \cdots, c_{1_n} + 2c_{2_n}v_r)$, $A_{22} = 0_{(n-1)\times(n-1)}$, $B = \text{diag}(\frac{1}{m_1}, \cdots, \frac{1}{m_n})$.

$$A_{12} = \begin{bmatrix} -\frac{k_1}{m_1} & 0 & \cdots & 0 & 0 \\ \frac{k_1}{m_2} & -\frac{k_2}{m_2} & \cdots & 0 & 0 \\ \cdots & \cdots & \cdots & \cdots & \cdots \\ 0 & \cdots & 0 & \frac{k_{n-2}}{m_{n-1}} & -\frac{k_{n-1}}{m_{n-1}} \\ 0 & \cdots & 0 & 0 & \frac{k_{n-1}}{m_n} \end{bmatrix},$$

$$A_{21} = \begin{bmatrix} 1 & -1 & 0 & \cdots & 0 & 0 \\ 0 & 1 & -1 & \cdots & 0 & 0 \\ \cdots & \cdots & \cdots & \cdots & \cdots & \cdots \\ 0 & 0 & 0 & \cdots & 1 & -1 \end{bmatrix},$$

The variables k_i, $i = 1, \cdots, n-1$ are chosen to be constant. Although different scheduling has different equilibria, the coefficients in the linearized model (3.22) are identical.

In simulation, however, the original nonlinear model has been used for the train model.

When an LQR controller is to be designed with the approach in [16], the performance function is chosen as

$$\begin{aligned} \delta J &= \int (X'QX + U'RU)\, dt \\ &= \int \left(\sum_{i=0}^{n-1} K_f^o \delta x_i^2 + \sum_{i=0}^{n} K_e \delta u_i^2 + \sum_{i=0}^{n} K_v^o \delta v_i^2 \right) dt, \end{aligned} \tag{3.23}$$

where K_f^o, K_e, K_v^o are the weights for in-train forces, energy consumption and velocity tracking, respectively. When the coefficients K_f^o, K_e, K_v^o are chosen so that the first item of (3.23) dominates, the controller is an in-train force emphasized one. When the second item of (3.23) dominates, the controller is an energy emphasized one. It is speed emphasized control if the third item dominates.

Based on the optimization approach [27], one can get feedback control $U = -KX$, and the complete closed-loop control is

$$u = U + u^0. \tag{3.24}$$

3.5.2 Anti-windup technique

Within a closed-loop controller in this thesis, open loop scheduling is used to calculate the inputs when a train is running in its steady state with the reference velocity maintained and the input constraints are not considered in open loop scheduling. Since the

throttle of the locomotives takes discrete values and the braking capacities of the wagons are constrained, when the control inputs u of a closed-loop controller are applied to the train, an anti-windup technique is employed. For the wagons, the application of the anti-windup technique is very simple. For the locomotives, the inputs are discrete with some operation constraints. Similar methods as described in [29] are used to smooth continuous control inputs. Assuming the required force of jth locomotives is F_j and the output of the kth notch with the current velocity v_j is $g(k, v_j)$, the output force F_j^r for the jth locomotives can be defined as

$$\begin{aligned} F_j^r &= g(k, v_j) \quad \text{if} \quad G(k-1, v_j) \le F_j < G(k, v_j), \\ G(k, v) &= g(k, v_j) + \alpha \left(g(k+1, v_j) - g(k, v_j) \right). \end{aligned} \tag{3.25}$$

In (3.25), $G(k, v_j)$ and $G(k-1, v_j)$ are the upper and lower boundaries of the admitted notch k, respectively. The variable α is the ratio of the separation for the boundary. In simulation, α is chosen as 0.5.

3.5.3 Simulation settings of LQR controllers

In simulation, the model parameters of the train, the track profile and the reference speed profile are the same as those in the previous chapter, as well as the locomotive notch operation constraints.

The track profile shown in Fig. 3.1 is from the COALink line, which is typically downhill when the train is loaded. In this section of track, there are also two uphill segments, which make it difficult to drive a long train that may extend over several different gradient sections at any given time. The largest incline degree is 0.09152 and the largest decline one is -0.1, which are very similar to the slope degree (+/- 0.1) in [3].

A piecewise linear function is used to approximate the non-linear function of a coupler. In the controllers one chooses a greater value, namely 3×10^7 N/m for all the couplers' linearized coefficients in (3.22).

A safe-operation requirement for a train on the COALink is that the in-train forces should be less than $\pm 2,000$ kN. In simulation, $\overline{F_{in_i}}, \underline{F_{in_i}}$ are chosen as $1,200$ kN, considering the redundancy for a longer train with 800 wagons.

In the simulation, the weights for in-train force, energy and velocity are K_f, K_e, K_v, respectively, and $K_f^o = 3 \times 10^8 K_f, K_v^o = 5 \times 10^6 K_v$, which gives the same value for the in-train forces, speed deviation and input in (3.23) as would be obtained when $\delta x = 0.01m, \delta v = 0.1$ m/s^2, $\delta u = 200$ N with the weights $K_f = K_e = K_v$.

The acceleration limit a_{rr} is 0.07 m/s^2. This value is calculated on the assumption that the train is running on a flat track and all the traction power of the locomotives is

used to accelerate. The maximum acceleration can be $760 \times 2/(252 \times 2 + 417 \times 50) = 0.07118$ m/s^2. The maximum deceleration is more than the maximum acceleration, but in the simulation they are assumed to be the same for the sake of simplicity.

The initial state of the train is that the train is in its steady state with all the cars' velocities 10.5 m/s and all the in-train forces equal to zero.

3.5.4 Simulation results of LQR controllers

Simulation results of the three different strategies' closed-loop controllers based on the heuristic scheduling and optimal scheduling are shown from Fig. 3.11 to Fig. 3.16, where the weights are $K_f = 1$, $K_e = 1$, $K_v = 1$. The energy consumption in these figures is shown in Table 3.6.

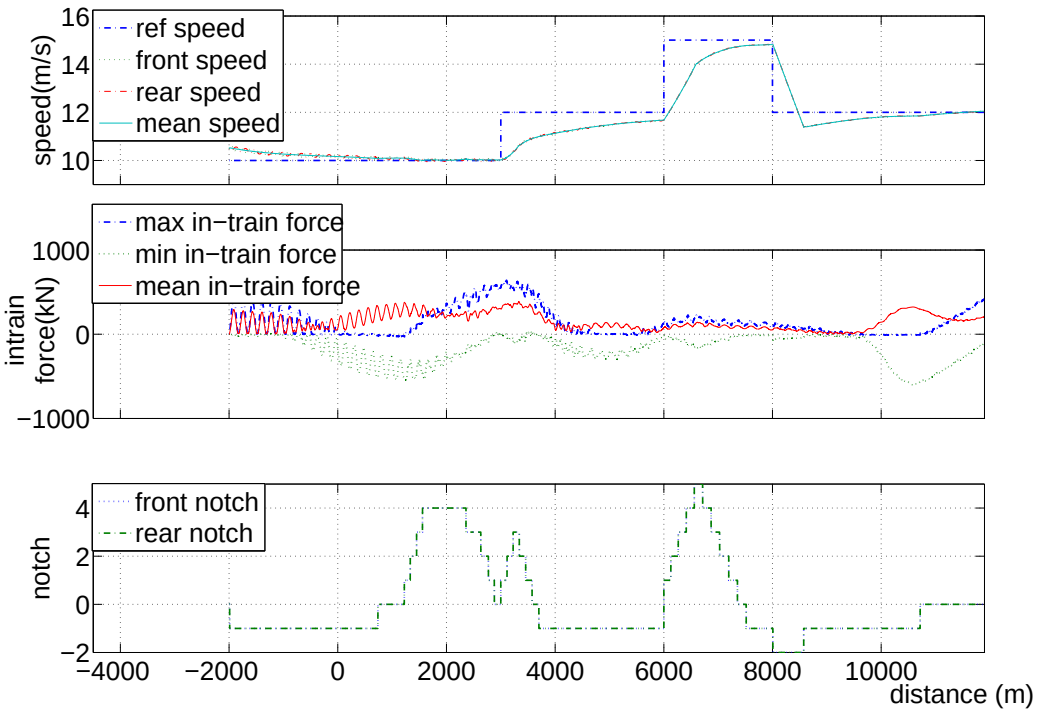

Figure 3.11: 1-1 strategy closed-loop control based on heuristic scheduling

When comparing the figures of the closed-loop controllers with those of the open loop scheduling, it is obvious that the steady velocity error is much smaller and better in closed-loop controllers than in open loop scheduling. For heuristic scheduling, the performances of the in-train force and the energy consumption of the open loop scheduling are similar to those of closed-loop controllers. For optimal scheduling, the performances of the energy consumption with the closed-loop controllers of the three

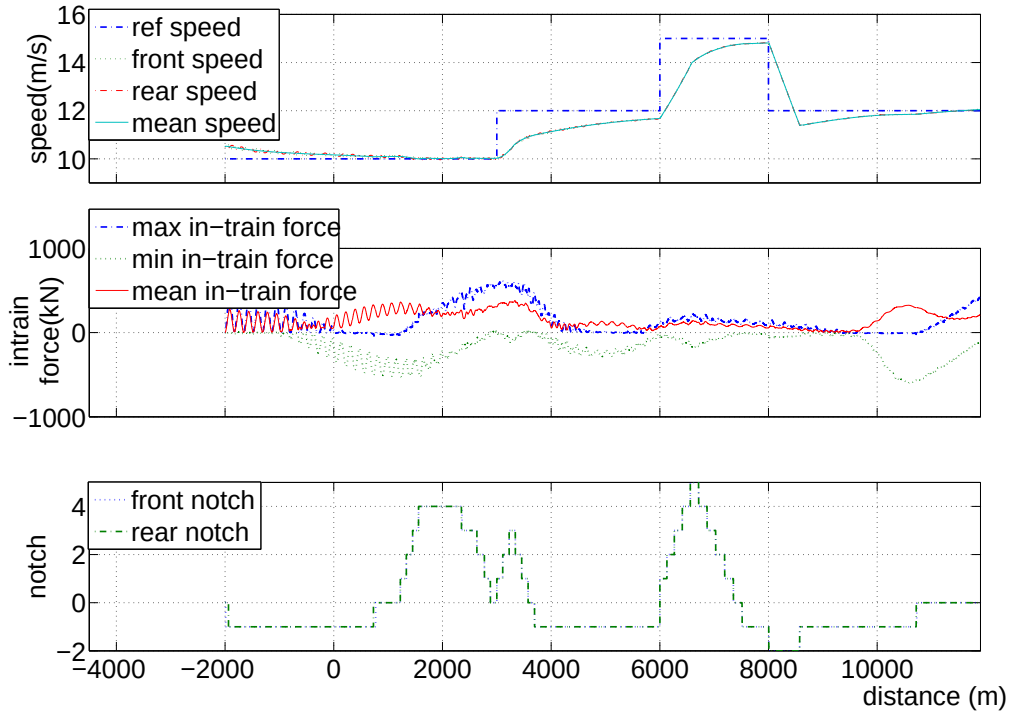

Figure 3.12: 2-1 strategy closed-loop control based on heuristic scheduling

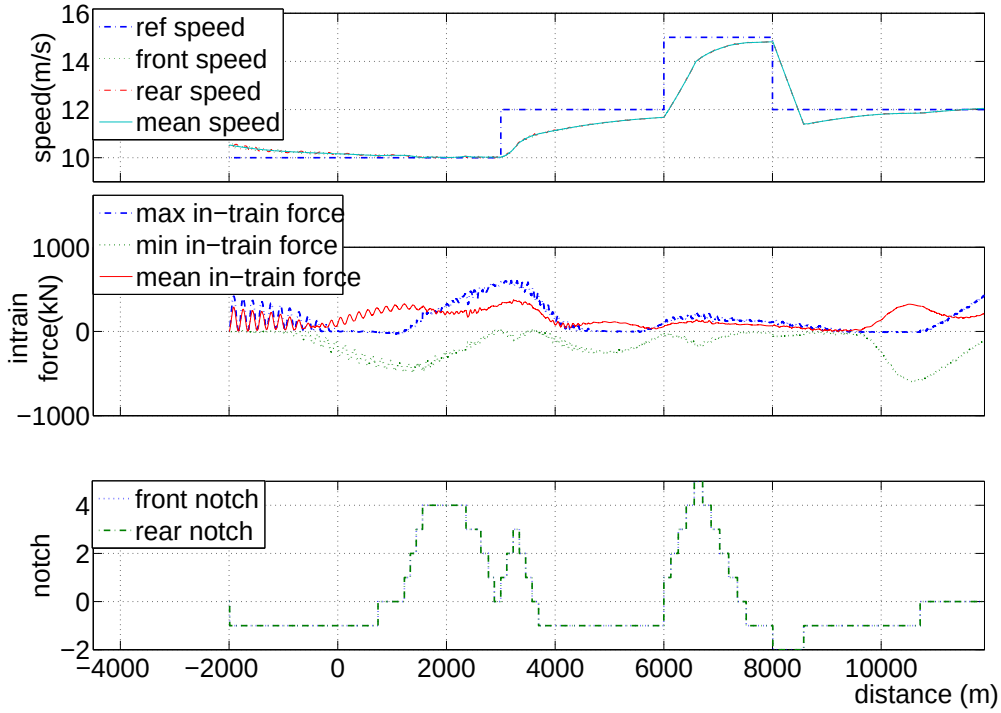

Figure 3.13: 2-2 strategy closed-loop control based on heuristic scheduling

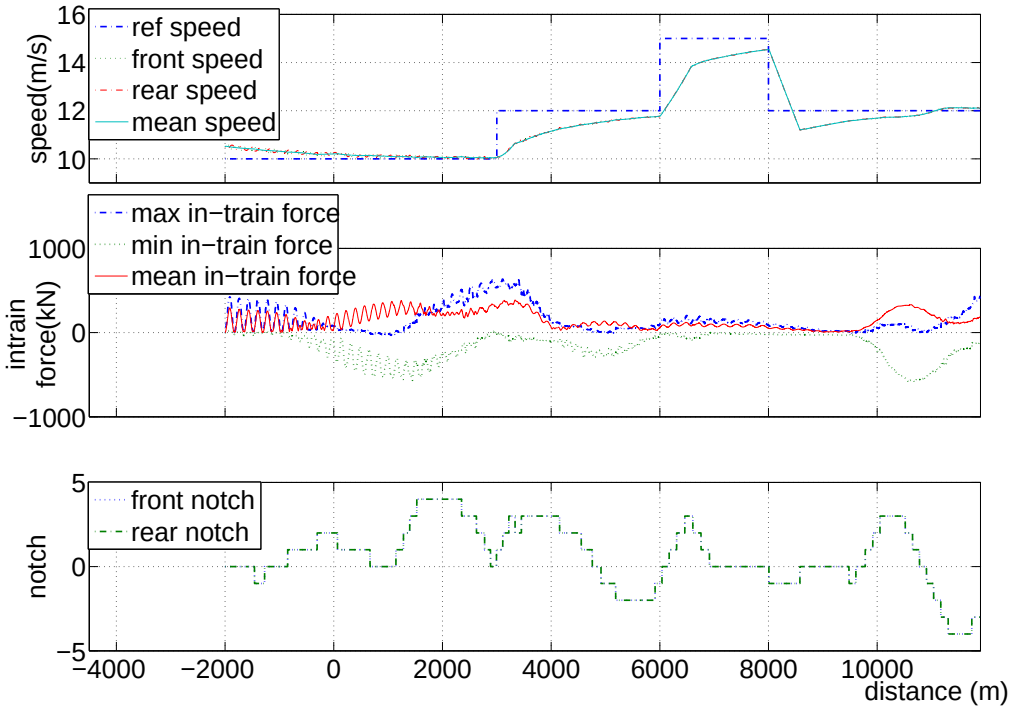

Figure 3.14: 1-1 strategy closed-loop control based on optimal scheduling

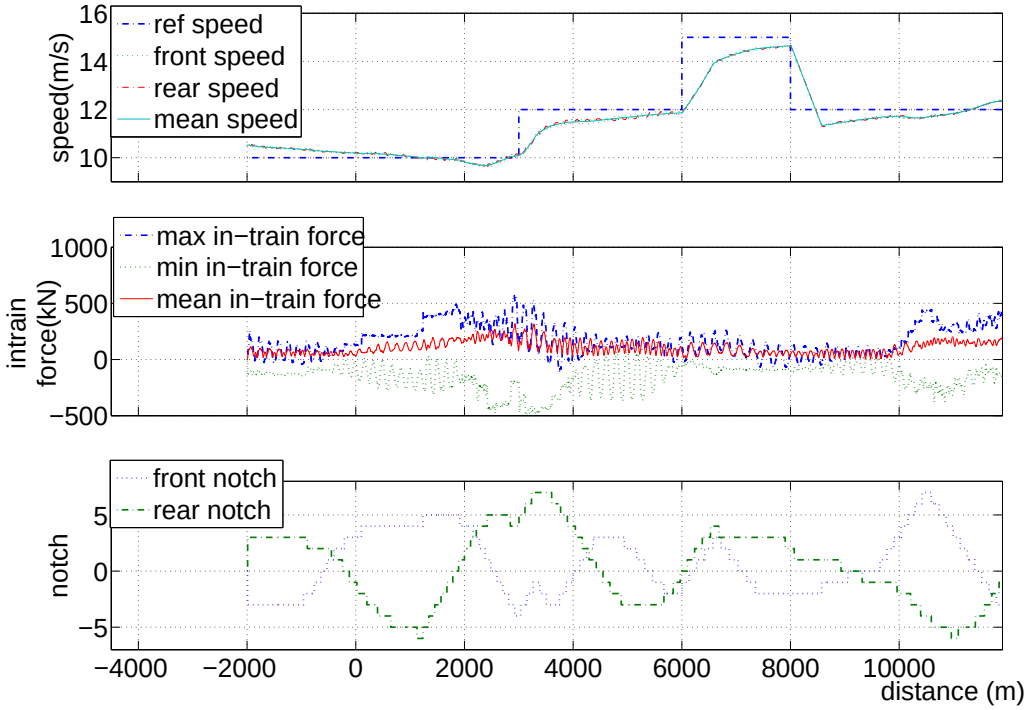

Figure 3.15: 2-1 strategy closed-loop control based on optimal scheduling

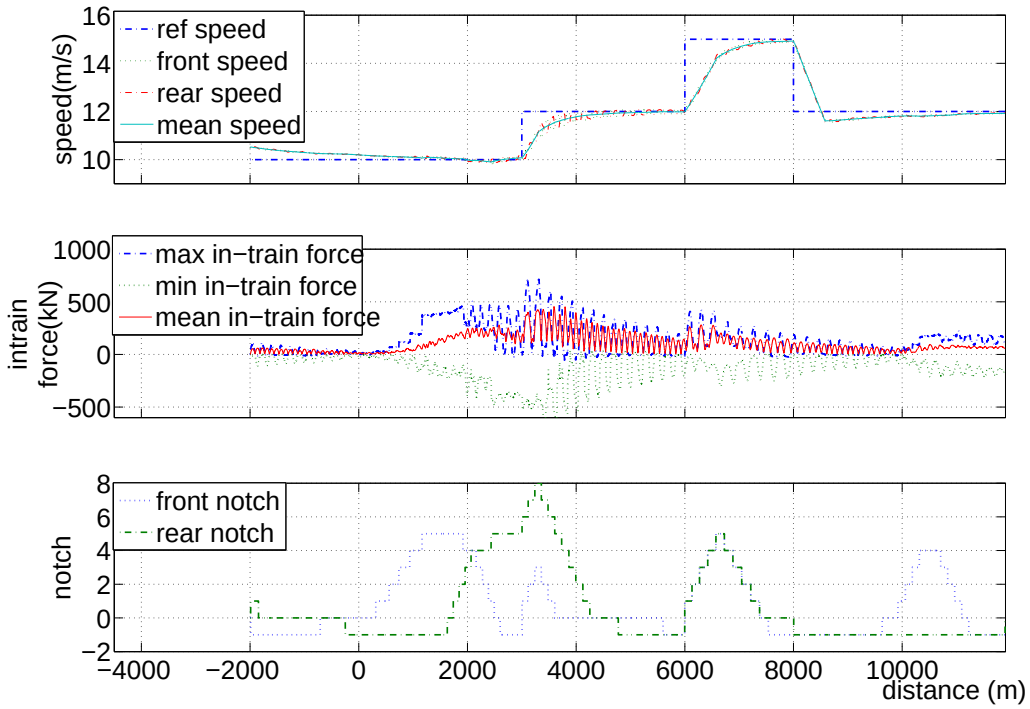

Figure 3.16: 2-2 strategy closed-loop control based on optimal scheduling

strategies are similar to those of the corresponding open loop scheduling. The 2-1 strategy and 2-2 strategy closed-loop control give better in-train force performances than the corresponding scheduling.

When comparing the three different strategies' closed-loop controllers based on heuristic scheduling, the performances are very similar.

When comparing the closed-loop controllers of the three different strategies based on corresponding optimal scheduling, the performances of the velocity and in-train force with the 2-2 strategy are best and those with the 1-1 strategy are worst. The energy consumption with the 1-1 is a little better than that with the 2-2 strategy, which is also a little better than that with the 2-1 strategy.

When comparing the corresponding strategy closed-loop controllers based on optimal scheduling and heuristic scheduling, the energy consumption with the three different strategies based on heuristic scheduling is less than that based on the corresponding optimal scheduling. The performances of the velocity and the in-train force with the 2-2 strategy based on optimal scheduling are better than those based on heuristic scheduling. The performance of the velocity with the 1-1 strategy based on optimal scheduling is worse than that based on heuristic scheduling, while the performances of the in-train force based on the two scheduling approaches are similar. The performances of the velocity with the 2-1 strategy based on the two scheduling approaches are similar and

the performance of in-train force with the 2-1 strategy based on optimal scheduling is better than that based on heuristic scheduling.

From the above comparison, it can be seen that the performances of the in-train force and the velocity with the 2-2 strategy based on optimal scheduling are best. In this strategy, it is very interesting to see, as depicted in Fig. 3.16, the variation of the traction efforts of the front and rear locomotives (groups) when the train travels from 0 m to 4,000 m and from 9,500 m to 11,000 m; those sections are hills in the track. When the front locomotives (groups) are climbing uphill and the rear ones are driving downhill, the front locomotives make increasing traction efforts and the rear ones are braking. When more and more cars are climbing uphill, the rear locomotives begin to make traction efforts, increasing gradually. When the front locomotives pass the top of the hill and begin to drive down, their efforts begin to decrease and the rear ones increase their efforts gradually. When the front locomotives are driving downhill and the rear ones are climbing uphill, the front ones are braking and the rear ones make traction efforts. At 3,000 m, the train begins to accelerate from 10 m/s to 12 m/s. The front and rear locomotives begin to increase their traction efforts simultaneously, which can also be seen from distance points 6,000 m and 8,000 m. That is consistent with common sense.

Table 3.6: Performance with $K_e = 1, K_f = 1, K_v = 1$

	$\|\delta\bar{v}\|$(m/s)			$\overline{\|f_{in}\|}$(kN)			E
	max	mean	std	max	mean	std	(MJ)
C01	3.3241	0.4573	0.58	386.94	145.82	100.27	8,700
C02	3.3244	0.4539	0.57	376.78	145.30	99.32	8,610
C03	3.3241	0.4613	0.58	373.60	144.45	97.50	8,470
C1	3.2274	0.4992	0.56	387.04	147.52	102.65	11,760
C2	3.1405	0.4585	0.53	318.97	106.16	59.35	22,100
C3	3.0182	0.3166	0.48	454.50	97.40	86.44	16,500

Table 3.7: Performance with $K_e = 1, K_f = 1, K_v = 10$

	$\|\delta\bar{v}\|$(m/s)			$\overline{\|f_{in}\|}$(kN)			E
	max	mean	std	max	mean	std	(MJ)
C01	3.0412	0.3062	0.55	394.39	145.72	99.57	8,620
C02	3.0413	0.3080	0.55	394.50	144.54	100.07	8,550
C03	3.0412	0.3085	0.55	369.24	144.61	96.63	8,586
C1	3.0070	0.3372	0.57	382.57	147.38	102.40	11,100
C2	2.9891	0.3629	0.53	344.95	103.57	67.20	21,800
C3	3.0225	0.2443	0.50	408.70	74.07	76.34	16,500

Tables 3.6, 3.7, 3.8 and 3.9 are the simulation results of the six closed-loop controllers with different weights in the performance function for the in-train force, the energy consumption and the velocity tracking. Table 3.6 is the performance comparison of Fig.s from 3.11 to 3.16. In these tables, C01, C02 and C03 are 1-1 strategy, 2-1

Table 3.8: Performance with $K_e = 1, K_f = 10, K_v = 1$

	$\lvert\delta\bar{v}\rvert$(m/s)			$\overline{\lvert f_{in}\rvert}$(kN)			E
	max	mean	std	max	mean	std	(MJ)
C01	3.3251	0.4611	0.57	385.83	146.17	100.43	8,790
C02	3.3234	0.6609	0.57	377.25	145.96	98.68	8,610
C03	3.3243	0.4604	0.58	368.28	144.61	96.40	8,460
C1	3.2663	0.5312	0.58	384.58	147.53	101.76	11,460
C2	3.1379	0.4542	0.52	331.48	105.82	62.57	22,300
C3	3.0090	0.3670	0.47	405.70	70.77	78.04	15,000

Table 3.9: Performance with $K_e = 100, K_f = 1, K_v = 1$

	$\lvert\delta\bar{v}\rvert$(m/s)			$\overline{\lvert f_{in}\rvert}$(kN)			E
	max	mean	std	max	mean	std	(MJ)
C01	3.8039	0.7383	0.56	392.08	145.01	99.50	8,795
C02	3.8056	0.7361	0.56	389.83	146.27	99.24	8,600
C03	3.8041	0.7415	0.56	386.49	144.19	99.08	8,560
C1	3.6744	0.6889	0.57	390.46	143.61	101.44	9,550
C2	3.4603	0.6388	0.53	300.06	110.47	61.90	16,800
C3	3.247	0.4918	0.47	297.27	78.90	63.27	13,400

strategy and 2-2 strategy closed-loop controllers based on heuristic scheduling, and C1, C2 and C3 are 1-1 strategy, 2-1 strategy and 2-2 strategy closed-loop controllers based on optimal scheduling. $|\delta\bar{v}|$ is the absolute value of the difference between the reference velocity and the mean value of all the cars' velocities at a specific point. The variable $\overline{|f_{in}|}$ is the mean value of the absolute values of all the couplers' in-train forces at a specific point. The item E is the energy consumed during travel. The items max, mean and std are the maximum value, mean value and standard deviation of the statistical variable, respectively.

From these tables, it can be seen that the three strategies based on heuristic scheduling have similar performances. This is because their scheduling is the same. However, based on optimal scheduling, the 2-2 strategy yields a better performance in terms of velocity, in-train force and energy consumption than the 2-1 strategy with the same parameters. The performance of velocity in Table 3.7, which is with the velocity emphasized optimal parameters, is the best compared with the corresponding operational strategy of the other tables. The performance of the in-train force based on heuristic scheduling of the corresponding operational strategy is approximate in the four tables, while the performance of the in-train force based on optimal scheduling is best in Table 3.8, which is with the in-train force emphasized parameters, but only the improvement of the 2-2 strategy is obvious and that of the other two is only approximate. In Table 3.9, with the energy consumption emphasized parameters, the performance of energy consumption with all the corresponding controllers based on optimal scheduling, is the best among the four tables. On the whole, local optimization does work and leads to

global optimization in some degree.

From simulation, it is shown that the train tracks the reference speed quickly when the reference speed changes and tracks the reference speed very well when the train is cruising. So the track length is enough for simulation of the driving profile. On a longer track, the same result can be reached, which will be shown in the next chapter. However, it should be pointed out that when the objective is to test the optimization combination of a driving profile and a reference speed profile, a longer track might be necessary.

Based on the observation of the 2-2 strategy, another approach to controller design is proposed in the following chapter by assuming only the locomotives' speed measurement. Performance comparisons are detailed further in the following chapter.

3.6 Conclusion

This chapter emphasizes open loop scheduling for the handling of heavy haul trains, which constitutes a basic problem about the trim point. In this chapter the cascade-mass-point model is adopted for a long heavy haul train. Three control strategies are proposed and then followed by the open loop optimal scheduling algorithms for them. Simulation results of these control strategies for a traditional heavy haul train and a train equipped with an ECP braking system are shown. It is noticed that ECP braking systems show superb performance compared with pneumatic braking systems.

Optimal scheduling and heuristic scheduling in [15] are compared when they are applied to trains equipped with ECP braking systems. It is shown that optimal scheduling can improve performance and the ECP/iDP is the best of the three strategies. A closed-loop controller based on an LQR approach is used to verify the result.

Chapter 4

Speed regulation

4.1 Introduction

In the previous chapter, optimal scheduling shows a better start for the design of a closed-loop controller for train handling. An LQR closed-loop controller is designed to verify the advantage of optimal scheduling. However, the closed-loop controller is based on full state feedback, which is not practical in train handling to measure all states. If partial states are measured, an observer can be designed to supplement the LQR controller. This is, however, not the approach employed in this chapter. Instead, output regulation with measurement feedback is adopted for the full ECP/iDP mode subject to the assumption that only speed measurement of locomotives is available: while optimality is retained in open loop control design, closed-loop control is done by employing a nonlinear system regulator theory.

In this chapter, the output regulation of nonlinear systems with measured output feedback is first formulated and solved for the global version and the local version. Then the result of the local version is applied to train control. The simulation result shows the feasibility of such a speed regulator with only measurement of the locomotives' speeds, in terms of its simplicity, cost-effectiveness and its implementation convenience.

4.2 Output regulation with measured output feedback

The output regulation problem in linear systems has been studied in [30, 31, 32]. The internal model principle is proposed in [30], enabling the conversion of output regulation problems into stabilization problems. The details on the solvability of the problem can

be found in [31, 32].

The internal model principle is extended to nonlinear systems in [33], which shows that the error-driven controller of the output tracking necessarily incorporates the internal model of the exosystem. The conditions of the existence of regulators for nonlinear systems are detailed for different kinds of exosystems with bounded signals in [34, 35, 36]. The necessary and sufficient conditions are given in [37] for the local output regulation problem of nonlinear systems, which is the solvability of regulator equations. With an assumption added to the conditions in [37], the results in [37] have been improved in [38]. A differential vector space approach is used in [39] to develop solutions of state feedback for nonlinear systems with both bounded and unbounded exogenous signals. An approach for robust local output regulation problems is presented in [40] in a geometric insight. In [41], an output regulation problem of a class of single-input single-output (SISO) nonlinear systems is reformulated into an output feedback stabilization problem.

The robust version of output regulation problem of nonlinear systems with uncertain parameters is studied in [42]. Furthermore, the output regulation problem of nonlinear systems driven by linear, neutrally stable exosystems with uncertain parameters is presented in [72], in terms of the parallel connection of a robust stabilizer and an internal model, which has recently been in [73]. Recently, the concept of the steady-state generator has been advanced in [43] as well as that of the internal model candidate. Based on these dynamic systems, a framework for global output regulation of nonlinear systems with autonomous exosystems is proposed in [43] for bounded signals, in [44] for unbounded signals, and in [47] for nonlinear exosystems. The frameworks are in the form of output feedback or plus (partial) state feedback.

All the controller design approaches in these papers cannot be extended directly to the form of measurement (measured output) feedback. Measurement feedback is considered in this chapter instead of the output feedback, because generally the measurable output is different from the output to regulate. For example in this study, in the handling of heavy-haul trains, the outputs to be regulated are all the cars' speeds; however, only part of the speeds (for example, the first and last locomotives' speeds) can be practically measured. On the other hand, the measurable output covers the form of the output or output plus (partial) state, as considered in [44].

In the above papers, an important idea is to design an internal model to eliminate the effect of the unknown states of the exosystem. In the controllers of [37] for the local version of output regulation problem, the internal model is given together with the stabilizer directly. In the global version, it is proposed in [43] and [44] firstly to design an internal model candidate, and thus the solvability of the output regulation problem is transformed into the solvability of the stabilization problem. This is a very smart technique to deal with the output regulation problem. The internal model candidates incorporate the output (or plus [partial] state, dependent on the measurability of the state) and the input to design. It does not incorporate the information of the stabilizer,

which will be known in the controller. In this chapter, another approach is proposed to solve output regulation problems. Similar to [43] and [44], an output regulation problem is transformed into a stabilization problem of a simplified system with the assumption that the states of the exosystem are known, and a stabilizer is designed for it. It will be shown that the existence of the stabilizer is sometimes necessary for the solvability of the output regulation problem. Then an internal model *with respect to the stabilizer* for the original system is constructed. Specifically, the internal model can incorporate the information of the stabilizer. This approach is more natural than the ones in [43] and [44], where the internal model is a prerequisite and first designed. It can be seen that the existence of the internal model is sometimes not necessary. However, the existence of the stabilizer is necessary when the output zeroing manifold is unique, which is the case in all the examples given in [43, 44] and examples 1, 2 and 4 in this chapter.

The definition of the output regulation problem of nonlinear systems in [44] is borrowed, but the feedback is in the form of measurement feedback. A stabilizer for the simplified system is firstly designed. Then with respect to the stabilizer, an internal model is constructed to estimate the exosystem states. If successful, the output regulation problem is solved. In this study, the exosystem may be linear or nonlinear, the signals of which may be bounded or unbounded. The results for both the global version and the local version of dynamic measurement feedback output regulation problem (DMFORP) are reported.

4.2.1 Problem formulation and preliminaries

In this chapter, as well as in the subsequent chapter, extensive use of the differential geometric concepts and notations will be made to show the application of two most recent nonlinear control techniques in the case of heavy haul trains. The prerequisite for these two chapters are [45] and [46], A. Isidori's classic books.

Consider a nonlinear system,

$$\begin{aligned} \dot{x} &= f(x,u,w), \\ \dot{w} &= s(w), \\ e &= h(x,w), \\ y_m &= h_m(x,w). \end{aligned} \tag{4.1}$$

The first equation describes the original system, with state $x \in X \subset R^n$, and input $u \in U \subset R^m$. The second one defines an exosystem, with state $w \in W$ with $W \in R^s$ a compact set. The exosystem models the class of disturbance and/or reference signals taken into consideration. The third one is the error equation. The fourth one is the measured output $y_m \in R^{p_m}$. The vector fields $f(x,u,w)$ and $s(w)$ are smooth, and the mappings $h(x,w)$ and $h_m(x,w)$ are smooth, too.

It is assumed that $f(0,0,0) = 0$, $s(0) = 0$, $h(0,0) = 0$, *i.e.*, the system (4.1) has the equilibrium state $col(x,w) = col(0,0)$ for $u = 0$ with zero track error $h(0,0) = 0$.

Before the problem is formulated, some concepts in [45, 46] are stated firstly.

A continuous function $f : [0,a) \to [0,+\infty)$ is a class-$\mathcal{K}$ function if $f(0) = 0$ and it is strictly increasing.

A continuous function $f : [0,+\infty) \to [0,+\infty)$is a class-$\mathcal{L}$ function if it is decreasing and

$$\lim_{t\to\infty} f(t) = 0.$$

The function $f(r,s)$ is a class-$\mathcal{K}L$ function if $f(\cdot,s) \in \mathcal{K}$ for all $s \geq 0$, and $f(r,\cdot) \in \mathcal{L}$ for all $r \geq 0$.

The equilibrium $x = 0$ of the system $\dot{x} = f(x)$ with $f(0) = 0$ is said to be globally (locally) asymptotically stable in the sense of $\mathcal{K}L$ functions if from any initial state $x_0 \in R^n$ (some initial state $x_0 \in X$ with $X \subset R^n$ through the origin), the solution of system satisfies $\|x\| \leq \varrho(\|x_0\|, t)$ for some class-$\mathcal{K}L$ functions $\varrho(\cdot,\cdot)$.

A system of $\dot{x} = f(x,u), y = h(x)$, with $f(0,0) = 0$ is said to be globally (locally) stabilizable if there exists a control law $\dot{z} = \eta(z,y), u = \vartheta(z,y)$ satisfying $\eta(0,0) = 0, \vartheta(0,h(0)) = 0$ so that the origin of the closed-loop system $\dot{x} = f(x,\vartheta(z,h(x))), \dot{z} = \eta(z,h(x))$ is globally (locally) asymptotically stable in the sense of $\mathcal{K}L$ functions.

The dynamic measurement feedback output regulation problem of the system (4.1) considered here is to design a controller, in the form of

$$\begin{aligned} u &= \vartheta(z, y_m), \\ \dot{z} &= \eta(z, y_m). \end{aligned} \tag{4.2}$$

An advantage of a controller in the form of (4.2) is that it depends only on the current values of the measured variables, instead of differentiated signals of the measured variables, as introduces noise, and stably filtered signals of the measured variables. As a result, the closed-loop system can be written as

$$\begin{aligned} \dot{x}_c &= f_c(x_c, w), \\ \dot{w} &= s(w), \\ e &= h_c(x_c, w), \\ y_m &= h_{m_c}(x_c, w), \end{aligned} \tag{4.3}$$

where $x_c = col(x,z)$, $f_c(x_c,w) = col(f(x,\vartheta(z,y_m),w),\eta(z,y_m))$, $h_c(x_c,w) = h(x,w)$, $h_{m_c}(x_c,w) = h_m(x,w)$.

The formulation of the output regulation problem involves two requirements from the closed-loop system (4.3). One is the asymptotical convergence to zero of the error output, that is,

P1
$$\lim_{t\to\infty} e(t) = \lim_{t\to\infty} h(x(t), w(t)) = 0.$$

This property reflects the objective of the output regulation problem.

The other one is the internal stability of the closed-loop system (4.3). The system (4.3) is said to be globally (locally) asymptotically stable, irrespective of w, when for all $w(0) \in W$ with W any (a) compact set (containing the origin), the subsystem, parameterized by w, of the first equation of the system (4.3) is globally (locally) asymptotically stable in the sense of $\mathcal{KL}$ functions.

When the local version of the output regulation problem is considered, assuming the exosystem is Poisson stable at the origin (neutrally stable), the internal stability is given in [37] by

P2 the equilibrium of the closed-loop system (4.3) with $w = 0$ is asymptotically stable (or exponentially stable).

Actually, this property guarantees the boundedness of the trajectories of the closed-loop system with sufficiently small exosystem signals. But once the signals of the exosystem are large, the boundedness may not be kept [44].

Example Consider the following system

$$\begin{aligned} \dot{x}_1 &= -x_1 + v, \\ \dot{x}_2 &= -x_2 + x_2 w, \\ \dot{w} &= 0, \\ e &= x_1 - w. \end{aligned} \tag{4.4}$$

The solution is

$$\begin{aligned} x_1 &= (x_1(0) - w)e^{-t} + w, \\ x_2 &= x_2(0)e^{(-1+w)t}, \\ e &= (x_1(0) - w)e^{-t}. \end{aligned} \tag{4.5}$$

It is easy to check that the condition P2 is satisfied, but when $w > 1$, the state x_2 approaches infinity. So P2 cannot be used for the global version of output regulation problem. The internal stability of a global version of output regulation problem is given in [43] as

P3 for all $w \in W$ with W any compact set, the trajectories of the closed-loop system (4.3) starting from any initial state x_{c_0} exist and are bounded for all $t > 0$.

This interpretation of internal stability is meaningful if the states of the exosystem are bounded. When they are unbounded, the condition is modified [44] as the following two properties:

P4 for all $w_0 \in W$, there exists a sufficiently smooth functions $\pi_c(w)$ with $\pi_c(0) = 0$ satisfying

$$\begin{aligned} \frac{\partial \pi_c(w)}{\partial w} s(w) &= f_c(\pi_c(w), w), \\ 0 &= h_c(\pi_c(w), w). \end{aligned} \tag{4.6}$$

P5 for all $w_0 \in W$, $x_c = \pi_c(w)$ of the closed-loop system of (4.3) is globally asymptotically stable, irrespective of w, in the sense of some class $\mathcal{KL}$ functions.

The property P4 actually defines an invariant flow for the closed-loop system (4.3), on which the output error is exactly zero. The property P5 is about the asymptotical convergence of the invariant flow. From any initial state, the trajectories will converge to the invariant flow.

When the exosystem is neutrally stable, a closed-loop system satisfying properties P4 and P5 satisfies the properties P1 and P2.

If the P4 is fulfilled, then there exists an invariant manifold $x_c = \pi_c(w)$, on which the output is exactly zero. And for $\pi_c(0) = 0$, and from P5

$$\|x_c - \pi_c(w)\| \leq \varrho(\|x_c(0) - \pi_c(w_0)\|, t)$$

for some class-$\mathcal{KL}$ functions $\varrho(\cdot, \cdot)$, one has $\|x_c\| \leq \varrho(\|x_c(0)\|, t)$ when $w = 0$. Thus the asymptotical stability of P2 is satisfied. With the continuity of the output $h(x, w)$, $x_c \to \pi_c(w)$ as $t \to 0$, and w is bounded, P1 is satisfied. So the property P2 can be interpreted by

P4' for some compact set W through the origin, there exists sufficiently smooth functions $\pi_c(w)$ with $\pi_c(0) = 0$ satisfying the equations of (4.6).

P5' the equilibrium $x_c = \pi_c(w(t))$ of the closed-loop system (4.3) is locally asymptotically stable, irrespective of w, in the sense of $\mathcal{KL}$ functions.

It is pointed out that the asymptotical stability in the sense of $\mathcal{KL}$ functions is more general than the exponential stability. So the properties P4' and P5' are more general than the requirement P2 in [37].

The properties P4 and P5 are also sufficient conditions for the property P3 when the exosystem is Poisson stable. Because the $\pi_c(w)$ is bounded, and from the asymptotically stability, the state $x_c(t)$ is also bounded.

The global DMFORP is to find, if possible, a controller in a form (4.2) that allows the closed-loop system (4.3) to satisfy the properties P1, P4 and P5 for any compact set $W \subset R^s$.

The local DMFORP is to find, if possible, a controller in a form (4.2) that allows the closed-loop system (4.3) to satisfy P1, P4' and P5' for a compact set $W \subset R^s$ through the origin.

In the problem formulation, measurement feedback, instead of output feedback, is considered because the measured output is usually different from the output to regulate, and measurement feedback is more universal than output or plus (partial) state feedback. If measured output is the output error to regulate, then measurement feedback is output feedback. If it is just partial output, the feedback is in the form of partial output feedback, as in *example 1*. If the measurement includes the (partial) state, then the feedback includes (partial) state feedback. It is common for the measurement to be completely different from the output or/and state. When only measurement feedback can be used, such as in *example 2 and example 3*, the output regulation problem cannot be solved with output feedback or plus partial state feedback.

Remark 1 *The zeroing output is guaranteed by the property P1. The properties P4 and P5 usually imply P1. However, when the state of exosystem is unbounded, the output cannot be definitely zero sometimes, which can be seen in [44].*

Remark 2 *The exosystem considered in this study is given as $\dot{w} = s(w)$. In the global version of DMFORP, the exosystem may be Poisson stable or not, linear or nonlinear, bounded or unbounded. However, in the local version, the exosystem is required to be neutrally stable.*

Remark 3 *Even though the exosystem may be unbounded in global version, a constraint should be put on the exosystem. The state of the exosystem should not vary too quickly. This is because in that case it is difficult to design an observer to estimate or track the state of the exosystem $\dot{w} = s(w)$.*

4.2.2 Assumptions

In this chapter, one makes some assumptions. The first one is as follows:

A1 There exist sufficiently smooth functions $\pi(w)$ and $c(w)$ with $\pi(0) = 0$ and $c(0) = 0$, for all $w \in R^s$, satisfying,

$$\begin{aligned} \frac{\partial \pi(w)}{\partial w} s(w) &= f(\pi(w), c(w), w), \\ 0 &= h(\pi(w), w). \end{aligned} \tag{4.7}$$

Remark 4 *The above assumption is a standard one. It is a necessary condition for the solvability of the output regulation problem [37]. The equation* (4.7) *is called regulator equation.*

With this assumption, the original system can be written as the following (called *simplified system*) with the coordinate change $\bar{x} = x - \pi(w)$, $\bar{u} = u - c(w)$,

$$\begin{aligned} \dot{\bar{x}} &= \bar{f}(\bar{x}, \bar{u}, w), \\ y_m &= \bar{h}_m(\bar{x}, w), \end{aligned} \tag{4.8}$$

where $\bar{f}(\bar{x}, \bar{u}, w) = f(\bar{x} + \pi(w), c(w) + \bar{u}, w) - f(\pi(w), c(w), w)$, $\bar{h}_m(\bar{x}, w) = h_m(\bar{x} + \pi(w), w)$.

Furthermore, one makes another assumption.

A2 The above simplified system is globally stabilizable, irrespective of w, by a controller in the form of measurement feedback.

With this assumption, there exists a (dynamic) measurement feedback stabilizer in the form of

$$\begin{aligned} \dot{z}_1 &= \eta_1(z_1, y_m, w), \qquad & \eta_1(0, \bar{h}_m(0, w), w) = 0, \\ \bar{u} &= \psi_1(z_1, y_m, w), \qquad & \psi_1(0, \bar{h}_m(0, w), w) = 0, \end{aligned} \tag{4.9}$$

with which the equilibrium $col(\bar{x}, z_1) = col(0, 0)$ of the closed-loop simplified system composed of (4.8) and (4.9), for any $w \in W$, is globally asymptotically stable, irrespective of w, in the sense of $\mathcal{K}L$ functions.

Remark 5 *The assumption A2 is also necessary for the solvability of the output regulation problem on the zeroing output manifold* $\{(x, w) \mid x = \pi(w), w \in W\}$. *It is obvious that in this case, the state of the exosystem is assumed to be known. This is a middle case between full information feedback and output feedback [37], where the measurement is the output.*

The necessity is as follows:

Lemma 6 *If the global output regulation problem is solvable with a unique output zeroing manifold* $\{(x,w)|x=\pi(w), w\in W\}$*, then there must exist a stabilizer in the form of* (4.9) *such that for any* $w\in W$*, the equilibrium* $col(\bar{x},z_1)=col(0,0)$ *of the closed-loop simplified system is globally asymptotically stable, irrespective of* w*, in the sense of* $\mathcal{KL}$ *functions.*

Proof: Assume the condition P4 is satisfied, then there exists sufficiently smooth function $col(x,z)=\pi_c(w)=col(\pi(w),z^*(w))$ satisfying

$$\begin{aligned}\frac{\partial\pi(w)}{\partial w}s(w)&=f(\pi(w),\vartheta(z^*(w),h_m(\pi(w),w)),w),\\ \frac{\partial z^*(w)}{\partial w}s(w)&=\eta(z^*(w),h_m(\pi(w),w),w)\\ 0&=h(\pi(w),w).\end{aligned}$$

Choosing

$$\begin{aligned}z_1&=z-z^*(w),\\ \bar{x}&=x-\pi(w),\\ c(w)&=\vartheta(z^*(w),h_m(\pi(w),w)),\\ \psi_1(z_1,y_m,w)&=\vartheta(z_1+z^*(w),y_m,w)-c(w),\\ \eta_1(z_1,y_m,w)&=\eta(z_1+z^*(w),y_m)-\eta(z^*(w),h_m(\pi(w),w)),\end{aligned}$$

one has the equation of (4.9) and the system (4.8).

Furthermore if the condition P5 is fulfilled, i.e, for all $w_0\in W$, the trajectories of the closed-loop system (4.3) starting from any initial state $x_c(0)$ exist for all $t>0$, and satisfying

$$\|x_c(t)-\pi_c(w(t))\|\le\varrho(\|x_c(0))-\pi_c(w0)\|,t),$$

which can be written as $\|col(\bar{x},z_1)\|\le\varrho(\|col(\bar{x}_0,z_{1_0})\|,t)$.

Thus the equilibrium $col(\bar{x},z_1)=col(0,0)$ of the closed-loop simplified system composed of (4.8) and (4.9), is globally asymptotically stable, irrespective of w, in the sense of $\mathcal{KL}$ functions.

Remark 7 *The above necessity is true when the original system has a unique output zeroing manifold. It is not difficult to give some conditions under which the output zeroing manifold is unique. For example, if the maximal output zeroing manifold of* (4.1) *takes the form* $N^*=\{x-\phi(w)=0\}$ *for some smooth functions* $\phi(w)$*, then uniqueness is guaranteed. This, together with more general cases, are under separate study. It is nevertheless worth noting that all examples given in [43, 44] and* Example 1, 2 *and* 4 *given in this chapter admit unique output zeroing manifolds. When the original system has more than one output zeroing manifold, there are more than*

one corresponding simplified system. The existence of the stabilizer for one simplified system may be unnecessary for the solvability of DMFORP. However, if the DMFORP is solvable on a specific output zeroing manifold, there must exist a stabilizer for the corresponding simplified system. It is demonstrated in Example 3.

For the observability of the states of the exosystem, one makes the following assumption.

A3 there exist mappings $\theta(w) : R^s \to R^d, \alpha : R^d \to R^d, \beta : R^d \to R^s$ satisfying

$$\begin{aligned} \frac{d\theta(w)}{dt} &= \alpha(\theta(w)), \\ w &= \beta(\theta(w)). \end{aligned} \tag{4.10}$$

Remark 8 *The dynamic system of* (4.10) *is very similar to the definition of the steady-state generator in [43]. The difference is that the output of* (4.10) *is exactly the state of the exosystem while it is the steady input or input plus (partial) state of the original system of* (4.1) *in [43] and [44]. With the output of this dynamic system, all the steady input and state of the original system can be generated. In this study it is therefore still called* steady-state generator.

When it comes to the local DMFORP, the first two assumptions are as follows:

A1' There exist sufficiently smooth functions $x = \pi(w)$, $u = c(w)$ with $\pi(0) = 0$, $c(0) = 0$, satisfying, $\forall w \in W$ with W a neighbourhood of the origin, regulator equation (4.7) is solved.

A2' The system (4.8) is locally stabilizable, irrespective of w, by a controller in the form of measurement feedback.

With the assumption A2', there exists a dynamic measurement feedback control law in the form of (4.9) with which the closed-loop simplified system composed of the simplified system (4.8) and the stabilizer (4.9) is locally asymptotically stable at $col(\bar{x}, z_1) = col(0, 0)$ for all $w \in W$.

4.2.3 Solution of the global DMFORP

Definition 1: An internal model candidate with respect to the stabilizer (4.9) and the steady-state generator (4.10) is as (4.11) satisfying $\eta_2(0, \theta(w), h_m(\pi(w), w)) = \alpha(\theta(w))$.

$$\dot{z}_2 = \eta_2(z_1, z_2, y_m). \tag{4.11}$$

Remark 9 *This definition is consistent with the one in [43] and [44], which also requires* $\eta_2(0, \theta(w), h_m(\pi(w), w), w)) = \alpha(\theta(w))$ *when* $h_m(\pi(w), w) = e = 0$. *Here the concept is extended to the case of the measurement feedback form. Furthermore, this internal model candidate incorporates the information of the stabilizer, which is different from that in [43] and [44].*

The following system is called the *closed-loop stabilized system* in this chapter,

$$\begin{aligned} \dot{\bar{x}} &= f_{\bar{x}}(\bar{x}, z_1, \bar{z}_2, w), \\ \dot{z}_1 &= \eta_{z_1}(\bar{x}, z_1, \bar{z}_2, w), \\ \dot{\bar{z}}_2 &= \bar{\eta}_{\bar{z}_2}(\bar{x}, z_1, \bar{z}_2, w), \end{aligned} \tag{4.12}$$

where $f_{\bar{x}}(\bar{x}_1, z_1, \bar{z}_2, w) = f(\bar{x} + \pi(w), u_z, w) - f(\pi(w), c(w), w)$, $u_z = c(\beta(\bar{z}_2 + \theta(w))) + \psi_1(z_1, h_m(\bar{x} + \pi(w), w), \beta(\bar{z}_2 + \theta(w)))$, $\eta_{z_1}(\bar{x}, z_1, \bar{z}_2, w) = \eta_1(z_1, h_m(\bar{x} + \pi(w), w), \beta(\bar{z}_2 + \theta(w)))$, $\bar{\eta}_{\bar{z}_2}(\bar{x}, z_1, \bar{z}_2, w) = \eta_2(z_1, \bar{z}_2 + \theta(w), h_m(\bar{x} + \pi(w), w)) - \eta_2(0, \theta(w), h_m(\pi(w), w))$.

Definition 2: The internal model candidate (4.11) is called a global (local) internal model with respect to the stabilizer (4.9) and the steady-state generator (4.10) for the original system (4.1), if for any $w \in W$, the closed-loop stabilized system of (4.12) is globally (locally) asymptotically stable, irrespective of w, in the sense of $\mathcal{K}L$ functions $\varrho(\cdot, \cdot)$.

Remark 10 *An additional restriction is added to the internal model candidate. Thus the candidate becomes a "real one". The restriction gives an approach to modify the candidate to get a real internal model.*

In the original system, the output function $h(x, w)$ is globally Lipschitz with respect to x if there exists a class-$\mathcal{K}$ function l_0 such that for all $x^1, x^2 \in R^n, w \in R^s$,

$$\|h(x^1, w) - h(x^2, w)\| \leq l_0(\|x^1 - x^2\|). \tag{4.13}$$

Theorem 11 *If A1, A2, A3 hold, there exists a global internal model* (4.11) *with respect to the stabilizer* (4.9) *and the steady-state generator* (4.10), *and the output function* $h(x, w)$ *is globally Lipschitz with respect to* x, *then the global DMFORP of the original system* (4.1) *is solvable.*

Proof Consider the following controller,

$$\begin{aligned} \dot{z}_1 &= \eta_1(z_1, y_m, \beta(z_2)), \\ \dot{z}_2 &= \eta_2(z_1, z_2, y_m), \\ u &= c(\beta(z_2)) + \psi_1(z_1, y_m, \beta(z_2)). \end{aligned} \tag{4.14}$$

Given any compact set W, the origin of the closed-loop stabilized system of (4.12) is globally asymptotically stable from initial state $(\bar{x}_0, z_{1_0}, \bar{z}_{2_0}, w_0)$. The state of the augmented system composed of the original system (4.1) and the controller (4.14) is $x_c = col(x, z_1, z_2)$, and the state of system (4.12) is $\bar{x}_c = col(\bar{x}, z_1, \bar{z}_2)$, with a relation

$$col(x, z_1, z_2) = col(\bar{x}, z_1, \bar{z}_2) + col(\pi(w), 0, \theta(w)).$$

It is easy to verify that $\pi_c(w) = col(\pi(w), 0, \theta(w))$ satisfies the equations (4.6) for the augmented system composed of the original system (4.1) and the controller (4.14). Thus the condition P4 is satisfied.

On the other hand, $x_c - \pi_c(w) = col(x, z_1, z_2) - col(\pi(w), 0, \theta(w)) = col(\bar{x}, z_1, \bar{z}_2) = \bar{x}_c$, and from the definition of the internal model, one has $\|\bar{x}_c(t)\| \leq \varrho(\|\bar{x}_c(0)\|, t)$, then

$$\|x_c(t) - \pi_c(w(t))\| \leq \varrho(\|x_c(0) - \pi_c(w_0)\|, t).$$

The condition P5 is satisfied.

With the Lipschitz condition, and $\bar{x}(t) \to 0$ as $t \to 0$,

$$\begin{aligned} \lim_{t\to\infty} \|e(t)\| &= \lim_{t\to\infty} h(\bar{x}(t) + \pi(w), w) - h(\pi(w), w) \\ &\leq \lim_{t\to\infty} l_0(\|\bar{x}\|) = 0, \end{aligned} \tag{4.15}$$

i.e., the requirement P1 of the asymptotical convergence to zero of the error output is satisfied.

Thus the global DMFORP is solvable.

Remark 12 *In the theorem, if the solution of* (4.12) *satisfies*

$$\lim_{t\to\infty} (h(\bar{x} + \pi(w), w) - h(\pi(w), w)) = 0 \tag{4.16}$$

for any $w \in W$, the Lipschitz condition is not necessary for the solvability of DMFORP.

Remark 13 *This theorem gives an approach to solve the output regulation problem. The first step is to design a stabilizer for the simplified system on the assumption that the states of the exosystem are known. Then an internal model candidate is constructed with respect to the stabilizer and a steady-state generator for the exosystem. If the internal model is found and the condition of* (4.16) *is satisfied, then the DMFORP is solved.*

Remark 14 *If w is not explicit in $\psi_1(z_1, y_m, w) + c(w)$ and the mapping $\eta_1(z_1, y_m, w)$, the internal model is unnecessarily constructed, and the dynamic measurement feedback output regulation problem is solved by the following controller.*

$$\begin{aligned} \dot{z}_1 &= \eta_1^0(z_1, y_m), \\ u &= \psi_1^0(z_1, y_m), \end{aligned} \tag{4.17}$$

where $\eta_1^0(z_1, y_m) = \eta_1(z_1, y_m, w)$, $\psi_1^0(z_1, y_m) = \psi_1(z_1, y_m, w) + c(w)$. *From the proof of the above proposition, one can see that the internal model is to estimate the functions in the stabilized system related to* w. *So in the steady-state generator definition, the output of the generator can be just the functions related to* w. *This is also consistent with the origin of the internal model candidate, which is to estimate the unknown parameters in the controller. The internal model can be thought of as an observer for the exosystem and its design can be thought of as an observer design for nonlinear systems, which is another problem. So the design techniques of the internal model are not detailed in this thesis.*

Proposition 15 *If the output regulation problem is solvable by the approach proposed in [43] and [44] with the measurement being the output or the output plus the (partial) state, it is also solvable with the above theorem.*

Proof In [43] and [44], output regulation problem of the following system

$$\begin{aligned} \dot{x} &= f(x, u, w), \\ e &= h(x, u, w), \end{aligned} \tag{4.18}$$

is solved by the controller

$$\begin{aligned} \dot{\eta} &= \gamma(\eta, x, u, e), \\ \dot{\xi} &= \zeta(\bar{x}_1, \cdots, \bar{x}_d, \xi, e), \\ u &= \beta_u(\eta) + k(\bar{x}_1, \cdots, \bar{x}_d, \xi, e), \end{aligned} \tag{4.19}$$

where the solution of the regulator equation is $x = \pi(w), u = c(w)$, and

$$\frac{d\theta(w)}{dt} = \alpha(\theta(w)),$$

$$col(\pi_1(w), \cdots, \pi_d(w), c(w)) = \beta(\theta(w)),$$

$$\beta_u = col(\beta_{d+1}, \cdots, \beta_{d+m}),$$

$$\gamma(\theta(w), \pi(w), c(w), 0) = \alpha(\theta(w)),$$

$$k(0, \cdots, 0, 0, 0) = 0,\ \zeta(0, \cdots, 0, 0, 0) = 0,$$

$$\bar{x}_i = x_i - \beta_i(\eta),\ i = 1, 2, \cdots, d.$$

With the approach proposed in this chapter, the stabilizer for the simplified system can be chosen as

$$\begin{aligned} \dot{\bar{\eta}} &= \bar{\gamma}(\bar{\eta}, x_1, \cdots, x_d, w), \\ \dot{\xi} &= \zeta(\bar{\bar{x}}_1, \cdots, \bar{\bar{x}}_d, \xi, e), \\ \bar{u} &= \beta_u(\eta) + k(\bar{\bar{x}}_1, \cdots, \bar{\bar{x}}_d, \xi, e) - c(w), \end{aligned} \tag{4.20}$$

where

$$\bar{\bar{x}}_i = x_i - \beta_i(\bar{\eta} + \theta(w)),\ i = 1, 2, \cdots, d,$$

$$\bar{\gamma}(\bar{\eta}, x_1, \cdots, x_d, w) = \gamma(\bar{\eta} + \theta(w), \bar{\bar{x}}_1, \cdots, \bar{\bar{x}}_d, \bar{u} + \alpha(\theta(w)), e) - \alpha(\theta(w)).$$

In the closed-loop stabilized system, only the function $\theta(w)$ is related to w. So the output of the internal model can be just the function $\theta(w)$. It is obvious that the dynamic system $\eta = \gamma(\eta, x, u, e)$ is naturally the internal model candidate. Actually this candidate is a "real one". This internal model is principally the same as part of the stabilizer. Combining the stabilizer and the internal model, the controller of (4.19) solves the global DMFORP.

All in all, if an output regulation problem is solvable by the approach proposed in [43] and [44], it must be solvable by the approach proposed in this chapter.

4.2.4 Solution of the local DMFORP

Similar to the global version, there is a theorem for the local DMFORP.

Theorem 16 *If A1', A2' and A3 hold, the exosystem is neutrally stable, and if there exists a local internal model with respect to a stabilizer* (4.9) *and a steady-state generator* (4.10)*, then the local DMFORP is solvable.*

Proof Consider the controller (4.14). The closed-loop stabilized system of (4.12) is locally asymptotically stable from the initial state $\bar{x}_0, z_{1_0}, \bar{z}_{2_0}, w_0$. The state of the augmented system composed of the original system (4.1) and the controller (4.14) is $x_c = col(x, z_1, z_2)$, and the state of the system (4.12) is $\bar{x}_c = col(\bar{x}, z_1, \bar{z}_2)$, with a relation

$$col(x, z_1, z_2) = col(\bar{x}, z_1, \bar{z}_2) + col(\pi(w), 0, \theta(w)).$$

It is easy to verify that $\pi_c(w) = col(\pi(w), 0, \theta(w))$ satisfies the equations (4.6) for the augmented system composed of the original system (4.1) and the controller (4.14). Thus the condition P4' is satisfied.

On the other hand, $x_c - \pi_c(w) = col(x, z_1, z_2) - col(\pi(w), 0, \theta(w)) = col(\bar{x}, z_1, \bar{z}_2) = \bar{x}_c$, and from the definition of the local internal model, one has $\|\bar{x}_c(t)\| \leq \varrho(\|\bar{x}_c(0)\|, t)$, then

$$\|x_c(t) - \pi_c(w(t))\| \leq \varrho(\|x_c(0) - \pi_c(w_0)\|, t).$$

The condition P5' is satisfied.

With continuity of $h(x, w)$, $\bar{x}(t) \to 0$ as $t \to 0$, and with w bounded,

$$\lim_{t\to\infty} e(t) = \lim_{t\to\infty} h(\bar{x}(t) + \pi(w), w) = h(\pi(w), w) = 0,$$

that is, the requirement P1 is satisfied.

Thus the DMFORP is solved by the controller (4.14). If the state w of the exosystem is not explicit in the mapping $\eta_1(z_1, y_m, w)$ and the controller $u = \psi_1(z_1, y_m, w) + c(w)$, then the internal model need not be constructed.

For a nonlinear system (4.1), one has the notations:

$$A = \frac{\partial f(0,0,0)}{\partial x}, \quad S = \frac{\partial s}{\partial w}(0), \quad C_m = \frac{\partial h_m}{\partial x}(0,0), \quad P = \frac{\partial f}{\partial w}(0,0,0),$$
$$B = \frac{\partial f}{\partial u}(0,0,0), \quad C = \frac{\partial h}{\partial x}(0,0), \quad Q = \frac{\partial h}{\partial w}(0,0), \quad Q_m = \frac{\partial h_m}{\partial w}(0,0).$$

Proposition 17 *For* (4.1)*, if the exosystem is neutrally stable,* (A, B) *is controllable [28] and*

$$\left(\begin{bmatrix} A & P \\ 0 & S \end{bmatrix}, [C_m, Q_m] \right)$$

is detectable [28], furthermore the condition A1' is satisfied, then the local DMFORP is solvable.

Proof With the assumption A1', using the coordinate change $\bar{x} = x - \pi(w)$, $\bar{u} = u - c(w)$, the simplified system (4.8) can be stabilized by the following controller.

$$\begin{aligned} \dot{z}_{11} &= f(z_{11} + \pi(w), c(w) + \bar{u}, z_{12} + w) - f(\pi(w), c(w), w) \\ &\quad + G_1(h_m(\bar{x} + \pi(w), w) - h_m(z_{11} + \pi(w), z_{12} + w)), \\ \dot{z}_{12} &= s(z_{12} + w) - s(w) \\ &\quad + G_2(h_m(\bar{x} + \pi(w), w) - h_m(z_{11} + \pi(w), z_{12} + w)), \\ \bar{u} &= c(z_{12} + w) + H(z_{11} + \pi(w) - \pi(z_{12} + w)) - c(w), \end{aligned} \tag{4.21}$$

where H, G_1, G_2 are chosen such that

$$A + BH$$

and

$$\begin{bmatrix} A - G_1 C_m & P - G_1 Q_m \\ -G_2 C_m & S - G_2 Q_m \end{bmatrix}$$

are Hurwitz, which guarantees the following Jacobian matrix of the closed-loop simplified system is Hurwitz [28].

$$\begin{bmatrix} A & BH & BK \\ G_1 C_m & A + BH - G_1 C_m & P + BK - G_1 Q_m \\ G_2 C_m & -G_2 C_m & S - G_2 Q_m \end{bmatrix}, \tag{4.22}$$

where $K = (\frac{\partial c(w)}{\partial w} - H\frac{\partial \pi(w)}{\partial w})|_{w=0}$. Since the pair of (A, B) is controllable and the pair of $\left(\begin{bmatrix} A & P \\ 0 & S \end{bmatrix}, [C_m, Q_m] \right)$ is detectable, it is possible to choose H, G_1, G_2 satisfying the above conditions. With the Lyaponov theory, the Hurwitz Jacobian matrix means the

system is exponentially stable, which leads to asymptotical stability in the sense of $\mathcal{K}L$ functions. So the above controller can be thought of as a stabilizer. The assumption A2' is satisfied.

Now the steady state generator is chosen as $\theta(w) = \begin{bmatrix} \pi(w) \\ w \end{bmatrix}$, $\beta(\theta(w)) = w$, and the internal model candidate $\dot{z}_2 = \eta_2(z_2, z_{11}, z_{12}, \bar{h}_m(\bar{x}, w))$ is constructed. If one chooses $z_2 = col(z_{21}, z_{22})$ satisfying $z_{21} = z_{11} + \pi(w)$, $z_{22} = z_{12} + w$, then one gets

$$\begin{aligned} \dot{z}_{21} &= f(z_{11}, u_z, z_{21}) + G_1(y_m - h_m(z_{21}, z_{12})), \\ \dot{z}_{22} &= s(z_{22}) + G_2(y_m - h_m(z_{21}, z_{22})), \\ u_z &= c(z_{22}) + H(z_{21} - \pi(z_{12}), \end{aligned} \tag{4.23}$$

The stabilizer (4.21) is rewritten as (4.24).

$$\begin{aligned} \frac{d(z_{11} + \pi(w))}{dt} &= f(z_{11} + \pi(w), u, z_{12} + w) \\ &\quad + G_1(h_m(\bar{x} + \pi(w), w) - h_m(z_{11} + \pi(w), z_{12} + w)), \\ \frac{d(z_{12} + w)}{dt} &= s(z_{12} + w) \\ &\quad + G_2(h_m(\bar{x} + \pi(w), w) - h_m(z_{11} + \pi(w), z_{12} + w)), \\ u &= c(z_{12} + w) + H(z_{11} + \pi(w) - \pi(z_{12} + w)). \end{aligned} \tag{4.24}$$

With the internal model candidate (4.23), replacing the functions $z_{11}+\pi(w)$, $z_{12}+w$ in the stabilizer (4.24) with $z_{21} = \bar{z}_{21} + \pi(w) = z_{11} + \pi(w)$ and $z_{22} = \bar{z}_{22} + w = z_{12} + w$, respectively, the closed-loop stabilized system can be written as

$$\begin{aligned} \dot{\bar{x}} &= f(\bar{x} + \pi(w), u, w) - f(\pi(w), c(w), w), \\ \dot{z}_{11} &= f(z_{11} + \pi(w), u, z_{12} + w) - f(\pi(w), c(w), w) \\ &\quad + G_1(y_m - h_m(z_{11} + \pi(w), z_{12} + w)), \\ \dot{z}_{12} &= s(z_{12} + w) - s(w) + G_2(y_m - h_m(z_{11} + \pi(w), z_{12} + w)), \\ u &= c(z_{12} + w) + H(z_{11} + \pi(w) - \pi(z_{12} + w), \end{aligned} \tag{4.25}$$

whose Jacobian matrix is the same as (4.22). That is, the internal model candidate (4.23) is a "real one".

It is noticed that in the closed-loop stabilized system (4.25), the dynamics of the internal model disappears because when one changes the coordinates of the internal model candidate, and replaces the functions of w in the stabilizer, the dynamics of the stabilizer is the same as the internal model candidate.

With the theorem 16, the local DMFORP is solved by the controller (4.23).

Remark 18 *From the proof, it can be seen that the problem is locally solved by the following controller,*

$$\begin{aligned}\dot{z}_{21} &= f(z_{11}) + g(z_{11})u_z + p(z_{11})z_{22} + G_1(y_m - h_m(z_{21}, z_{12})),\\ \dot{z}_{22} &= s(z_{22}) + G_2(y_m - h_m(z_{21}, z_{22})),\\ u_z &= c(z_{22}) + H(z_{21} - \pi(z_{12})),\end{aligned} \tag{4.26}$$

where H, G_1, G_2 *can simply be chosen such that*

$$A + BH$$

and

$$\begin{bmatrix} A - G_1C_m & P - G_1Q_m \\ -G_2C_m & S - G_2Q_m \end{bmatrix}$$

are Hurwitz, which guarantees the following Jacobean matrix of the closed-loop simplified system is Hurwitz,

$$\begin{bmatrix} A & BH & BK \\ G_1C_m & A + BH - G_1C_m & P + BK - G_1Q_m \\ G_2C_m & -G_2C_m & S - G_2Q_m \end{bmatrix},$$

where

$$K = (\frac{\partial c(w)}{\partial w} - H\frac{\partial \pi(w)}{\partial w})|_{w=0}.$$

In particular, when the state of the exosystem w *is known, for example,* $y_m = col(y_m^1,\ w)$, *the problem can be solved by*

$$\begin{aligned}\dot{z} &= f(z) + g(z)u + p(z)w + G_1(y_m^1 - h_m(z, w)),\\ u &= c(w) + H(z - \pi(w)),\end{aligned} \tag{4.27}$$

where G_1, H *are chosen such that* $A+BH$ *and* $A-G_1C_m^1$ *are Hurwitz* ($C_m^1 = \frac{\partial y_m^1(0,0)}{\partial x}$.)

Remark 19 *The parameters* K (H), G *can be chosen with different kinds of methods, such as with pole placement or a linear-quadratic state-feedback regulator approach. Although* K (H), G *are chosen with a linear system theory, the nonlinear regulator problem is solved by the controller* (4.26) *with them.*

If the measurement is the output, the above proposition leads to the theorem in [37]. However, Theorem 16 is not limited to processing the case of the proposition; as can be seen in *Example 4*, this theorem can process a nonlinear system whose closed-loop simplified system has a Jacobian matrix which is not Hurwitz but is stable in the sense of some class $\mathcal{KL}$ functions.

Consider a simplified system

$$\dot{\bar{x}} = \bar{f}(\bar{x}, \bar{u}, w)$$

can be stabilized by a stabilizer

$$\begin{aligned} \dot{z}_1 &= \eta_1(z_1, y_m, w), \\ \bar{u} &= \psi_1(z_1, y_m, w). \end{aligned} \tag{4.28}$$

The Jacobian matrix of the closed-loop simplified system at the origin is not Hurwitz, but it is still stable in the sense of some class $\mathcal{KL}$ functions.

Assuming an internal model candidate $\dot{z}_2 = \eta_2(z_1, z_2, y_m)$ with respect to the above stabilizer and a steady-state generator $\frac{d\theta(w)}{dt} = \alpha(\theta(w))$, $w = \beta(\theta(w))$ is a "real one", and with a coordinate change $\bar{z}_2 = z_2 - \theta(w)$, the closed-loop stabilized system can be written as

$$\begin{aligned} \dot{\bar{x}} &= \bar{f}(\bar{x}, \bar{u}, w), \\ \dot{z}_1 &= \eta_1(z_1, y_m, \beta(\bar{z}_2 + \theta(w))), \\ \dot{\bar{z}}_2 &= \eta_2(z_1, \bar{z}_2 + \theta(w), y_m) - \alpha(\theta(w)), \\ \bar{u} &= \psi_1(z_1, y_m, \beta(\bar{z}_2 + \theta(w))), \\ y_m &= \bar{h}_m(\bar{x}, w). \end{aligned} \tag{4.29}$$

When $\bar{z}_2 = 0$ in (4.29), it is the closed-loop simplified system, which is stable although its Jacobian matrix is not Hurwitz. So according to the reduction principle [45], it is possible to find a linear change of coordinates $col(p_1, p_2) = T col(\bar{x}, z_1) + K\bar{z}_2$, with T nonsingular, such that the closed-loop stabilized system (4.29) can be rewritten as

$$\begin{aligned} \dot{p}_1 &= F_1 p_1 + g_1(p_1, p_2, \bar{z}_2), \\ \dot{p}_2 &= F_{21} p_1 + F_2 p_2 + G_2 \bar{z}_2 + g_2(p_1, p_2, \bar{z}_2), \\ \dot{\bar{z}}_2 &= A_1 p_1 + A_2 p_2 + A\bar{z}_2 + g_3(p_1, p_2, \bar{z}_2), \end{aligned} \tag{4.30}$$

where F_1 has all the eigenvalues with zero real part, F_2 has all the eigenvalues with negative real part, and the functions g_1, g_2, g_3 vanish at $(p_1, p_2, \bar{z}_2) = (0, 0, 0)$ together with their first order derivatives.

When $\bar{z}_2 = 0$ in (4.30), the first two equations are as follows.

$$\begin{aligned} \dot{p}_1 &= F_1 p_1 + g_1(p_1, p_2, 0), \\ \dot{p}_2 &= F_{21} p_1 + F_2 p_2 + g_2(p_1, p_2, 0), \end{aligned} \tag{4.31}$$

which is the transformation of the closed-loop simplified system with the linear change of coordinates $col(p_1, p_2) = T col(\bar{x}, z_1)$. For the origin $col(\bar{x}, z_1) = col(0, 0)$ of the closed-loop simplified system is locally asymptotically stable in the sense of $\mathcal{KL}$ functions, the origin $col(p_1, p_2) = col(0, 0)$ of the (4.31) is also locally asymptotically stable in the sense of $\mathcal{KL}$ functions. So according to the reduction principle, there must exist a center manifold $p_2 = \pi_2(p_1)$ for the system (4.31) and the origin $x = 0$ of the reduced system $\dot{x} = F_1 x + g_1(x, \pi_2(x), 0)$ is necessarily locally asymptotically stable in the sense of $\mathcal{KL}$ functions.

If $A_1 z_1 + A_2 \pi_2(z_1) + g_3(z_1, \pi_2(z_1), 0) = 0$ and $\begin{bmatrix} F_2 & G_2 \\ A_2 & A \end{bmatrix}$ is Hurwitz, then $p_2 = \pi_2(p_1)$, $\bar{z}_2 = 0$ is a center manifold for the system (4.30) and the reduced system

is the same as that of the system (4.31), the origin of which is locally asymptotically stable in the sense of $\mathcal{K}L$ functions. According to the reduction principle, $col(p_1, p_2, \bar{z}_2) = (0, 0, 0)$ of the system (4.30) is locally asymptotically stable in the sense of $\mathcal{K}L$ functions. In addition, T is nonsingular in the linear change of coordinates, the origin $col(\bar{x}, z_1, \bar{z}_2) = col(0, 0, 0)$ of the closed-loop stabilized system is locally asymptotically stable in the sense of $\mathcal{K}L$ functions. According to the definition of the internal model, the internal model candidate is a "real one", that is, the aforementioned assumption is true. According to Theorem 16, the local DMFORP is solved.

The above analysis gives an approach to check if the observer (internal model candidate) is a "real one" in the local DMFORP.

Remark 20 *The above condition is sufficient for the solvability of the local DMFORP.*

4.2.5 Examples

Four examples are employed to show the application cases of the proposed theories. Example 1 will show the solution of DMFORP with partial output feedback (static stabilizer and measured output being partial of the regulated output), Example 2 will show the solution of DMFORP with measured output feedback (static stabilizer and measured output being different from the regulated output) and Example 3 will show the solution of DMFORP with measured output feedback (dynamic stabilizer and measured output being different from the regulated output). These three examples are application cases of Theorem 10 while Example 4 is an application case of Theorem 15.

Example 1 Here, consider the system [44],

$$\begin{aligned} \dot{x}_1 &= x_1 + u_1, \\ \dot{x}_2 &= -x_2 + 1.2(x_1 - w) + 0.3u_2, \\ \dot{w} &= 2w, \\ e_1 &= x_1 - w, \\ e_2 &= x_1 x_2 - 0.2w^2, \\ y_m &= e_1 = x_1 - w. \end{aligned} \tag{4.32}$$

The solution of the regulator equation is $x = \pi(w) = \begin{bmatrix} w \\ 0.2w \end{bmatrix}$, $u = c(w) = \begin{bmatrix} w \\ 2w \end{bmatrix}$. One can get the following simplified system with $\bar{x} = x - \pi(w)$, $\bar{u} = u - c(w)$,

$$\begin{aligned} \dot{\bar{x}}_1 &= \bar{x}_1 + \bar{u}, \\ \dot{\bar{x}}_2 &= -\bar{x}_2 + 1.2\bar{x}_1 + 0.3\bar{u}_2. \end{aligned} \tag{4.33}$$

It is obvious that the above linear system is globally asymptotically stable if one chooses the stabilizer $\bar{u}_1 = -k_1\bar{x}_1 = -k_1 y_m,\ \bar{u}_2 = 0,\ k_1 > 1$.

One considers a steady-state generator with $\theta(w) = w, \beta(\theta(w)) = \theta(w)$, and an internal model candidate with respect to the stabilizer in the form of $\dot{z}_2 = ky_m + 2z_2 = k\bar{x}_1 + 2z_2, k \in R$. Then one can get the following closed-loop stabilized system with $\bar{z}_2 = z_2 - \theta(w)$,

$$\begin{aligned} \dot{\bar{x}}_1 &= (1 - k_1)x_1 + \bar{z}_2, \\ \dot{\bar{x}}_2 &= 1.2\bar{x}_1 - \bar{x}_2 + 0.6\bar{z}_2, \\ \dot{\bar{z}}_2 &= k\bar{x}_1 + 2\bar{z}_2 \end{aligned} \tag{4.34}$$

If $k_1,\ k$ is chosen such that $k_1 - 3 > 0,\ k + 2(k_1 - 1) < 0$, for example, $k_1 = 7,\ k = -15$, the above system is globally asymptotically stable and thus $\dot{z}_2 = ky_m + 2z_2$ is an internal model with respect to the stabilizer. Then the output regulation problem of (4.32) is solved by

$$\begin{aligned} \dot{z}_2 &= ky_m + 2z_2, \\ u_1 &= -k_1 y_m + z_2, \\ u_2 &= 2z_2. \end{aligned} \tag{4.35}$$

Remark 21 *This example is in the form of (partial) output feedback. And the stabilizer is designed for a linear system. Some parameters in the stabilizer can be tuned together with some parameters in the internal model such that the origin of the closed-loop stabilized system is globally asymptotically stable in the sense of some class-$\mathcal{KL}$ functions.*

Example 2 Consider the following system with some changes in the above example,

$$\begin{aligned} \dot{x}_1 &= x_1 + u_1, \\ \dot{x}_2 &= -x_2 + 1.2(x_1 - w) + 0.3u_2, \\ \dot{w} &= 2w, \\ e_1 &= x_1 - w, \\ e_2 &= x_1 x_2 - 0.2w^2, \\ y_m &= x_1 - w/2. \end{aligned} \tag{4.36}$$

The solution of the regulator equation and the simplified system are the same as in *Example 1*. But the stabilizer is in the form of $\bar{u}_1 = -k_1\bar{x}_1 = -k_1(y_m - w/2),\ \bar{u}_2 = 0,\ k_1 > 1$.

One considers a steady-state generator with $\theta(w) = w, \beta(\theta(w)) = \theta(w)$, and an internal model candidate with respect to the stabilizer in the form of $\dot{z}_2 = ky_m - kz_2/2 + 2z_2 = k\bar{x}_1 - kz_2/2 + kw/2 + 2z_2, k \in R$. Then one can get the following

closed-loop stabilized system with $\bar{z}_2 = z_2 - \theta(w)$,

$$\begin{aligned}\dot{\bar{x}}_1 &= (1-k_1)x_1 + (1+k_1/2)\bar{z}_2,\\ \dot{\bar{x}}_2 &= 1.2\bar{x}_1 - \bar{x}_2 + 0.6\bar{z}_2,\\ \dot{\bar{z}}_2 &= k\bar{x}_1 + (2-k/2)\bar{z}_2.\end{aligned} \tag{4.37}$$

If $k_1,\ k$ is chosen such that $k_1 > 1,\ k_1 - 3 + k/2 > 0,\ -3k/2 - 2(k_1 - 1) < 0$, for example, $k_1 = 10, k = -13$, the above system is globally asymptotically stable. Then the output regulation problem of (4.36) is solved by

$$\begin{aligned}\dot{z}_2 &= ky_m + (2+k/2)z_2,\\ u_1 &= -k_1 y_m + (1+k_1/2)z_2,\\ u_2 &= 2z_2.\end{aligned} \tag{4.38}$$

Remark 22 *From the above examples, one can see that not all stabilizers have the corresponding internal model such that the closed-loop stabilized system is globally asymptotically stable. It should be pointed out that all the examples in [44] can be dealt with in the framework proposed in this chapter with stabilizers in the form of static feedback. Next, a system that cannot be stabilized by a static measurement feedback controller is considered.*

Example 3 Consider the following system

$$\begin{aligned}\dot{x}_1 &= -2x_1 - x_2 + u + 3w,\\ \dot{x}_2 &= x_1 + 3x_2 - 3w,\\ \dot{w} &= w,\\ e &= x_1 x_2 - w^2,\\ y_m &= x_2.\end{aligned} \tag{4.39}$$

A solution of the regulator equation is $x = \pi(w) = col(w, w), u = c(w) = w$. One can get the following simplified system with $\bar{x} = x - \pi(w),\ \bar{u} = u - c(w)$,

$$\begin{aligned}\dot{\bar{x}}_1 &= -2\bar{x}_1 - \bar{x}_2 + \bar{u},\\ \dot{\bar{x}}_2 &= \bar{x}_1 + 3\bar{x}_2,\end{aligned} \tag{4.40}$$

with measurement $y_m = \bar{x}_2 + w$. This system cannot be stabilized by a static feedback controller even if w is known. However, it can be globally stabilized by a dynamic feedback controller,

$$\begin{aligned}\dot{z}_{11} &= -(y_m - w) - 8z_{11} - 29z_{12} &&= -\bar{x}_2 - 8z_{11} - 29z_{12},\\ \dot{z}_{12} &= 9.5(y_m - w) + z_{11} - 6.5z_{12} &&= 9.5\bar{x}_2 + z_{11} - 6.5z_{12},\\ \bar{u} &= -6z_{11} - 29z_{12},\end{aligned} \tag{4.41}$$

Consider a steady-state generator with $\theta(w) = w, \beta(\theta(w)) = \theta(w)$, and an internal model candidate $\dot{z}_2 = k_1(y_m - z_{12} - z_2) + z_2 = k_1\bar{x}_2 - k_1 z_{12} - k_1(z_2 - w) + z_2, k_1 \in R$. Then one can get the closed-loop stabilized system with $\bar{z}_2 = z_2 - \theta(w)$,

$$\begin{aligned}
\dot{\bar{x}}_1 &= -2\bar{x}_1 - \bar{x}_2 - 6z_{11} - 29z_{12} + \bar{z}_2, \\
\dot{\bar{x}}_2 &= \bar{x}_1 + 3\bar{x}_2, \\
\dot{z}_{11} &= -(y_m - z_2) - 8z_{11} - 29z_{12} \qquad = -\bar{x}_2 - 8z_{11} - 29z_{12} + \bar{z}_2, \\
\dot{z}_{12} &= 9.5(y_m - z_2) + z_{11} - 6.5z_{12} \qquad = 9.5\bar{x}_2 + z_{11} - 6.5z_{12} - 9.5\bar{z}_2, \\
\dot{\bar{z}}_2 &= k_1\bar{x}_2 - k_1 z_{12} + (1 - k_1)\bar{z}_2.
\end{aligned} \tag{4.42}$$

If $k_1 = -3$, the above system is globally asymptotically stable and the internal model candidate is a "real one". So the output regulation problem is solved by

$$\begin{aligned}
\dot{z}_{11} &= -(y_m - z_2) - 8z_{11} - 29z_{12}, \\
\dot{z}_{12} &= 9.5(y_m - z_2) + z_{11} - 6.5z_{12}, \\
\dot{z}_2 &= -3(y_m - z_{12} - z_2) + z_2, \\
u &= -6z_{11} - 29z_{12} + z_2.
\end{aligned} \tag{4.43}$$

Another solution of the regulator equation is $x = \pi(w) = col(2w, 0.5w)$, $u = c(w) = 3.5w$. With a similar approach, one can get another solution of the output regulation problem as follows,

$$\begin{aligned}
\dot{z}_{11} &= -(y_m - 0.5z_2) - 8z_{11} - 29z_{12}, \\
\dot{z}_{12} &= 9.5(y_m - 0.5z_2) + z_{11} - 6.5z_{12}, \\
\dot{z}_2 &= -6(y_m - z_{12} - 0.5z_2) + z_2, \\
u &= -6z_{11} - 29z_{12} + 3.5z_2.
\end{aligned} \tag{4.44}$$

From this example, one can see that the DMFORP may be solved on different manifolds.

Remark 23 *Not all stabilizers have the corresponding internal model such that the closed-loop stabilized system is globally asymptotically stable. It should be pointed out that all the examples in [44] can be processed by the framework proposed in this chapter with stabilizers in the form of static feedback. The output regulation problem in this example cannot be solved by a static measurement feedback even if the state w of the exosystem is known. When a dynamic measurement feedback controller is considered, it is possible to find an internal model to incorporate the exosystem. In the example, the design of the stabilizer is not detailed, for there are a number of methods to go about it. However, it really concerns the example of how to apply the idea of this chapter to solve dynamic measurement feedback output regulation problems.*

Example 4 Consider the following system,

$$\begin{aligned} \dot{x}_1 &= -x_1^3, \\ \dot{x}_2 &= x_1(x_2 - w) + x_2 + u + 2w, \\ \dot{w} &= 0, \\ e &= x_2 - w, \\ y_m &= x_2. \end{aligned} \tag{4.45}$$

The unique solution of the regulator equation is $\pi(w) = col(0, w)$, $c(w) = -3w$. A1' holds. With $\bar{x} = x - \pi(w), \bar{u} = u - c(w)$, the simplified system is

$$\begin{aligned} \dot{\bar{x}}_1 &= -\bar{x}_1^3, \\ \dot{\bar{x}}_2 &= \bar{x}_2 + \bar{x}_1\bar{x}_2 + \bar{u}. \end{aligned} \tag{4.46}$$

It can be stabilized by a static controller $\bar{u} = -k_1 y_m + k_1 w, k_1 > 1$. A2' holds. Consider a steady-state generator $\theta(w) = w, \alpha(\theta(w)) = 0, \beta(w) = w$, and an internal model candidate $\dot{z}_2 = k_2 y_m - k_2 z_2 = k_2\bar{x}_2 - k_2(z_2 - w)$. With $\bar{z}_2 = z_2 - w$, the stabilized closed-loop system is

$$\begin{aligned} \dot{\bar{x}}_1 &= -\bar{x}_1^3, \\ \dot{\bar{x}}_2 &= (1 - k_1)\bar{x}_2 + (k_1 - 3)\bar{z}_2 + \bar{x}_1\bar{x}_2, \\ \dot{\bar{z}}_2 &= k_2\bar{x}_2 - k_2\bar{z}_2. \end{aligned} \tag{4.47}$$

The above system is actually locally asymptotically stable in the sense of $\mathcal{KL}$ functions when $k_1 > 1, k_2 > 0$. The internal model is a "real one". According to Theorem 16, the local DMFORP is solvable. With w in the stabilizer $u = \bar{u} + c(w) = (-k_1 y_m + k_1 w) - 3w$ replaced by z_2, the controller is as follows,

$$\begin{aligned} \dot{z}_2 &= k_2 y_m - k_2 z_2, & k_2 > 0, \\ u &= -k_1 y_m + (k_1 - 3)z_2, & k_1 > 1. \end{aligned} \tag{4.48}$$

4.3 Speed regulation

In the previous chapter, it is shown that optimal scheduling can improve the performance of the closed-loop controller, and that the 2-2 strategy, the ECP/iDP mode, is the best of all the strategies.

In this section, one considers the application of output regulation of nonlinear systems with measured output feedback to the control of heavy haul trains. Optimal scheduling is still based on "trading off" the equilibria. Thus the balance between energy consumption and in-train forces is still maintained. For closed-loop control, speed regulation is imposed. This approach to design is practically feasible and manageable,

and by its nature, is also easily integrable with human drivers. Instead of the linear system theory, a nonlinear system theory is adopted so that without a linear approximation philosophy, the control is closer to reality. Another advantage of the approach is the assumption that only the locomotives' speeds are available for measurement.

4.3.1 Application of output regulation in heavy haul trains

The mathematical model of train is repeated as follows,

$$\begin{aligned} m_s\dot{v}_s &= u_s + f_{in_{s-1}} - f_{in_s} - f_{a_s}, \quad s = 1, 2, \cdots, n, \\ \dot{x}_j &= v_j - v_{j+1}, \quad j = 1, 2, \cdots, n-1, \end{aligned} \tag{4.49}$$

For the model of a train (4.49), some changes are required to be made for the application of output regulation. On the one hand, the origin is not an equilibrium of the system (4.49). On the other hand, there are many trajectories to annihilate the output (to regulate the output to the reference). However, for train handling, the choice of trajectories involves the balance between energy consumption and in-train forces. So in the application scheme, a quadratic programming algorithm is firstly applied to calculate the equilibrium of the system (4.49) with the reference speed held. Then, based on the equilibrium, a difference system between state of the origin system (4.49) and the equilibrium is formed, which can be stabilized with output regulation in the form of measurement feedback.

Optimal scheduling is referred to in section 3.4.2, where the equilibrium calculation is a quadratic programming problem. The performance function, considering the "trade-off" between the in-train forces and the energy consumption, is as (3.15).

In open loop control, the dynamic process in the train is ignored and the train is assumed to be in its steady state with the reference speed maintained, that is,

$$\begin{aligned} \frac{dv_i}{dt} &= 0, \quad i = 1, 2, \cdots, n, \\ \frac{dx_j}{dt} &= 0, \quad i = 1, 2, \cdots, n-1. \end{aligned} \tag{4.50}$$

Applying (4.50) to (4.49), one has

$$u_s + f_{in_{s-1}} - f_{in_s} - f_{a_s} = 0, \qquad s = 1, 2, \cdots, n. \tag{4.51}$$

In practical operations, u_i and f_{in_i} have some constraints.

$$\begin{aligned} \underline{U}_i \le u_i \le \overline{U}_i, &\qquad i = 1, 2, \cdots, n; \\ \underline{F}_{in_j} \le f_{in_j} \le \overline{F}_{in_j}, &\quad j = 1, 2, \cdots, n-1, \end{aligned} \tag{4.52}$$

where $\underline{U}_i, \overline{U}_i$ are the upper and the lower constraints for the ith input, and $\underline{F}_{in_j}, \overline{F}_{in_j}$ are the upper and lower constraints for the jth in-train force, respectively. For wagons,

$\overline{U_i} = 0$ and the values of $\underline{U_i}$ depend on the braking capacities of the wagons. For locomotives, the constraints $\underline{U_i}, \overline{U_i}$ depend on the locomotives' capacities in traction efforts and the running states. The constraints $\underline{F}_{in_j}, \overline{F}_{in_j}$ are limited because of the requirement of safe operation and low maintenance cost.

Thus optimal scheduling is a standard quadratic programming (QP) problem with objective function (3.15), equality constraints (4.51) and inequality constraints (4.52). The input operation limits are not considered. When the inputs are applied to the model, an anti-windup technique, detailed later, is applied.

With the above scheduling, the equilibrium can be denoted as $f^0_{in_j}(x^0_j)$, $v^0_i(v_r)$, u^0_i, $j = 1, 2, \cdots, n-1$, $i = 1, 2, \cdots, n$, which are the in-train forces (static displacement of coupler), the velocities (reference velocity) and the efforts of the cars. Then one can rewrite the train model as:

$$\begin{aligned} \delta\dot{v}_s &= (\delta u_s + \delta f_{in_{s-1}} - \delta f_{in_s} - \delta f a_s)/m_s, \qquad s = 1, \cdots, n, \\ \delta\dot{x}_j &= \delta v_j - \delta v_{j+1}, \qquad j = 1, \cdots, n-1, \end{aligned} \tag{4.53}$$

where $\delta v_s = v_s - v^0_s = v_s - v_r$, $\delta u_s = u_s - u^0_s$, $\delta f_{in_s} = f_{in_s} - f^0_{in_s}$, $\delta x_j = x_j - x^0_j$.

Thus in the controller design, the system (4.53) can be rewritten as

$$\dot{X} = f(X) + g(X)U, \tag{4.54}$$

where

$$X = col(\delta v_1, \cdots, \delta v_n, \delta x_1, \cdots, \delta x_{n-1});$$

$$U = col(\delta u_1, \cdots, \delta u_n);$$

$$f_i(X) = \frac{1}{m_i}(k_{i-1}X_{n+i-1} - k_i X_{n+i}) - (c_{i_1} + 2c_{i_2}v_r)X_i - c_{i_2}X_i^2, \ i = 1, 2\cdots, n,$$

$$f_{n+i}(X) = X_i - X_{i+1}, \ i = 1, 2, \cdots, n-1;$$

$$g(x) = \begin{bmatrix} \mathrm{diag}(\frac{1}{m_1}, \cdots, \frac{1}{m_n}) \\ 0_{(n-1)\times n} \end{bmatrix}.$$

The outputs to regulate are the cars' speeds, *i.e.*, assuming the reference speed is w_1, which is to be designed later, $e_i = v_i - w_1 = X_i + v_r - w_1$. The measured output is part of the cars' speeds, *i.e.*, $y_m = C_m(X + v_r)$, where $C_m = (C_{ij})_{p_m \times (2n-1)}$ and all the entries of the row vectors of C_m are zeros, only except one of the first n ones, which is one. For example, $C_m = \begin{bmatrix} 1 & 0 & 0 & \cdots & 0 \\ 0 & 1 & 0 & \cdots & 0 \end{bmatrix}$ if only the first two cars' speeds are measured.

Notice that the measured output is different from the output error.

The linearized system of (4.54) has system matrixes

$$A = \begin{bmatrix} A_{11} & A_{12} \\ A_{21} & A_{22} \end{bmatrix},$$

$$A_{11} = -\text{diag}(c_{1_1} + c_{2_1}v_r, \cdots, c_{1_n} + c_{2_n}v_r),$$

$$A_{12} = \begin{bmatrix} -\frac{k_1}{m_1} & 0 & \cdots & 0 & 0 \\ \frac{k_1}{m_2} & -\frac{k_2}{m_2} & \cdots & 0 & 0 \\ \cdots & \cdots & \cdots & \cdots & \cdots \\ 0 & \cdots & 0 & \frac{k_{n-2}}{m_{n-1}} & -\frac{k_{n-1}}{m_{n-1}} \\ 0 & \cdots & 0 & 0 & \frac{k_{n-1}}{m_n} \end{bmatrix},$$

$$A_{21} = \begin{bmatrix} 1 & -1 & 0 & \cdots & 0 & 0 \\ 0 & 1 & -1 & \cdots & 0 & 0 \\ \cdots & \cdots & \cdots & \cdots & \cdots & \cdots \\ 0 & 0 & 0 & \cdots & 1 & -1 \end{bmatrix},$$

$$A_{22} = 0_{(n-1)\times(n-1)},$$

$$B = \begin{bmatrix} \text{diag}(\frac{1}{m_1}, \cdots, \frac{1}{m_n}) \\ 0_{(n-1)\times n} \end{bmatrix}.$$

It can be verified that the above linearized pair (A, B) is controllable and (A, C_m) is observable with the *PBH* criterion in [28]. First one verifies the controllability.

$$\begin{aligned} [\lambda I - A \mid B] &= \begin{bmatrix} \lambda I_{n\times n} - A_{11} & -A_{12} & \text{diag}(\frac{1}{m_i}) \\ -A_{21} & \lambda I_{(n-1)\times(n-1)} & 0_{(n-1)\times n} \end{bmatrix} \\ &\sim \begin{bmatrix} \lambda I_{n\times n} - A_{11} & -A_{12} & I_{n\times n} \\ -A_{21} & \lambda I_{(n-1)\times(n-1)} & 0_{(n-1)\times n} \end{bmatrix} \\ &\sim \begin{bmatrix} 0_{n-1\times n-1} & 0 & 0_{n\times(n-1)} & I_{n\times n} \\ I_{(n-1)\times(n-1)} & 0 & \lambda I_{(n-1)\times(n-1)} & 0_{(n-1)\times n} \end{bmatrix}, \end{aligned}$$

from which one can get rank $([\lambda I - A \mid B]) = 2n-1$, and the pair (A, B) is controllable according to the *PBH* criterion.

When it comes to observability, if the first or the last car's speed is measured, the pair (A, C_m) is observable. Assuming, for example, the first car's speed is available, one has

$$\begin{bmatrix} A - \lambda I \\ C_m \end{bmatrix} = \begin{bmatrix} A_{11} - \lambda I_{n\times n} & A_{12} \\ A_{21} & -\lambda I_{(n-1)\times(n-1)} \\ 1 \quad 0 \quad \cdots \quad 0 & 0_{1\times(n-1)} \end{bmatrix} \sim \begin{bmatrix} I_{(2n-1)\times(2n-1)} \\ 0_{1\times(2n-1)} \end{bmatrix},$$

from which one knows that rank $\left(\begin{bmatrix} A - \lambda I \\ C_m \end{bmatrix}\right) = 2n - 1$, and the pair (A, C_m) is observable according to the *PBH* criterion. Actually the first car of a train is usually a locomotive, which is often a leader and whose speed is available. So the above assumption does not lose generality.

4.3.2 Trajectory design of heavy haul trains

As described, only the speed maintenance phase, speed acceleration and speed deceleration phases are discussed in this study. The cars' speeds are the subject of regulation.

To apply Theorem 16 into train control, the trajectory of the reference speed should satisfy the condition of neutral stability. It can be designed as

$$\begin{aligned} \dot{w}_1 &= aw_2, \\ \dot{w}_2 &= -a(w_1 - w_3), \\ \dot{w}_3 &= 0, \end{aligned} \tag{4.55}$$

whose solution is

$$\begin{aligned} w_1 &= w_3(0) + A\sin(at + \phi_0), \\ w_2 &= A\cos(at + \phi_0), \\ w_3 &= w_3(0), \end{aligned} \tag{4.56}$$

where A and ϕ_0 are determined by the initial conditions $(w_1(0), w_2(0), w_3(0))$.

Within the cruise phase, the initial conditions are chosen as

$$(w_1(0), w_2(0), w_3(0)) = (v_r, 0, v_r),$$

where v_r is the cruise speed.

Assuming the reference speed before acceleration/deceleration is v_{r_1} and the reference speed after acceleration/deceleration is v_{r_2}, then the initial conditions are chosen such that $w_3(0) = v_{r_1}, \phi_0 = 0, A = \sqrt{2}(v_{r_2} - v_{r_1})$.

The variable a in (4.55) is chosen considering the acceleration limit a_r or deceleration limit a_c of the train, which is determined by the effort capacity of the train. In simulation, $a = \frac{a_r}{A}$ within the acceleration phase and $a = \frac{a_c}{A}$ within the deceleration phase. For example, one chooses $a_r = 0.07$ m/s^2, $a_c = -0.2$ m/s^2, $\phi_0 = 0$, and the time interval $T_1 = \frac{\pi}{4a}$ as acceleration/deceleration phase. The modified speed file according to the speed profile is shown in Fig. 4.1.

The coefficient matrix of (4.55) is constant and its eigenvalues obviously lie on the imaginary axis, so the above designed trajectories are neutrally stable.

4.3.3 Speed regulation controller design

From the above designed trajectories, the conditions in Proposition 17 are satisfied if the regulator equations (4.7) are solved. Actually, one can verify that $X = \pi(w) =$

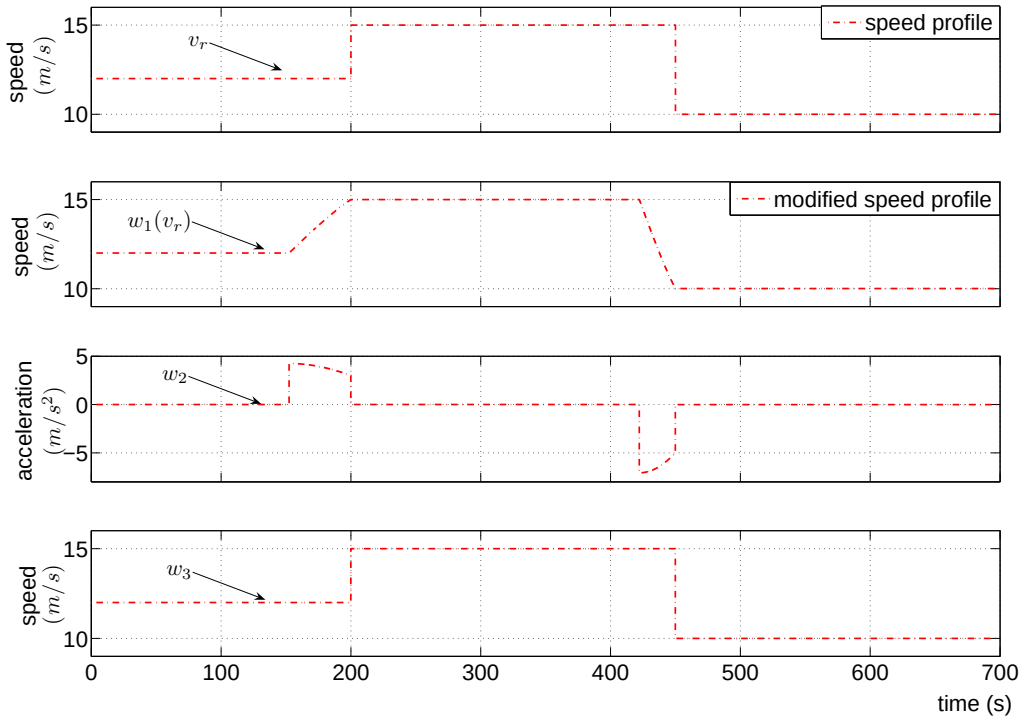

Figure 4.1: Modified speed profile

$(w_1 - w_3)[(1_{1\times n}, 0_{1\times(n-1)}]^T, U = c(w) = w_2 B_1^{-1} \cdot 1_{n\times 1} - B_1^{-1} f^1(\pi(w))$, where f^1 is the first n entries of f and B_1 is the first n rows of B, is a solution of (4.7).

According to Remark 18, the output regulating controller with measurement feedback is

$$\begin{aligned} \dot{z} &= f(z) + g(z)U + G_1(y_m - C_m z), \\ U &= c(w) + K(z - \pi(w)), \end{aligned} \tag{4.57}$$

where G_1, K are chosen such that $A + BK$ and $A - G_1 C_m$ are Hurwitz.

Based on the optimal scheduling and the output regulating controller, the complete closed-loop controller is

$$u = U + u^0. \tag{4.58}$$

In simulation, one chooses K with a linear quadratic algorithm in [15], where the performance function is

$$\delta J = \int (X'QX + U'RU)\, dt = \int \left(\sum_{i=0}^{n-1} K_f^o \delta x_i^2 + \sum_{i=0}^{n} K_e \delta u_i^2 + \sum_{i=0}^{n} K_v^o \delta v_i^2 \right) dt,$$

in which the variables K_f^o, K_e, K_v^o are the weights for in-train forces, energy consumption and velocity tracking, respectively. The different choices of the values of the

weights lead to speed emphasized control, in-train force emphasized control and energy consumption emphasized control, respectively.

The parameter G is also obtained by a quadratic programming algorithm in simulation where the weights for all the entries are equal.

These choices of K and G are consistent with Remark 19.

4.3.4 Simulation of speed regulation

Simulation setting

The simulation setting and parameters are the same as those in the previous chapter except that the deceleration limit is -0.2 m/s^2.

The weights for in-train forces, energy and velocity are K_f, K_e, K_v, respectively, and $K_f^o = 3\times10^8 K_f$, $K_v^o = 5\times10^6 K_v$, which leads to the same quantities of the items of the in-train forces, speed and input in (4.3.3) when $\delta x = 0.01$ m, $\delta v = 0.1$ m/s^2, $\delta u = 200$ N with $K_f = K_e = K_v$.

The acceleration limit a_r is 0.07 m/s^2. This value is calculated on the assumption that the train is running on a flat track and all the traction power of the locomotives is used to accelerate. The maximum acceleration can be $760 \times 2/(252 \times 2 + 417 \times 50) = 0.07118$ m/s^2. The absolute value of the deceleration a_c is more than that of the acceleration.

The observer is designed on the assumption that the front and rear locomotive group speeds are available. Since the exosystem is designed and its state is known, the observer is just to estimate the running state of the train model (deviations of the cars' speeds and the displacements of the couplers). The initial states of the observer are set to be zeros.

The observer is designed based on the difference system (4.53), which is related to w_3 of the exosystem. When w_3 is changed, the observer needs some time to track the state of the difference system. So in the control design, when w_3 is changed, the closed-loop controller is disabled (*i.e.*, only open loop scheduling is used) for some interval, during which the observer will track more closely to the state of the difference system. In simulation the interval is assumed to be a distance interval, whose length is equal to $15 \times w_3$.

Simulation result

A simulation result is shown in Fig. 4.2 with the optimal parameters $K_f = 1, K_v = 1, K_e = 1$.

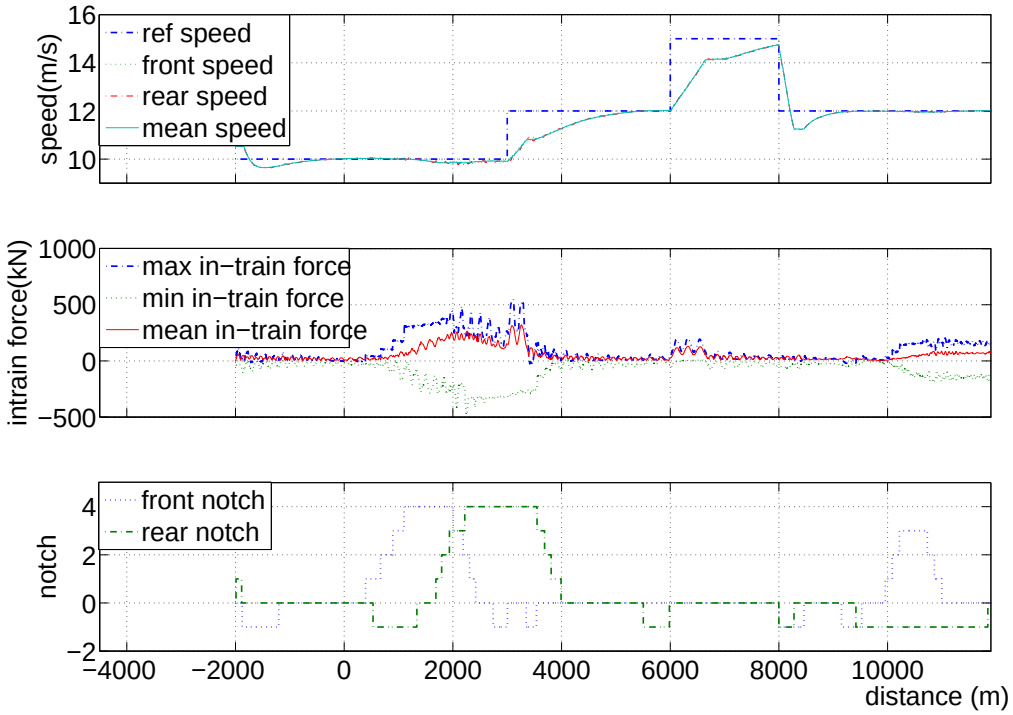

Figure 4.2: Output regulation with measurement feedback

In comparing the results shown in the above figure with Fig. 3.10 and Fig. 3.14, it can be seen that the oscillation is most obvious in open loop scheduling, while it is least in the output regulation with measurement feedback. The steady state error exists in open loop scheduling while it is smaller in optimal control with state feedback and output regulation with measurement feedback. However, it tracks the reference speed more quickly with state feedback than with measurement feedback. This is because of the application of the observer in the latter, which needs some time to track the state of the train. Coincidentally for the same reason, the in-train forces in Fig. 4.2 are smaller than those of the other two in the steady state. This is because the slower response of the observer leads to more gentle output.

Table 4.1 shows the simulation results of the state feedback controllers $S_i, i = 1, 2, 3, 4$ advanced in Section 3.5 and measurement feedback controllers $M_i, i = 1, 2, 3, 4$ proposed in this chapter with different tuning parameters. The indices $1, 2, 3, 4$ denote the different sets of parameters $(K_e, K_f, K_v) = (1, 1, 1)$, $(K_e, K_f, K_v) = (1, 1, 10)$, $(K_e, K_f, K_v) = (1, 10, 1)$, $(K_e, K_f, K_v) = (100, 1, 1)$. $|\delta\bar{v}|$ is the absolute value of the

Table 4.1: Performance comparison

	$\lvert\delta\bar{v}\rvert$(m/s)			$\overline{\lvert f_{in}\rvert}$(kN)			E
	max	mean	std	max	mean	std	(MJ)
S1	3.0182	0.3166	0.48	454.50	97.40	86.44	16,528
S2	3.0225	0.2443	0.50	408.70	74.07	76.34	16,524
S3	3.0090	0.3667	0.47	405.70	70.77	78.04	15,007
S4	3.2470	0.4918	0.47	297.27	78.90	63.27	13,422
M1	2.9827	0.3250	0.53	322.02	56.49	63.54	12,400
M2	2.9801	0.2969	0.53	329.39	54.28	65.28	12,713
M3	2.9692	0.3290	0.52	329.00	56.74	64.14	12,570
M4	3.6094	0.8942	0.62	405.34	98.41	73.50	10,493

difference between the reference velocity and the mean value of all the cars' velocities at a specific point. $\overline{|f_{in}|}$ is the mean value of the absolute values of all the couplers' in-train forces at a specific point. The items max, mean and std are the maximum value, mean value and standard deviation of the statistical variable.

These data reflect the working of the optimization parameters. From Table 4.1, it can be seen that more energy is consumed in the optimal controller with state feedback than in output regulating controller with measurement feedback, no matter which group of the optimal parameters is chosen. This is because the optimal controllers of state feedback are sensitive to the state deviation from the equilibrium, and the energy optimization is local, thus the locomotives' traction efforts and the cars' braking are more frequent, which leads to the consumption of more energy.

For speed tracking, the optimal controller with state feedback is a little better than the output regulating controller with measurement feedback, and for in-train forces, the former is worse than the latter. This confirms the above result, by comparing Fig. 3.14 and Fig. 4.2.

In the above chapter, it is said that the length of the track does not affect the result in this thesis. To show this, the above speed regulator will be simulated on a longer track (27 km), as indicated in Fig. 4.3. The simulation result is reflected in Fig. 4.4.

From Fig. 4.4, it can be seen that the train tracks the reference speed well except within the distance from 18 km to 21 km, where the train speed is much lower than the reference speed. This is because the train is passing over a hill during this period, which can be seen from Fig. 4.3. Because of the operational constraint (the time delay between two notch changes), the train has enough traction power to maintain or be closer to the reference speed.

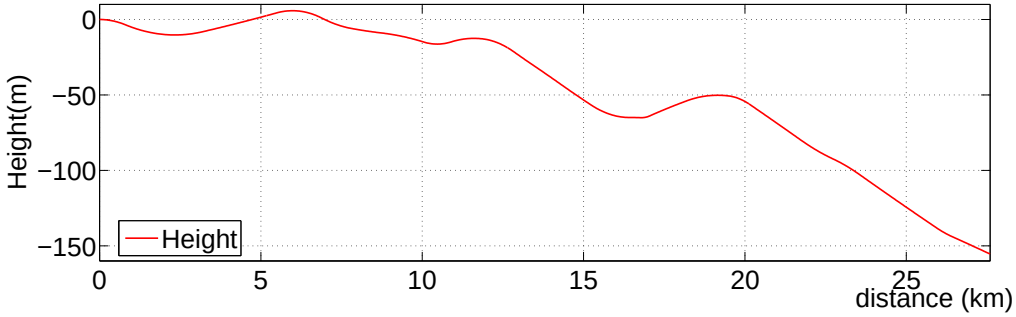

Figure 4.3: A longer track profile

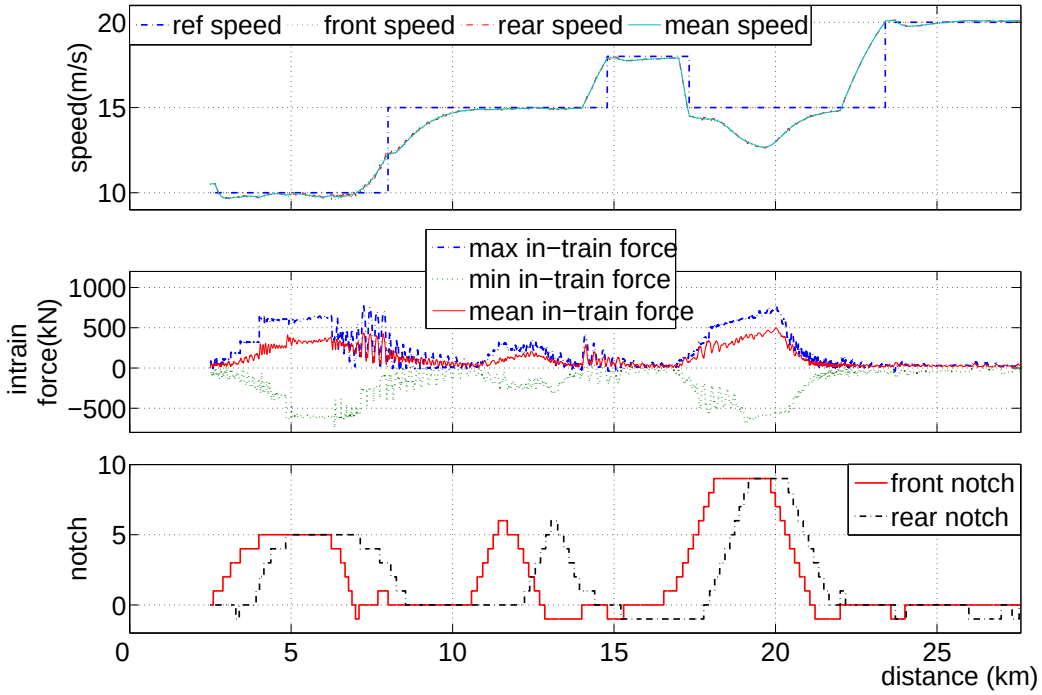

Figure 4.4: Speed regulation on a longer track profile

4.4 Conclusion

In this chapter, a framework is introduced to solve the output regulation problem using measurement feedback.

The measurement feedback is considered because the measurement can cover the output and/or (partial) state, even some measurable output different from the output and state, that is, it is more general.

This framework can also incorporate different kinds of exosystems with bounded signal or unbounded signal, Poisson stable or not. Some assumptions in this chapter are necessary.

Similar to [43] and [44], the solvability of the output regulation problem is transformed to the solvability of the corresponding stabilization problem. The difference is that in this chapter a stabilizer is firstly designed assuming the states of the exosystem are known, and then an internal model is designed with respect to this stabilizer and a steady-state generator. The internal model is in nature an observer of the state of the exosystem. The existence of the stabilizer is sometimes a necessary condition for the solvability of the output problem. The properties of the internal model, in which the state of the stabilizer and the measurement of the original system can appear, are also given.

It should be pointed out that not all stabilizers have the corresponding internal models. Sometimes the parameters in the stabilizer and the internal model candidate need to be tuned. The design techniques of the internal model, in essence an observer for nonlinear systems, are not detailed, nor are the design techniques of the stabilizer, which are out of the scope of this study.

The application of output regulation of nonlinear systems with measured output feedback to the control of heavy haul trains is investigated in section 4.3. The optimal scheduling of the open loop controller is still based on "trading off" the equilibria. Thus the balance between energy consumption and in-train forces is still maintained. For closed-loop control, speed regulation is imposed. This approach to design is practically feasible and manageable, and by its nature, is also easily integrable with human drivers, because the human drivers drive the train according to the train's speed.

Instead of the linear system theory, a nonlinear system theory is adopted so that without a linear approximation philosophy, the control is closer to the reality. Another advantage of the approach is the assumption that only the locomotives' speeds are available for measurement.

A controller of speed regulator is designed based on the result mentioned in the first part of this chapter. The conditions of the application are verified. In the controller design, Optimal scheduling is retained in the control of output regulation. It is noted

that when the difference system is changed with the variation of the reference speed, the state of the observer is changed suddenly and sufficient time should be given to the observer to track the state of the difference system, and thus the control of the output regulation is disabled during this period. Simulation shows the feasibility of the output regulating controller with only measurement of the locomotive speeds, in terms of its simplicity, cost-effectiveness and its implementation convenience.

Chapter 5

Fault-tolerant control

5.1 Introduction

In the existing papers on train handling as well as the previous chapters, all the controllers are designed on the assumption that the train is well set up and all the actuators (traction efforts and braking efforts of locomotives and wagons) and sensors (speed sensors) work as designed, which is an ideal condition. In practice, some of the actuators and/or sensors may be faulty, and even worse, the train structure may be changed. For example, the speed sensor has a constant bias, or the amplifier in the sensor circuit has a fault, which leads to a gain fault of the sensor. The air pressure in the braking pipe may be different from expected because of a fault in the pressure sensor in the air recharge system or air leakage, which makes the braking forces acting on the wheels less than expected. When a fault happens, the controller, designed on the basis of the faultless train model, cannot work as well as expected, and sometimes it even leads to unsafe running, such as train-breaking and derailment, *i.e.,* the safe running of trains cannot be promised. Some safe running methods are therefore necessary in train handling.

Actually, in some fault modes of train handling, it is possible to assure train performance with suitably redesigned controllers. That is what is studied in this chapter.

In nature, the above-mentioned controller redesign is a fault-tolerant control problem. In the literature, there are many papers about such problems. Some survey papers, such as [48, 49, 50, 51, 52, 53, 54, 55], provide excellent reviews on the subject of fault-tolerant control. For linear systems, geometric approaches are proposed for fault detection and isolation (FDI), e.g. in [56, 57, 58]. A combined input-output and local approach is proposed in [59] for the problem of FDI of nonlinear systems modelled by polynomial differential-algebraic equations. A high-gain observer-based approach for FDI of an affine nonlinear system is advanced in [60], where a sufficient condition is

given. In [61], a geometric approach to FDI of nonlinear systems is proposed, while a necessary condition for the existence of FDI is exploited based on a geometric concept– *unobservability distribution* introduced by the authors in [62]. For the solution of FDI, a sufficient condition is also given. A stability- and performance-vulnerable failure of sensors can be identified with the approach in [63] for nonlinear systems. The switch between two robust control strategies based on normal operation and faulty operation is used to realize fault-tolerant control. An information-based diagnostic approach is investigated in [64] for a class of SISO nonlinear system in a triangular structure. In [65], a fault diagnosis approach is proposed based on adaptive estimation by combining a high gain observer and a linear adaptive observer. As is known, the high-gain observer is sensitive to measurement noise. In speed regulation of heavy haul trains with measurement (speeds) feedback, noise is inevitable, so a high-gain observer is not considered in this study. Recently, compared to [61], a relaxed formulation of FDI of nonlinear systems is proposed in [66], where a residual has been designed to detect a set of faults.

In train handling, such problems have been investigated in [69, 70] for some faults with induction motors. The fault detection and isolation of diesel engines are seen in [67, 68]. Paper [70] is in essence on fault-tolerant control of the induction motor, which can also be seen in [71]. In this chapter, the fault-tolerant control of the whole train is studied. The faulty modes of a train include the gain faults of speed sensors, the locomotive actuators (induction motors, in this study), and wagon actuators (the braking systems). The locomotive fault signal is assumed to be acquired from other FDIs and is available in its fault-tolerant controller redesign. Based on the train model and fault modes, a fault-tolerant speed regulator (including the FDI part and FTC part) is designed for the faults of sensors and braking systems, respectively. The fault-tolerant speed regulator of sensors' faults is based on the approach in [61], while the fault-tolerant speed regulator of the braking system fault is based on steady state calculation.

In this chapter, a geometric approach to fault detectability is quoted from [61] in section 5.2. The approach in [61] is employed for the FDI of sensor faults. Then the fault modes of train handling are assumed with sensor faults and actuator faults, respectively. Considering the convenience of application considered, the sensor equipment structure of a train is suggested and the train structure is assumed for the subsequent study. The third part, the application condition of the result in section 5.2, is justified for the speed sensors as well as for the wagon actuators. An FDI for the sensor faults is designed on the basis of the approach in [61] and an FDI for the wagon actuator faults is designed on the basis of an approach proposed in this thesis. Based on the fault signals, the fault-tolerant controller is very convenient to be redesigned. Simulation for the proposed approaches is also given in the last part of this chapter.

5.2 Fault detectability

Based on a concept of the *observability co-distribution* in [62], a geometric approach is proposed in [61] for the fault detection problem of nonlinear systems. This approach will be adopted to justify the detectability of the train faults.

Consider a nonlinear system in the following form,

$$\begin{aligned} \dot{x} &= f(x) + g(x)u + l(x)u_f + p(x)w, \\ y &= h(x), \end{aligned} \tag{5.1}$$

where $x \in X \subset R^n$ is the state with X a neighbourhood of the origin, $u \in R^{m_u}$ is the control input, $u_f \in R$ is a fault signal (input), $w \in R^d$ is the disturbance and/or other fault signals, and $y \in R^q$ is the output. $g(x) = [g_1(x), \cdots, g_{m_u}(x)]$ and it is assumed $g_0(x) = f(x)$. $p(x) = [p_1(x), \cdots, p_d(x)]$. The vector fields $g_i(x), i \in [0, m_u], p_j(x), j \in [1, d], h(x)$ are assumed to be smooth and $f(0) = 0, h(0) = 0$.

The task of fault detection is to design a filter (*residual generator*) in the form of

$$\begin{aligned} \dot{\hat{x}} &= \hat{f}(\hat{x}, y) + \hat{g}(\hat{x}, y)u, \\ r &= \hat{h}(\hat{x}, y), \end{aligned} \tag{5.2}$$

where $\hat{x} \in \hat{X} \subset R^{\hat{n}}$, $r \in R^{\hat{q}}, \hat{q} \leq q$, and the vector fields $\hat{f}(\hat{x}, y), \hat{g}(\hat{x}, y), \hat{h}(\hat{x}, y)$ are smooth and $\hat{f}(0, 0) = 0, \hat{h}(0, 0) = 0$ such that the output r of the cascade system composed of (5.1) and (5.2) depends only on the fault signal u_f, is decoupled from the disturbance w and asymptotically converges to zero whenever u_f is identically zero with any input u.

This problem is formulated in a geometric concept in [61].

The system (5.1) can be rewritten as follows without the fault and disturbance signals considered:

$$\begin{aligned} \dot{x} &= g_0(x) + \sum_{i=1}^{m_u} g_i(x)u_i, \\ y &= h(x). \end{aligned} \tag{5.3}$$

Based on this system, some concepts are given below.

$\ker\{dh\}$ is the distribution annihilating the differentials of the rows of the mapping $h(x)$.

$\text{span}\{dh\}$ is the co-distribution spanned by the differentials of the rows of the mapping $h(x)$.

A distribution Δ is said to be conditioned invariant ((h, f) invariant, $f = g_0$) of the

system (5.3) if it satisfies

$$[g_i, \Delta \cap \ker\{dh\}] \subset \Delta, \forall i \in [0, m_u], \tag{5.4}$$

A co-distribution Ω is said to be conditioned invariant if

$$L_{g_i}\Omega \subset \Omega + \text{span}\{dh\}, \forall i \in [0, m_u]. \tag{5.5}$$

The symbol Ω_o denotes the smallest co-distribution invariant under $g_i, i \in [0, m_u]$ which contains $\text{span}\{dh\}$.

The cascade system of (5.1) and (5.2) can be written as

$$\begin{aligned} \dot{x}^e &= g_0^e(x^e) + \sum_{i=1}^{m_u} g_i^e(x^e)u_i + l^e(x^e)u_f + \sum_{i=1}^{d} p_i^e(x^e)w_i, \\ r &= h^e(x^e), \end{aligned} \tag{5.6}$$

where $x^e = \begin{pmatrix} x \\ \hat{x} \end{pmatrix}$, $g_0^e(x^e) = \begin{pmatrix} f(x) \\ \hat{f}(\hat{x}, h(x)) \end{pmatrix}$, $g_i^e(x^e) = \begin{pmatrix} g_i(x) \\ \hat{g}_i(\hat{x}, h(x)) \end{pmatrix}, i \in [1, m_u]$,
$l^e(x^e) = \begin{pmatrix} l(x) \\ 0 \end{pmatrix}$, $p_i^e(x^e) = \begin{pmatrix} p_i(x) \\ 0 \end{pmatrix}, i \in [1, d]$,

$h^e(x^e) = \hat{h}(\hat{x}, h(x))$. Let Ω_o^e denote the smallest co-distribution invariant under $g_i^e, i \in [0, m]$ which contains $\text{span}\{dh^e\}$.

The local nonlinear fundamental problem of residual generation (lNLFPRG) can be formulated in a geometric way [61].

Problem: Given a system (5.1)*, find, if possible, a dynamic system in the form of* (5.2) *such that the smallest co-distribution invariant* Ω_o^e *defined in* (5.6) *satisfies*

i) $\text{span}\{p_1^e, \cdots, p_d^e\} \subset (\Omega_o^e)^\perp$;

ii) $\text{span}\{l^e\} \not\subset (\Omega_o^e)^\perp$;

iii) there exists a neighbourhood of $X^e \in R^{n+\hat{n}}$ *containing the origin, such that the output* r *of system* (5.6) *asymptotically converges to zeros when* $u_f(t) = 0$ *and* $x^e(0) \in X^e$.

The fault detectability of nonlinear systems is incorporated with the *conditioned invariant distribution* and *observability co-distribution* [61].

An algorithm is given in [61] for a conditioned invariant distribution for the system (5.3) as follows. The nondecreasing sequence of distributions is defined:

$$\begin{aligned} S_0 &= \bar{P}, \\ S_{k+1} &= \bar{S}_k + \sum_{i=0}^{m_u} [g_i, \bar{S}_k \cap \ker\{dh\}], \end{aligned} \tag{5.7}$$

where $P = \text{span}\{p_1(x), \cdots, p_d(x)\}$ and $\bar{S}$ denotes the involutive closure of S. Then the following lemma holds.

Lemma. Suppose there exists an integer k^* such that

$$S_{k^*+1} = \bar{S}_{k^*}, \tag{5.8}$$

and set $\Sigma_*^P = \bar{S}_{k^*}$. Then Σ_*^P is involutive, contains P and is the smallest conditioned invariant.

One can see that $(\Sigma_*^P)^\perp$ is the maximal conditioned invariant co-distribution, which is locally spanned by exact differentials and contained in $P^\perp$.

An algorithm is also given for an observability co-distribution of the system (5.3). Let Θ be a fixed co-distribution and define the following nondecreasing sequence of co-distributions

$$\begin{aligned} Q_0 &= \Theta \cap \text{span}\{dh\}, \\ Q_{k+1} &= \Theta \cap \left(\sum_{i=0}^{m_u} L_{g_i} Q_k + \text{span}\{dh\} \right). \end{aligned} \tag{5.9}$$

Suppose that all co-distributions of this sequence are nonsingular, so that there exists an integer $k^* \leq n-1$ such that $Q_k = Q_{k^*}, \forall k > k^*$, and set $\Omega^* = \Omega_{k^*} = o.c.a(\Theta)$, where "o.c.a" stands for "observability co-distribution algorithm". Then the following holds.

Proposition. Suppose all the co-distributions generated by the algorithm above are nonsingular. Then repeat the algorithm above with $\Theta' = o.c.a(\Theta)$, that is,

$$\begin{aligned} Q_0 &= \Omega^* \cap span\{dh\}, \\ Q_{k+1} &= \Omega^* \cap \left(\sum_{i=0}^{m_u} L_{g_i} Q_k + span\{dh\} \right). \end{aligned} \tag{5.10}$$

As a consequence, $\Omega^* = o.c.a(\Omega^*)$. If the co-distribution Θ is conditioned invariant, so is Ω^*.

A co-distribution Ω is said to be an observability co-distribution for the system (5.3) if

$$\begin{aligned} &L_{g_i}\Omega \subset \Omega + \text{span}\{dh\}, \forall i \in [0, m_u], \\ &o.c.a(\Omega) = \Omega. \end{aligned} \tag{5.11}$$

A distribution Δ is an unobservability distribution if its annihilator $\Omega = (\Delta)^{\perp}$ is an observability co-distribution.

Also it is true that the co-distribution $o.c.a(\Theta)$ is the maximal observability co-distribution contained in Θ. If the distribution Σ_*^P is well-defined and nonsingular, and $\Sigma_*^P \cap \ker\{dh\}$ is a smooth co-distribution, then
$o.c.a((\Sigma_*^P)^{\perp})$ is the maximal observability co-distribution, which is locally spanned by exact differentials and contained in $P^{\perp}$.

A necessary condition for the solvability of lNLFPRG is that

$$\text{span}\{l\} \not\subset \left(o.c.a(\Sigma_*^P)^{\perp})\right)^{\perp}. \tag{5.12}$$

A sufficient condition is also given in [61].

Consider a system (5.1), determine the co-distribution $o.c.a(\Sigma_*^P)^{\perp})$, the largest observability co-distribution locally spanned by exact differentials and contained in $P^{\perp}$, and suppose the necessary condition (5.12) is satisfied. Then the system (5.1) can be rewritten as follows

$$\begin{aligned}
\dot{z}_1 &= f_1(z_1, z_2) + g_1(z_1, z_2)u + l_1(z_1, z_2, z_3)u_f, \\
\dot{z}_2 &= f_2(z_1, z_2, z_3) + g_2(z_1, z_2, z_3)u, \\
\dot{z}_3 &= f_3(z_1, z_2, z_3) + g_3(z_1, z_2, z_3)u, \\
y_1 &= h_1(z_1), \\
y_2 &= z_2,
\end{aligned} \tag{5.13}$$

with a coordinate change

$$z = \Phi(x) = \begin{pmatrix} z_1 \\ z_2 \\ z_3 \end{pmatrix} = \begin{pmatrix} \Phi_1(x) \\ H_2 h(x) \\ \Phi_3(x) \end{pmatrix}, \tag{5.14}$$

where $\Phi(x)$ is determined as described below.

When the fault signal and the disturbance signals are not considered, the system (5.1) is the one (5.3). Consider this system, let Ω be an observability co-distribution and $n_1 = \dim(\Omega)$. Suppose Ω is spanned by exact differentials and $\text{span}\{dh\}$ is nonsingular. $q - n_2 = \dim(\Omega \cap \text{span}\{dh\})$. Suppose there exists a surjection $\Psi_1 : R^p \to R^{p-n_2}$ such that

$$\Omega \cap \text{span}\{dh\} = \text{span}\{d(\Psi_1 \circ h)\}.$$

At $x^o \in X$, a neighourhood of the origin ($y^o = h(x^o)$), there exists a selection matrix H_2 (*i.e.,* a matrix in which any row has all zero entries but one, which is equal to one) such that

$$\Psi(y) = \begin{pmatrix} y_1 \\ y_2 \end{pmatrix} = \begin{pmatrix} \Psi_1(y) \\ H_2 y \end{pmatrix} \tag{5.15}$$

is a local diffeomorphism at $y^o \in R^p$. Choose a function $\Phi_1 : U^o \to R^{n_1}$, where U^o is a neighbourhood of x^o, such that in U^o,

$$\Omega = \text{span}\{d\Phi_1\}.$$

Then there exists a function $\Phi_3 : U^o \to R^{n-n_1-n_2}$ such that $\Phi(x)$ in (5.14) is a local diffeomorphism at $x^o \in U^o$. With this coordinate change, the system (5.3) is described in the following form,

$$\begin{aligned}
\dot{z}_1 &= f_1(z_1, z_2) + g_1(z_1, z_2)u \\
\dot{z}_2 &= f_2(z_1, z_2, z_3) + g_2(z_1, z_2, z_3)u, \\
\dot{z}_3 &= f_3(z_1, z_2, z_3) + g_3(z_1, z_2, z_3)u, \\
y_1 &= h_1(z_1), \\
y_2 &= z_2.
\end{aligned} \tag{5.16}$$

If $p(x)$ is a vector field in the annihilator of Ω, (which is true when $\Omega \subseteq \Sigma_*^P$,) and the condition (5.12) is satisfied, then in the new coordinates, the system (5.1) is in the form

$$\begin{aligned}
\dot{z}_1 &= f_1(z_1, z_2) + g_1(z_1, z_2)u + l_1(z_1, z_2, z_3)u_f, \\
\dot{z}_2 &= f_2(z_1, z_2, z_3) + g_2(z_1, z_2, z_3)u + l_2(z_1, z_2, z_3)u_f + p_2(z_1, z_2, z_3)w, \\
\dot{z}_3 &= f_3(z_1, z_2, z_3) + g_3(z_1, z_2, z_3)u + l_3(z_1, z_2, z_3)u_f + p_3(z_1, z_2, z_3)w, \\
y_1 &= h_1(z_1), \\
y_2 &= z_2.
\end{aligned} \tag{5.17}$$

It is very interesting to study the following z_1-system of (5.16), which is *locally weakly observable* with inputs u, y_1, and y_2 if $g_1(z_1, z_2)$ is a sum of a vector field of z_1 and a vector field of z_2.

$$\begin{aligned}
\dot{z}_1 &= f_1(z_1, y_2) + g_1(z_1, y_2)u, \\
y_1 &= h_1(z_1).
\end{aligned} \tag{5.18}$$

The following system is also locally weakly observable,

$$\begin{aligned}
\dot{z}_1 &= f_1(z_1, y_2) + g_1(z_1, y_2)u + l_1(z_1, z_2, z_3)u_f, \\
y_1 &= h_1(z_1).
\end{aligned} \tag{5.19}$$

As assumed in (5.12), $l_1(z_1, z_2, z_3)$ is non-zero. So the occurrence of the fault signal u_f may be detected by an appropriate observer.

5.3 Fault modes of trains

The previous train model is repeated as follows,

$$\begin{aligned}
m_i\dot{v}_i &= u_i + f_{in_{i-1}} - f_{in_i} - f_{a_i}, \qquad i = 1, \cdots, n, \\
\dot{x}_j &= v_j - v_{j+1}, \qquad j = 1, \cdots, n-1.
\end{aligned} \tag{5.20}$$

With open loop scheduling, one can get the equilibria. Then a difference system between the train model and the equilibria is as (3.21), which can be rewritten as

$$\begin{aligned} \delta\dot{v} &= f_{11}(\delta v) + A_{12}\delta x + B\delta u, \\ \delta\dot{x} &= A_{21}\delta v. \end{aligned} \tag{5.21}$$

where $\delta v = col(\delta v_1, \ ..., \delta v_n)$, $\delta x = col(\delta x_1, \ ..., \delta x_{n-1})$, $f_{11}(\delta v) = [f_{11}^1(\delta v_1), \ ..., f_{11}^n(\delta v_n)]^T$ in which $f_{11}^i(\delta v_i) = (c_{1_i} + 2c_{2_i}v_r)\delta v_i + c_{2_i}\delta v_i^2$,

$$B = \text{diag}(\frac{1}{m_1}, \cdots, \frac{1}{m_n}),$$

$$A_{12} = \begin{bmatrix} -\frac{k_1}{m_1} & 0 & \cdots & 0 & 0 \\ \frac{k_1}{m_2} & -\frac{k_2}{m_2} & \cdots & 0 & 0 \\ \cdots & \cdots & \cdots & \cdots & \cdots \\ 0 & \cdots & 0 & \frac{k_{n-2}}{m_{n-1}} & -\frac{k_{n-1}}{m_{n-1}} \\ 0 & \cdots & 0 & 0 & \frac{k_{n-1}}{m_n} \end{bmatrix},$$

$$A_{21} = \begin{bmatrix} 1 & -1 & 0 & \cdots & 0 & 0 \\ 0 & 1 & -1 & \cdots & 0 & 0 \\ \cdots & \cdots & \cdots & \cdots & \cdots & \cdots \\ 0 & 0 & 0 & \cdots & 1 & -1 \end{bmatrix}.$$

The variables $k_i, \ i = 1, \cdots, n-1$ are chosen to be constant.

In this thesis, the fault modes include speed senor faults and actuator faults.

5.3.1 Speed sensor faults

The states of a train include the speeds of cars and the relative displacement of the couplers (in-train forces). It is practical to measure the speeds of cars. The speed sensor may be faulty with a constant bias, and/or with a gain fault due to the gain change of the amplifier in the circuit. In the former case, such a fault can be corrected by the calibration before its application. In this chapter, the latter case is considered, that is, the sensor for the ith car's speed is faulty with a gain fault,

$$v_i = (1 + m_{v_i}^f)v_i^o, \tag{5.22}$$

where the variable v_i is the sensor output for the ith car's speed, v_i^o is the real speed, and $m_{v_i}^f$ is the constant gain fault of the sensor.

Assuming there are q sensors equipped for q cars of the train, and they are located at the positions $ls_1, \cdots, ls_q$, then, the dynamics of a train with speed measurement

(5.21) is as follows,

$$\begin{aligned} \delta\dot{v} &= f_{11}(\delta v) + A_{12}\delta x + Bu, \\ \delta\dot{x} &= A_{21}\delta v, \\ y_i &= (1 + m^f_{v_{ls_i}})v_{ls_i} - v_r, \qquad i = 1, \cdots, q, \end{aligned} \tag{5.23}$$

where the variable $m^f_{v_{ls_i}}$ is the constant gain fault of the ith sensor.

5.3.2 Actuator faults

The actuators of a train include the locomotives' engines (traction efforts or dynamic braking forces) and the wagons' brakes (braking efforts). However, the actuators are sometimes faulty. For example, one locomotive in a locomotive group (composed of n_l locomotives) does not work, then the actual output of the locomotive group is $\frac{n_l-1}{n_l}$ of the expected. The air pressure in the braking pipe is sometimes different from the designed one owing to air leakage or a fault of the pressure sensor in the air recharging system, which leads to less braking effort in the braking system. In train handling, every locomotive has its own engine, whose running condition is independent with the others while all wagons share the same braking pressure in the air pipe along the train, whose fault leads to the same faults on all wagons.

In the above cases, the outputs of the actuators may not be equal to those expected, but proportional to the expected ones, *i.e.,*

$$u^f_i = (1 - m^i_f)u_i, \qquad i = 1, \cdots, n, \tag{5.24}$$

in which u_i, u^f_i are expected output and real output, respectively. The output includes the open loop part u^o_i and the closed-loop part U_i. The coefficient m^i_f is a fault coefficient. In (5.24), $0 \leq m^i_f \leq 1$.

In the following analysis, one assumes the locomotives' faults are independent and the wagons' faults are the same, *i.e.,*

$$\begin{aligned} u^f_{l_i} &= (1 - m^{l_i}_f)u_{l_i}, \quad i = 1, \cdots, k, \\ u^f_j &= (1 - m^w_f)u_j, \quad j = 1, \cdots, n, j \neq l_i. \end{aligned} \tag{5.25}$$

5.4 Fault detection and isolation

5.4.1 Sensor fault detection and isolation

The sensors in train handling are the speed sensors. When the faults of these sensors are considered and viewed as pseudo-actuators' faults, the train model described in

(5.23), is as follows.

$$\begin{aligned}
\delta\dot{v} &= f_{11}(\delta v) + A_{12}\delta x + BU,\\
\delta\dot{x} &= A_{21}\delta v,\\
\dot{v}^f_{ls_i} &= -v^f_{ls_i} + u^f_{ls_i} v_{ls_i},\\
y_i &= \delta v_{ls_i} + v^f_{ls_i}, \qquad i = 1, \cdots, q,
\end{aligned} \tag{5.26}$$

where $u^f_{ls_i}$ is the pseudo-actuator of the sensor fault. When there is no fault with the sensor, *i.e.*, $v^f_{ls_i} = 0$, the dynamics are $\dot{v}^f_{ls_i} = -v^f_{ls_i} + u^f_{ls_i} v_{ls_i}$, in which $u^f_{ls_i}$ must be zero. When there is a fault with the sensor, *i.e.*, $v^f_{ls_i} \neq 0$, one has $u^f_{ls_i} = \frac{v^f_{ls_i}}{v_{ls_i}} \neq 0$ in steady state. So $u^f_{ls_i}$ can be thought of as the sensor fault signal.

In the previous chapter, it is assumed that there is a speed sensor for the first car (usually a locomotive). It is convenient to assume that this sensor is always in good condition and the output of this sensor is y_1, which can be guaranteed by some hardware structures, for example, a hardware redundancy. With this assumption, for every sensor fault mode (the output of this sensor is $y_i, i = 2, \cdots, q$), the train is modelled as

$$\begin{aligned}
\delta\dot{v} &= f_{11}(\delta v) + A_{12}\delta x + BU,\\
\delta\dot{x} &= A_{21}\delta v,\\
\dot{v}^f_{ls_i} &= -v^f_{ls_i} + u^f_{ls_i} v_{ls_i},\\
y_1 &= \delta v_1,\\
y_i &= \delta v_{ls_i} + v^f_{ls_i}, \qquad i = 2, \cdots, q.
\end{aligned} \tag{5.27}$$

When the ith sensor fault $u^f_{ls_i}$ is considered as u_f in (5.1), the other sensor faults ($u^f_{ls_j},\ j \in [2, q],\ j \neq i$) are thought as w in (5.1) to be decoupled. Then in the form of (5.1), one has $x = [\delta v, \delta x, v^f_{ls}]^T$, $u = U$, $u_f = u^f_{ls_i}$, $w = (u^f_{ls_j}), j \in [2, q], j \neq i$,

$$f(x) = \begin{bmatrix} f_{11}(\delta v) + A_{12}\delta x \\ A_{21}\delta v \end{bmatrix},$$

$$g(x) = B,$$

$$l(x) = [\overbrace{0, \cdots, 0}^{n-2+i}, v_{ls_i}, \overbrace{0, \cdots, 0}^{q-i}]^T,$$

$$p_j(x) = [\overbrace{0, \cdots, 0}^{n-2+j}, v_{ls_j}, \overbrace{0, \cdots, 0}^{q-j}]^T, j \in [2, q], j \neq i,$$

and

$$h(x) = \begin{bmatrix} \delta v_1 \\ \delta v_{ls_2} \\ \cdots \\ \delta v_{ls_q} \end{bmatrix}.$$

For the system (5.27), assuming the co-distribution

$$\Theta = \Omega_0 = \text{span}\{d(\delta v_1), \cdots, d(\delta v_n), d(\delta x_1), d(\delta x_{n-1})\}$$

in the observability co-distribution algorithm (5.9), one has,

$$\begin{aligned}
\text{span}\{dh\} &= \text{span}\{d(\delta v_1), d(\delta v_{ls_2} + v^f_{ls_2}), \cdots, d(\delta v_{ls_q} + v^f_{ls_q})\},\\
Q_0 &= \Omega_0 \cap \text{span}\{dh\} = \text{span}\{d(\delta v_1)\},\\
\bar{Q}_0 &= \sum_{i=0}^{m} L_{g_i} Q_0 + \text{span}\{dh\}\\
&= \text{span}\{d(\delta v_1), d(\delta x_1), d(\delta v_{ls_2} + v^f_{ls_2}), \cdots, d(\delta v_{ls_q} + v^f_{ls_q})\},\\
Q_1 &= \Omega_0 \cap \bar{Q}_0 = \text{span}\{d(\delta v_1), d(\delta x_1)\},\\
\bar{Q}_1 &= \sum_{i=0}^{m} L_{g_i} Q_1 + \text{span}\{dh\}\\
&= \text{span}\{d(\delta v_1), d(\delta v_2), d(\delta x_1), d(\delta v_{ls_2} + v^f_{ls_2}), \cdots, d(\delta v_{ls_q} + v^f_{ls_q})\},\\
Q_2 &= \Omega_0 \cap \bar{Q}_1 = \text{span}\{d(\delta v_1), d(\delta v_2), d(\delta x_1)\},\\
&\cdots,\\
Q_{2n-1} &= \text{span}\{d(\delta v_1), \cdots, d(\delta v_{n-1}), d(\delta x_1), \cdots, d(\delta x_{n-1})\},\\
\bar{Q}_{2n-1} &= \sum_{i=0}^{m} L_{g_i} Q_1 + \text{span}\{dh\} = \text{span}\{d(\delta v_1), \cdots, d(\delta v_n),\\
&\quad d(\delta x_1), \cdots, d(\delta x_{n-1}), d(\delta v_{ls_2} + v^f_{ls_2}), \cdots, d(\delta v_{ls_q} + v^f_{ls_q})\},\\
Q_{2n} &= \text{span}\{d(\delta v_1), \cdots, d(\delta v_n), d(\delta x_1), \cdots, d(\delta x_{n-1})\}.
\end{aligned}$$

Then $Q_k = Q_{2n}, \forall k > 2n$, which results in $o.c.a(\Omega_0) = Q_{2n} = \Omega_0$.

Considering the co-distribution $\Omega = \Omega_0 + \text{span}\{d(v^f_{ls_j})\}$, *i.e.*,

$$\Omega = \text{span}\{d(\delta v_1), \cdots, d(\delta v_n), d(\delta x_1), d(\delta x_{n-1}), d(v^f_{ls_j})\}, \forall j \in [2, q],$$

one has $o.c.a(\Omega) \supseteq o.c.a(\Omega_0)$.

Then from (5.10), one has $Q'_i \supseteq Q_i$ and $\bar{Q}'_i \supseteq \bar{Q}_i$ where $\bar{Q}'_i$ and Q'_i are the calculation results with Ω and $\bar{Q}_i$ and Q_i with Ω_0. Then one has $\bar{Q}'_{2n-1} \supseteq \bar{Q}_{2n-1}$ and furthermore

$$\begin{aligned}
Q'_{2n} &= (\Omega \cap \bar{Q}'_{2n-1})\\
&\supseteq (\Omega \cap \bar{Q}_{2n-1})\\
&= \text{span}\{d(\delta v_1), \cdots, d(\delta v_n), d(\delta x_1), d(\delta x_{n-1}), d(v^f_{ls_j})\}\\
&= \Omega,
\end{aligned}$$

which means $o.c.a(\Omega) \supseteq Q'_{2n} \supseteq \Omega$. As is known, $o.c.a(\Omega) \subseteq \Omega$, so $o.c.a(\Omega) = \Omega$.

Furthermore, one has

$$L_{g_j}\Omega \subset \Omega = \Omega + \text{span}\{dh\}, \forall j \in [0, m]. \tag{5.28}$$

The conditions in (5.11) are satisfied, *i.e.,* Ω is an observability co-distribution.

It is obvious that the vector field $p_j, j \in [2,p], j \neq i$ is in the annihilator of Ω while $\text{span}\{l\} \subset \Omega$. So it is possible to transform the train dynamics with sensor faults (5.27) into the form of (5.17), which means the possibility of fault detection of ith sensor fault.

A residual generator for the ith sensor can be in the following form,

$$\begin{aligned}
\dot{\xi}_1 &= f_{11}(\xi_1) + A_{12}\xi_2 + BU + L_{11}(y_1 - \xi_{11}) + L_{13}(y_i - \xi_{1,ls_i}),\\
\dot{\xi}_2 &= A_{21}\xi_1 + L_{21}(y_1 - \xi_{11}) + L_{23}(y_i - \xi_{1,ls_i}),\\
\dot{\xi}_3 &= -\xi_3 + L_{31}(y_1 - \xi_{11}) + L_{33}(y_i - \xi_{1,ls_i}),\\
r_i &= (y_i - \xi_{1,ls_i})/(v_r + \xi_{1,ls_i}), \qquad i \in [2,p].
\end{aligned} \tag{5.29}$$

where $\xi_1 = col(\xi_{11}, \cdots, \xi_{1n}) \in R^n, \xi_2 = col(\xi_{21}, \cdots, \xi_{2,n-1}) \in R^{n-1}, \xi_3 \in R$. In the above equation, L_{ij} are chosen by observer design approaches, such as pole placement (Luenberger observer) or optimization control (Kalman filter).

Especially, when $L_{13} = 0, L_{23} = 0$, it is also possible for the above form of dynamics to be a residual generator, because the original system without the faulty output is also observable, which has been proved in the previous chapter. It is very interesting to observe that this residual generator is naturally a fault identifier because the fault signal does not affect the states ξ_1, ξ_2, and the residual signal is actually the identifier signal of the fault. Furthermore, in this way, the residual generators and identifiers of all the sensor faults can share the same dynamics with different outputs, *i.e.,*

$$\begin{aligned}
\dot{\xi}_1 &= f_{11}(\xi_1) + A_{12}\xi_2 + BU + L_{11}(y_1 - \xi_{11}),\\
\dot{\xi}_2 &= A_{21}\xi_1 + L_{21}(y_1 - \xi_{11}),
\end{aligned} \tag{5.30}$$

and the output (a residual generator as well as a identifier) for the ith sensor fault is

$$r_i = \frac{y_2 - \xi_{1,ls_i}}{\xi_{1,ls_i} + v_r}. \tag{5.31}$$

5.4.2 Actuator fault detection and isolation

A locomotive group effort is sometimes not the same as the expected one for some reasons, such as one locomotive of the locomotive group not working. The braking efforts of wagons may be different from the expected, because of the pressure change in the braking pipe. In the following, only the fault modes as in (5.24) are studied.

When this happens, the efforts of the cars are proportional to the expected efforts, that is, the fault mode described in (5.25) is repeated as follows,

$$\begin{aligned}
\delta\dot{v} &= f_{11}(\delta v) + A_{12}\delta x + BU + B_f(U + u^o),\\
\delta\dot{x} &= A_{21}\delta v,
\end{aligned} \tag{5.32}$$

where $B_f = \text{diag}(m_f^{l_1}/m_1, \overbrace{m_f^w/m_2, \cdots, m_f^w/m_{n-1}}^{n-2}, m_f^{l_2}/m_n)$.

To detect the actuators' faults, some states are assumed to be measurable. In this study, the train is assumed to be composed of n cars with one locomotive (group) at the front and one at the rear. The wagons are between these two locomotives (locomotive groups). The speeds of the two locomotives and the two wagons next to the locomotives are also available, *i.e.*,

$$y = \begin{bmatrix} v_1 \\ v_2 \\ v_{n-1} \\ v_n \end{bmatrix}. \tag{5.33}$$

The two kinds of fault modes (sensor fault and actuator fault) are studied separately, because there are some difficulties in studying these two kinds of faults simultaneously, which will be discussed later. So, in the study of actuator faults, the speed sensors are assumed to be in good condition.

Locomotive fault detection and isolation

The locomotive group fault diagnosis is not studied in this chapter. Some approaches may be used to supervise the running states of the locomotives, such as in [69, 70, 67, 68, 71]. In this thesis, one assumes that the fault diagnosis signals and fault isolation signals are given, and when a fault happens, one's task is to reconfigure/redesign the controller.

Wagon fault detection and isolation

When the wagon faults in the system (5.32) are concerned, in the form of (5.1) for the algorithms in section 5.2, one has

$$x = \begin{bmatrix} \delta v \\ \delta x \end{bmatrix} \in R^{2n-1},$$

$$u = U,$$

$$u_f = m_f^w,$$

$$w = \begin{bmatrix} m_f^1 \\ m_f^n \end{bmatrix},$$

$$f(x) = \begin{bmatrix} f_{11}(\delta v) + A_{12}\delta x \\ A_{21}\delta v \end{bmatrix},$$

$$g(x) = B,$$

$$l = [0, (U_2 + u_2^o)/m_2, \cdots, (U_{n-1} + u_{n-1}^o)/m_{n-1}, \overbrace{0, \cdots, 0}^{n}]^T,$$
$$p_1 = [(U_1 + u_1^o)/m_1, \overbrace{0, \cdots, 0}^{n-2}, \overbrace{0, \cdots, 0}^{n}]^T,$$
$$p_2 = [\overbrace{0, \cdots, 0}^{n-1}, (U_n + u_n^o)/m_n, \overbrace{0, \cdots, 0}^{n-1}]^T,$$

and

$$h(x) = [\delta v_1, \delta v_2, \delta v_{n-1}, \delta v_n]^T.$$

According to the algorithm (5.7), one has

$$\begin{aligned} &S_0 = \bar{P} = \text{span}\{p_1, p_2\}, \\ &\bar{S}_0 \cap \ker\{dh\} = 0, \\ &\cdots, \\ &S_{k^*} = \text{span}\{p_1, p_2\}. \end{aligned}$$

from which one has

$$(\Sigma_*^P)^\perp = \text{span}\{\delta v_2, \cdots, \delta v_{n-1}, \delta x_1, \ldots, \delta x_{n-1}\}.$$

Furthermore, applying the algorithm (5.9) with $\Theta = (\Sigma_*^P)^\perp$, one has

$$\begin{aligned} \text{span}\{dh\} &= \text{span}\{d(\delta v_1), d(\delta v_2), d(\delta v_{n-1}), d(\delta v_n)\}, \\ Q_0 &= \Theta \cap \text{span}\{dh\} = \text{span}\{\delta v_2, \delta v_{n-1}\}, \\ \bar{Q}_0 &= \sum_{i=0}^{m} L_{g_i} Q_0 + \text{span}\{dh\} = \text{span}\{d(\delta v_1), d(\delta v_2), d(\delta v_{n-1}), d(\delta v_n), \\ &\quad d(k_1\delta x_1 - k_2\delta x_2), d(k_{n-2}\delta x_{n-2} - k_{n-1}\delta x_{n-1})\}, \\ Q_1 &= \Theta \cap \bar{Q}_0 = \text{span}\{d(\delta v_2), d(\delta v_{n-1}), \\ &\quad d(k_1\delta x_1 - k_2\delta x_2), d(k_{n-2}\delta x_{n-2} - k_{n-1}\delta x_{n-1})\}, \\ \bar{Q}_1 &= \sum_{i=0}^{m} L_{g_i} Q_1 + \text{span}\{dh\} \\ &= \text{span}\{d(\delta v_1), d(\delta v_2), d(\delta v_3), d(\delta v_{n-2}), d(\delta v_{n-1}), d(\delta v_n), \\ &\quad d(k_1\delta x_1 - k_2\delta x_2), d(k_{n-2}\delta x_{n-2} - k_{n-1}\delta x_{n-1})\}, \\ Q_2 &= \Theta \cap \bar{Q}_1 = \text{span}\{d(\delta v_2), d(\delta v_3), d(\delta v_{n-2}), d(\delta v_{n-1}), \\ &\quad d(k_1\delta x_1 - k_2\delta x_2), d(k_{n-2}\delta x_{n-2} - k_{n-1}\delta x_{n-1})\}, \\ &\quad \cdots, \\ Q_{k^*} &= \text{span}\{d(\delta v_2), \cdots, d(\delta v_{n-1}), d(k_1\delta x_1 - k_2\delta x_2), \\ &\quad \cdots, d(k_{n-2}\delta x_{n-2} - k_{n-1}\delta x_{n-1})\}, \end{aligned}$$

that is,

$$\begin{aligned} \Omega = o.c.a((\Sigma_*^P)^\perp) = \text{span}\{&d(\delta v_2), \cdots, d(\delta v_{n-1}), d(k_1\delta x_1 - k_2\delta x_2), \\ &\cdots, d(k_{n-2}\delta x_{n-2} - k_{n-1}\delta x_{n-1})\}. \end{aligned} \tag{5.34}$$

Repeat the above algorithm with $\Theta = \Omega$, and one has

$$\Omega = o.c.a(\Omega).$$

The second condition in (5.11) is satisfied. Then one can verify the first condition in (5.11).

$$\begin{aligned} L_g\Omega = \text{span}\{&d(k_1\delta v_1 - (k_1+k_2)\delta v_2 + k_2\delta v_3),\\ &\cdots,\\ &d(k_{n-2}\delta v_{n-2} - (k_{n-2}+k_{n-1})\delta v_{n-1} + k_{n-1}\delta v_n),\\ &d(k_1\delta x_1 - k_2\delta x_2),\\ &\cdots,\\ &d(k_{n-2}\delta x_{n-2} - k_{n-1}\delta x_{n-1})\}, \end{aligned}$$

and

$$\begin{aligned} \Omega + \text{span}\{dh\} = \text{span}\{&d(\delta v_1), d(\delta v_2), \cdots, d(\delta v_{n-2}), d(\delta v_{n-1}),\\ &d(k_1\delta x_1 - k_2\delta x_2), \cdots, d(k_{n-2}\delta x_{n-2} - k_{n-1}\delta x_{n-1})\}, \end{aligned}$$

so $L_{g_j}\Omega \subset \Omega + \text{span}\{dh\}, \forall j \in [0, m]$.

The conditions in (5.11) are satisfied with Ω defined above, which means the co-distribution Ω is the maximal observability co-distribution contained in $P^{\perp}$.

Assuming $z_{11} = \delta v_2, z_{12} = \delta v_3, \cdots, z_{1,n-2} = \delta v_{n-1}$, and $z_{1,n-1} = k_1\delta x_1 - k_2\delta x_2, \cdots, z_{1,2n-4} = k_{n-2}\delta x_{n-2} - k_{n-1}\delta x_{n-1}$, the z_1-system of (5.13) is as follows:

$$\begin{aligned} &\dot{z}_{11} = f_{11}^2(z_{11}) + z_{1,n-1}/m_2 + U_2/m_2,\\ &\cdots,\\ &\dot{z}_{1,n-2} = f_{11}^{n-1}(z_{1,n-2}) + z_{1,2n-4}/m_{n-1} + U_{n-1}/m_{n-1},\\ &z_{1,n-1} = k_1\delta v_1 - (k_1+k_2)z_{11} + k_2 z_{12},\\ &z_{1,n} = k_2 z_{11} - (k_2+k_3)z_{12} + k_3 z_{13},\\ &\cdots,\\ &z_{1,2n-5} = k_{n-3}z_{1,n-4} - (k_{n-3}+k_{n-2})z_{1,n-3} + k_{n-2}z_{1,n-2},\\ &z_{1,2n-4} = k_{n-2}z_{1,n-3} - (k_{n-2}+k_{n-1})z_{1,n-2} - k_{n-1}\delta v_n\\ &y_1 = col(z_{11}, z_{1,n-2}),\\ &y_2 = col(\delta v_1, \delta v_n). \end{aligned} \tag{5.35}$$

It can also be seen that $\text{span}\{l\} \subset \Omega$, which means the possibility of detectability of the wagon fault.

A residual generator is in the following form,

$$\begin{aligned}
\dot{\xi}_{11} &= f_{11}^2(\xi_{11}) + \xi_{21}/m_2 + U_2/m_2 + L_{11}(\xi_{11} - y_{11}) + L_{12}(\xi_{1,n-2} - y_{12}),\\
&\cdots,\\
\dot{\xi}_{1,n-2} &= f_{11}^{n-1}(\xi_{1,n-2}) + \xi_{2,n-2}/m_{n-1} + U_{n-1}/m_{n-1}\\
&\quad + L_{n-2,1}(\xi_{11} - y_{11}) + L_{n-2,2}(\xi_{1,n-2} - y_{12}),\\
\dot{\xi}_{2,1} &= k_1 y_{21} - (k_1 + k_2)\xi_{11} + k_2\xi_{12}\\
&\quad + L_{n-1,1}(\xi_{11} - y_{11}) + L_{n-1,2}(\xi_{1,n-2} - y_{12}),\\
\dot{\xi}_{2,i} &= k_i\xi_{11} - (k_i + k_{i+1})\xi_{1,i} + k_{i+1}\xi_{1,i+1}\\
&\quad + L_{i+n-2,1}(\xi_{11} - y_{11}) + L_{i+n-2,2}(\xi_{1,n-2} - y_{12}), \quad i = 2, \cdots, n-3,\\
\dot{\xi}_{2,n-2} &= k_{n-2}\xi_{1,n-3} - (k_{n-2} + k_{n-1})\xi_{1,n-2} + k_{n-1}y_{22} + L_{2n-4,1}(\xi_{11} - y_{11})\\
&\quad + L_{2n-4,2}(\xi_{1,n-2} - y_{12}),\\
y_1 &= col(\delta v_2, \delta v_{n-1}),\\
y_2 &= col(\delta v_1, \delta v_n),
\end{aligned} \tag{5.36}$$

where the matrix $L = (L_{ij})$ is suitably chosen with observer design approaches, such as pole placement (Luenberger observer) or optimization control (Kalman filter).

From (5.36), it can be seen that the dimension of the observer is $2n-4$. For a long train, n is very large. To avoid such a high-dimension observer, one considers another approach to identify the wagons' faults. The full train model is repeated as follows:

$$\begin{aligned}
m_i\dot{v}_i &= (1 - m_f^i)u_i + f_{in_{i-1}} - f_{in_i} - m_i(c_{0_i} + c_{1_i}v_i + c_{2_i}v_i^2) - f_{p_i}, \ i = 1, \cdots, n,\\
\dot{x}_j &= v_j - v_{j+1}, \qquad j = 1, \cdots, n-1,
\end{aligned} \tag{5.37}$$

where $f_{in_0} = 0, f_{in_n} = 0$.

When $m_f^i = 0$, one has reached an equilibrium (steady state, $\dot{v} = 0, \dot{x} = 0$) $v_i = v_r, i = 1, \cdots, n$, and $f_{in_j}^0(x_j^0)$, with $u_i = u_i^0$.

$$\begin{aligned}
\dot{v}_r &= u_i^0 + f_{in_{i-1}}^0 - f_{in_i}^0 - m_i(c_{0_i} + c_{1_i}v_r + c_{2_i}v_r^2) - f_{p_i}, \qquad i = 1, \cdots, n,\\
\dot{x}_j^0 &= v_r - v_r, j = 1, \cdots, n-1.
\end{aligned} \tag{5.38}$$

Thus one has a difference system (5.21) with $\delta v_i = v_i - v_r, \delta x_j = x_j - x_j^0$, which is also denoted as follows,

$$\dot{X} = f(X) + BU. \tag{5.39}$$

A speed regulator designed in the previous chapter for this difference system is repeated as follows,

$$\begin{aligned}
\dot{z} &= f(z) + BU + G_1(y_m - C_m z),\\
U &= c(w) + K(z - \pi(w)),
\end{aligned} \tag{5.40}$$

The closed-loop dynamics are

$$\begin{aligned} \dot{X} &= f(X) + BU, \\ \dot{z} &= f(z) + BU + G_1(y_m - C_m z), \\ U &= c(w) + K(z - \pi(w)). \end{aligned} \tag{5.41}$$

When the train is faultless, the train speed will track the reference speed under the above controller. How are the train's dynamics when $m_f^i \neq 0$? One first checks whether the train dynamics are stable. If they are, then one will study the new steady states.

The locomotives' faults are assumed to be detected and isolated through other approaches, so only the faults of the wagons with $m_f^i = m_f^w, i = 2, \cdots, n-1$ are considered in the following identification.

When $m_f^w \neq 0$, the closed-loop dynamics (5.41) in cruise phase is as follows

$$\begin{aligned} \dot{X} &= f(X) + BU - B_f(U + u^o), \\ \dot{z} &= f(z) + BU + G_1(y_m - C_m z), \\ U &= Kz, \end{aligned} \tag{5.42}$$

where $B_f = \text{diag}(0, \overbrace{m_f^w/m_2, \cdots, m_f^w/m_{n-1}}^{n-2}, \overbrace{0, \cdots, 0}^{n})$.

Assuming $A = \frac{\partial f(0)}{\partial X}$, (from the above, one knows $A + BK < 0, A + G_1 C_m < 0$,) one has a linearized model as follows:

$$\begin{aligned} \dot{X} &= AX + (B - B_f)Kz - B_f u^o, \\ \dot{z} &= -GC_m X + (A + G_1 C_m + BK)z. \end{aligned} \tag{5.43}$$

If the K, G are chosen such that

$$\begin{bmatrix} A & (B - B_f)K \\ -GC & A + GC + BK \end{bmatrix} < 0,$$

then the above system (5.43) is stable.

The steady state of the train can be denoted as $(\dot{v} = 0, \dot{x} = 0)$ $v_i = v_r^f, i = 1, \cdots, n$, and $f_{in_j}^f(x_j^f)$, with u_i,

$$\begin{aligned} m_1 \dot{v}_r^f &= u_1 - f_{in_1}^f - m_1(c_{0_1} + c_{1_1} v_r^f + c_{2_1}(v_r^f)^2) - f_{p_1}, \\ m_i \dot{v}_r^f &= u_i + f_{in_{i-1}}^f - f_{in_i}^f - m_i(c_{0_i} + c_{1_i} v_r^f + c_{2_i}(v_r^f)^2) - f_{p_i} - m_f^i u_i, i = 2, \cdots, n-1, \\ m_n \dot{v}_r^f &= u_n + f_{in_n}^f - m_n(c_{0_n} + c_{1_n} v_r^f + c_{2_n}(v_r^f)^2) - f_{p_n}, \end{aligned} \tag{5.44}$$

The locomotive fault is identifiable with other approaches and only the fault of wagons with $m_f^i = m_f^w, 2, \cdots, n-1$ is considered. Furthermore if v_r^f is known, then there are only n unknown variables $f_{in_i}^f, i = 1, \cdots, n-1, m_f^w$ in the above n equations. Especially when summing up the first n equations, one has

$$0 = \sum_{i=1}^{n} u_i - \sum_{i=1}^{n} m_i(c_{0_i} + c_{1_i} v_r^f + c_{2_i}(v_r^f)^2) - \sum_{i=1}^{n} f_{p_i} - \sum_{j=2}^{n-1} m_f^i u_i. \tag{5.45}$$

It is possible to solve them, which means the identifiability of the wagon fault.

Although it is impossible for a train to reach steady states in practical running, it is practical to assume that the train can approximate its steady state, at least within a cruise phase. The practical steady-state speed of the running train is defined with the analysis of differences of the measurable speeds (v_1, v_2, v_{n-1}, v_n) in this chapter.

When all the wagon are faultless and the train is running in its steady state, one has,

$$0 = \sum_{i=1}^{n} u_i^o - \sum_{i=1}^{n} \left(m_i(c_{0_i} + c_{1_i} v_r + c_{2_i}(v_r)^2) + f_{p_i} \right). \tag{5.46}$$

With (5.45) and (5.46), if all the wagons' faults are the same, *i.e.*, $m_f^i = m_f^w, i = 2, \cdots, n-1$, one has

$$(1 - m_f^w) \sum_{i=1}^{n} u_i - \sum_{i=1}^{n} u_i^o = \sum_{i=1}^{n} m_i \left(c_{1_i} v_r^f + c_{2_i}(v_r^f)^2 - (c_{1_i} v_r + c_{2_i} v_r^2) \right), \tag{5.47}$$

from which one can get m_f^w.

5.5 Fault-tolerant control (FTC)

5.5.1 FDI and FTC in the case of sensor faults

The residual generator in the case of sensor faults is as in equations (5.30) and (5.31), where function f_{11} is linearized and thus the observer is a linear system. The matrices L_{11}, L_{21} are determined through the function LQR in MATLAB. If the sensor fault model is linearized as

$$\begin{aligned} \dot{z} &= Az + BU, \\ y_m &= C_m z, \\ y_i &= (1 + m_{v_i}^f) v_i - v_r, \qquad i = 2, \cdots, p, \end{aligned} \tag{5.48}$$

then one assumes $C_{m1} = C_m(1,:)$, $Q = I_{(2n-1)\times(2n-1)}$, $R = 1$, and with the function $L = lqr(A', C_{m1}', Q, R)$, $L = L'$, one gets the residual generator.

In the controller, one assumes the outputs of the residual generator are $\bar{v}_i$ and the measured speeds v_{mi}. The reference speed is v_r. In the control process, for the output v_{mi} of the ith speed sensor, one will take $K_i^{sensor} \times v_{mi}$ as the real speed of the corresponding car, where K_i^{sensor} is a coefficient, which will be modified when the sensor fault is detected and isolated. A constant V_{th} is set as the threshold of fault diagnosis. For the fault detection and isolation, one has other arrays in the programme, $KD_{i,1:11}^{sensor}, Nsensor_i$. The former is used to store the past 11 coefficients of the sensor and the latter the times of continuous violations of the fault-free condition.

The fault detection and isolation programme is shown as Fig. 5.1, where $KD_{i,1:11}^{sensor} = 0_{1\times 11}, N_i^{sensor} = 0$ and $K_i^{sensor} = 1$ are initialized. This programme is executed once a second.

It is known that there is a possibility of false rejections and a possibility of false acceptances for a fault-tolerant controller, which should be considered. The first possibility is that it does not detect or isolate the fault well when a fault occurs. The second is that it takes a faultless system as a fault system. The choice of the thresholds affect these two possibilities. Generally, when one possibility is reduced with a set of thresholds, the other one is increased. When the threshold is to be determined, the balance between the two possibilities should be considered. From Fig. 5.1, it is impossible to avoid the above two possibilities. However, the effects of the possibility of false acceptance can be discussed qualitatively. If a fault is falsely accepted, for example, a sensor with a gain 1 is falsely identified with a gain 1.05, then with the FTC, the speed of the train will be underestimated, and thus the train will be overspeed. In that case, the FDI will further identify a gain fault lower than 1 to correct the false acceptance. It is in the way of "negative feedback" to track the real value of the gain. Such an approach in Fig. 5.1 does not obviously affect the train performance. That can be seen from the simulation results of an FTC in a faultless system.

In this thesis, the two possibilities from theoretic viewpoints will not be discussed, nor will the time delay between the fault occurrence and fault isolation. Instead, they will be discussed on the basis of the simulation results.

5.5.2 Controller redesign in the case of a locomotive fault

As described before, fault detection and isolation of locomotive faults are not studied in this thesis. Here, only the fault-tolerant control of a locomotive fault is considered.

In the following simulation, one assumes the fault is detected and identified 60 seconds after it occurs. When it is identified, the controller will be redesigned. According to the fault, the parameters of the train are modified and then the controller is redesigned with the new parameters. For example, assuming the coefficient of its input in the train model is $Bt(i,:)$, if the locomotive group $u(i)$ loses half its effort, the new coefficient is $Bt(i,:)/2$.

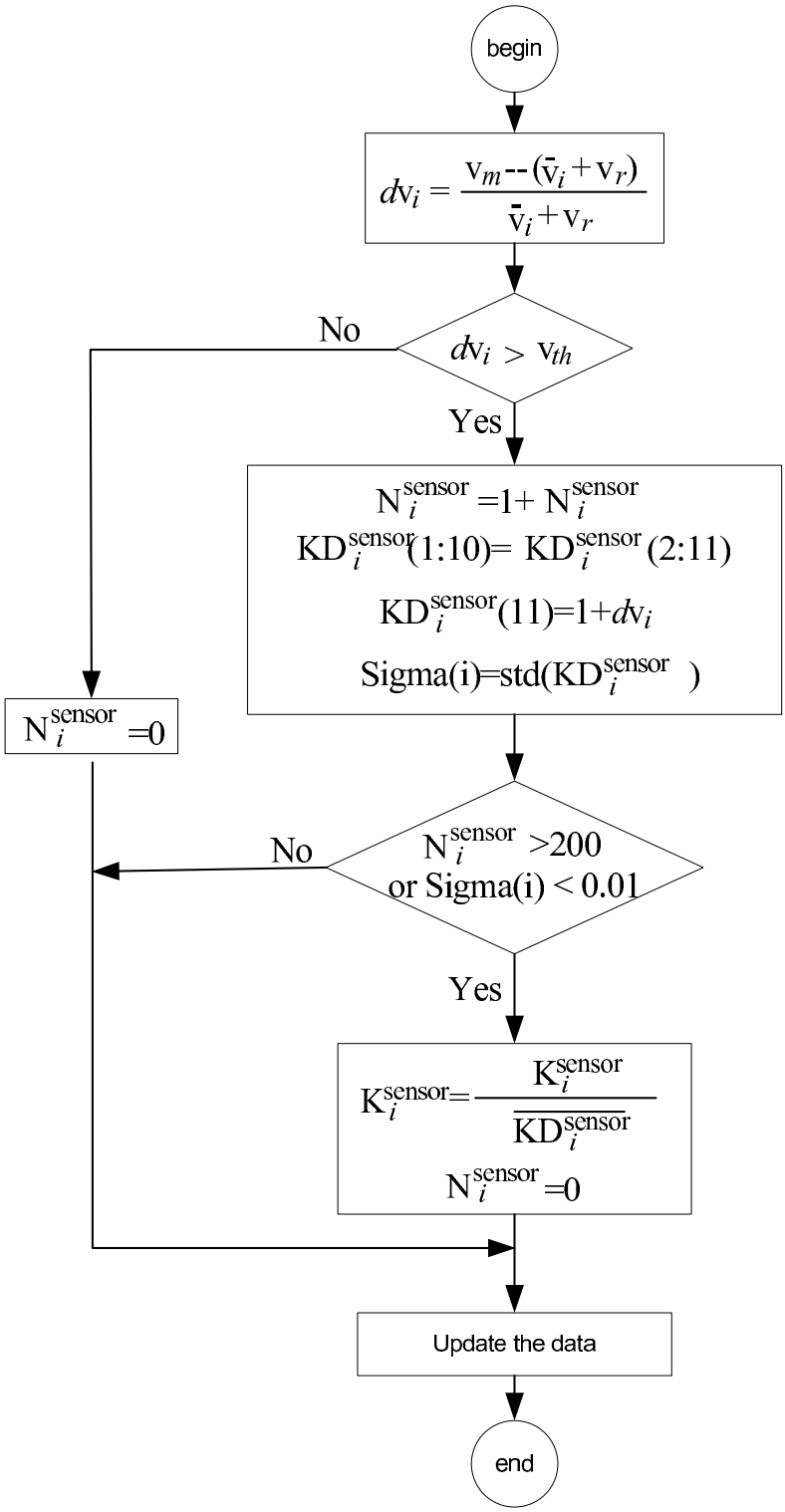

Figure 5.1: Sensor fault detection and isolation programme

5.5.3 FDI and FTC in the case of a wagon fault

When a wagon fault is detected and identified, similar to the case of a locomotive fault, the controller will be redesigned according to the updated parameters of the train. The key is fault detection and isolation. In the current simulation, this is done following the approach proposed in section 5.4.2.

In this approach, one employs the algorithm as Fig. 5.2 to detect and identify the fault; this is executed once a second. In the figure, the matrix Bb is the coefficient matrix of the brake inputs in the train model, which is equal to $\text{diag}(1/m_i)$ when the braking system is faultless. The variables v_m, v_r are the measured speed and reference speed, respectively. The variable K^f_{brake} is a ten-dimension array used to store the past ten estimated fault signals, while N^f_{brake} is a counter number of the continuous violation of fault condition.

There are the same possibilities in the FDI of a wagon fault as in the FDI of a sensor fault. Similar to the latter, the FDI of wagon faults is also "negative feedback" to track the real value of the wagon actuator. The effect of false acceptance on the train performance will not be discussed in a theoretic way, but is discussed with the simulation results. The time delay between the fault occurrence and fault isolation will not be discussed either.

5.6 Simulation

The simulation setting of the train is the same as previous chapters as well as the speed profile and track profile. When all sensors and actuators are faultless, the controller is the speed regulator with $K_e = 1, K_f = 1, K_v = 1$, designed in part 4.3. When a fault occurs, the controller will be redesigned. The controller redesign includes two parts: the redesign of the optimal scheduling and the redesign of the speed regulator.

5.6.1 Simulation of sensor faults

In simulation, the sensor fault detection and isolation programme is only working during the cruise phase. The simulation setting is the same as in section 4.3. The fault diagnosis parameter setting is as in Fig. 5.1.

There are two kinds of errors with the gains of speed sensors. One is a random error, which depends on the accuracy of speed sensor. The other one is a systematic error with gain, which is a real fault and should be corrected. From the simulation, it will be seen that the former has little impact on the performance of controllers, while

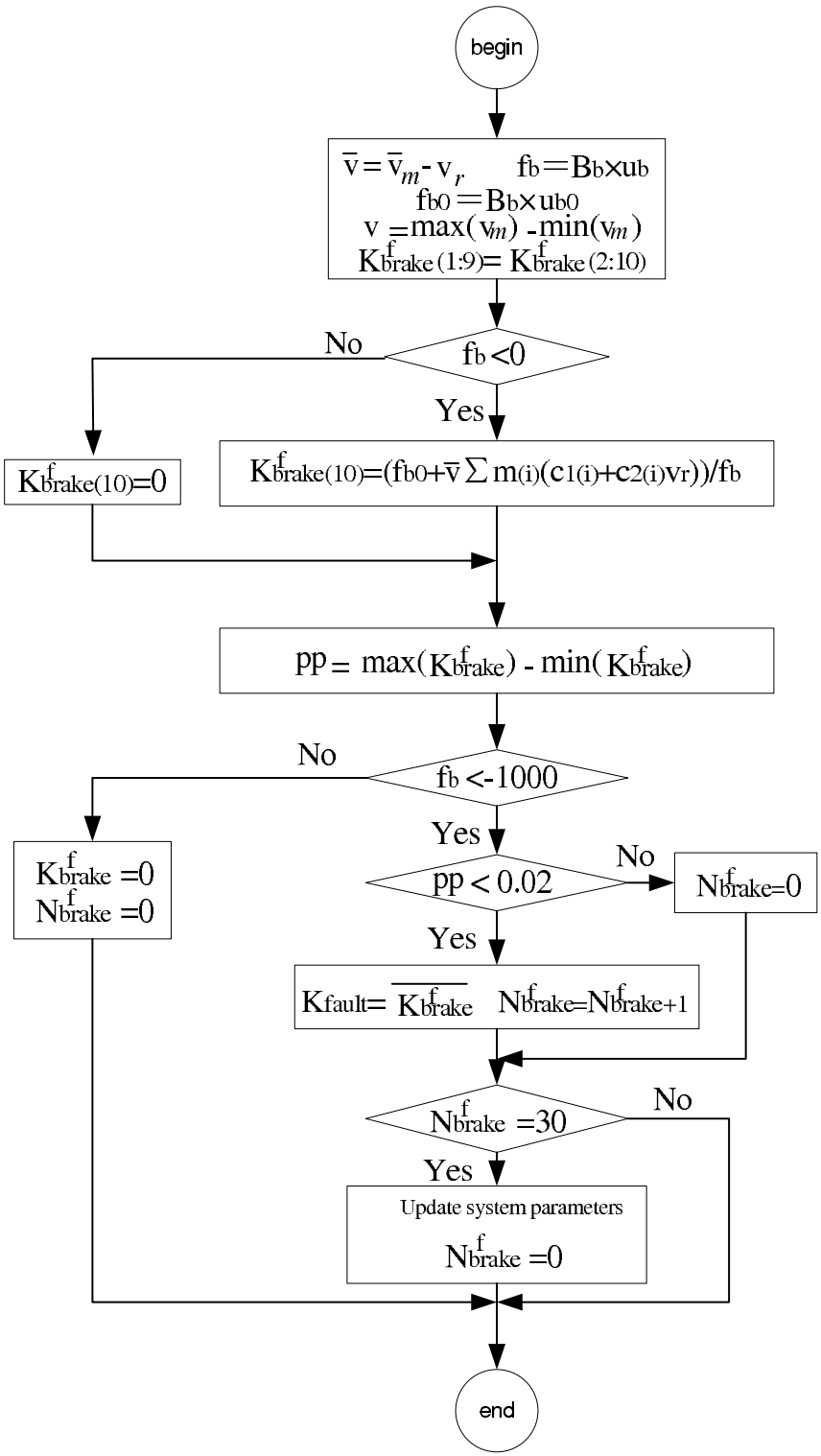

Figure 5.2: Wagon fault detection and isolation programme

the latter has much greater impact.

In the following description, the accuracy $1\pm\alpha\%$ of a speed sensor means the output of the sensor is randomly $1 \pm \alpha\%$ of the measured speed, while the gain fault $\beta\%$ of a sensor means the output of the sensor is $1 + \beta\%$ of the measured speed with the accuracy 1.

The effects of the random errors of the speed sensors on the non-FTC (a controller without fault-tolerant capacity) and the FTC (a controller with fault-tolerant capacity) are discussed firstly. The following three groups of figures are the simulation results with non-FTC of a faultless system, FTC of a faultless system and FTC of a faulty system, respectively.

Fig. 5.3 and Fig. 5.4 are the simulation results of a faultless system with non-FTC. All sensors in the former case have accuracies of 100%, while those in the latter have accuracies of $1 \pm 5\%$ from the beginning.

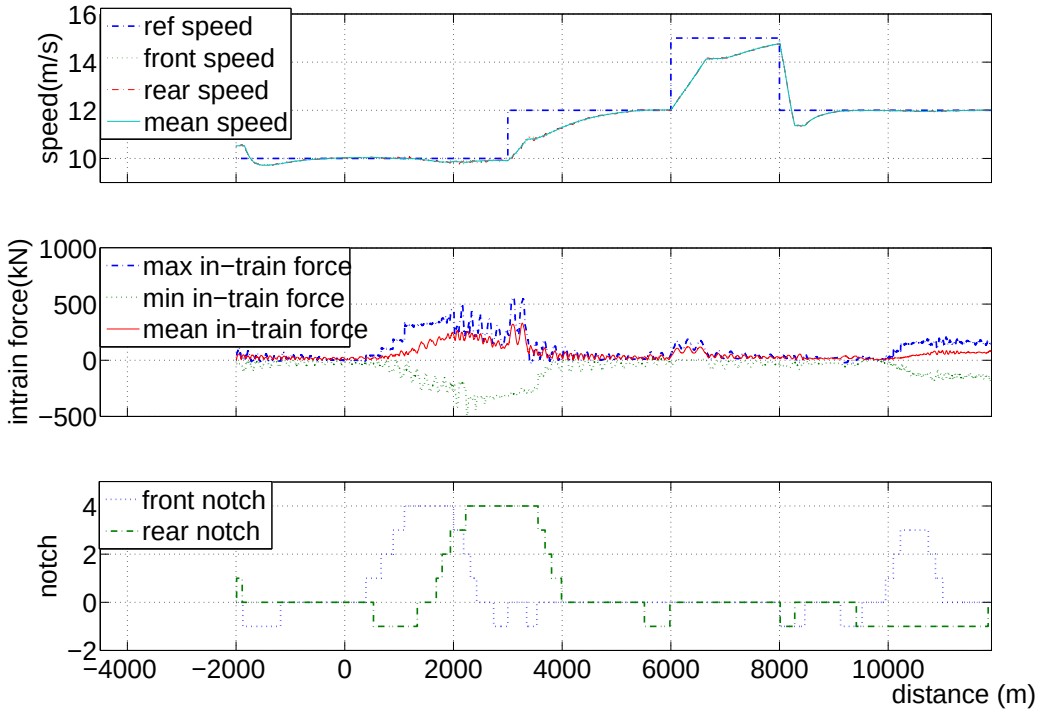

Figure 5.3: Non-FTC (sensor accuracy of 100%)

Fig. 5.5 and Fig. 5.6 are simulation results of a faultless system with an FTC. All sensors in the former case have accuracies of 100%, while those in the latter have accuracies of $1 \pm 5\%$ from the beginning.

Fig. 5.7 and Fig. 5.8 are the simulation results of a faulty system (the second sensor

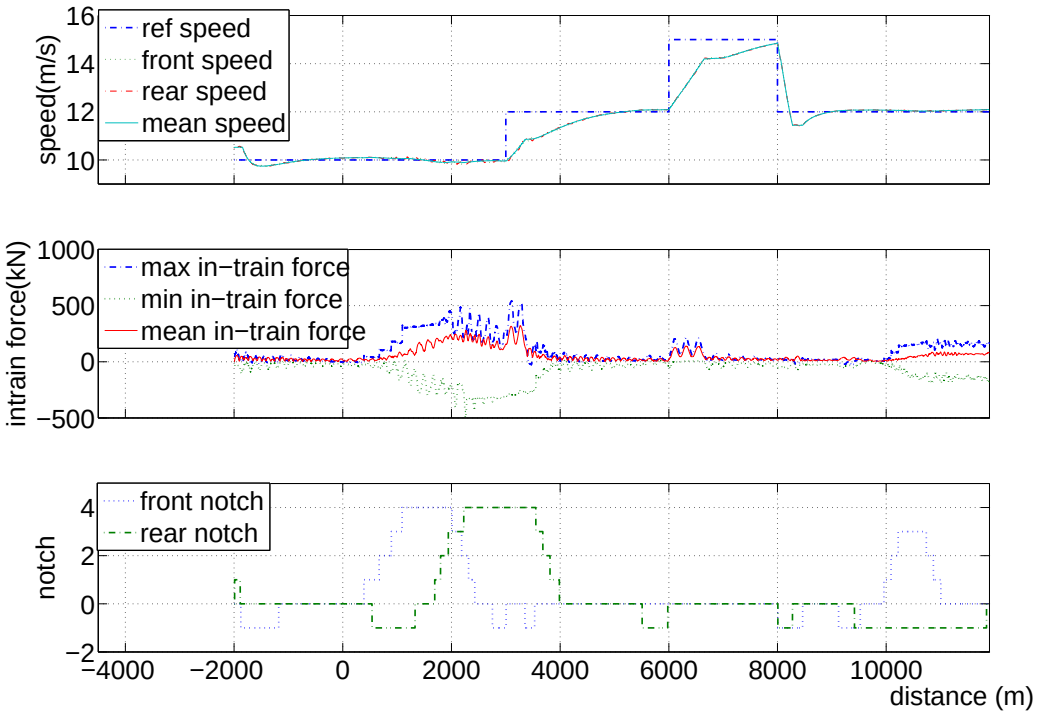

Figure 5.4: Non-FTC (sensor accuracy of $1 \pm 5\%$)

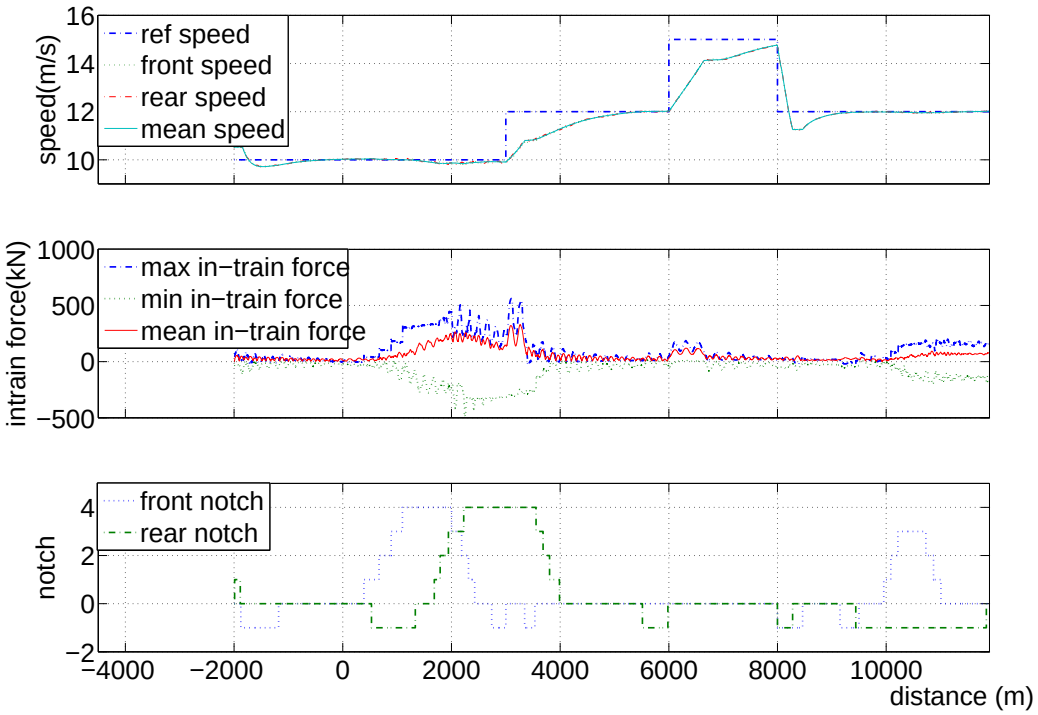

Figure 5.5: FTC (sensor accuracy of 100%)

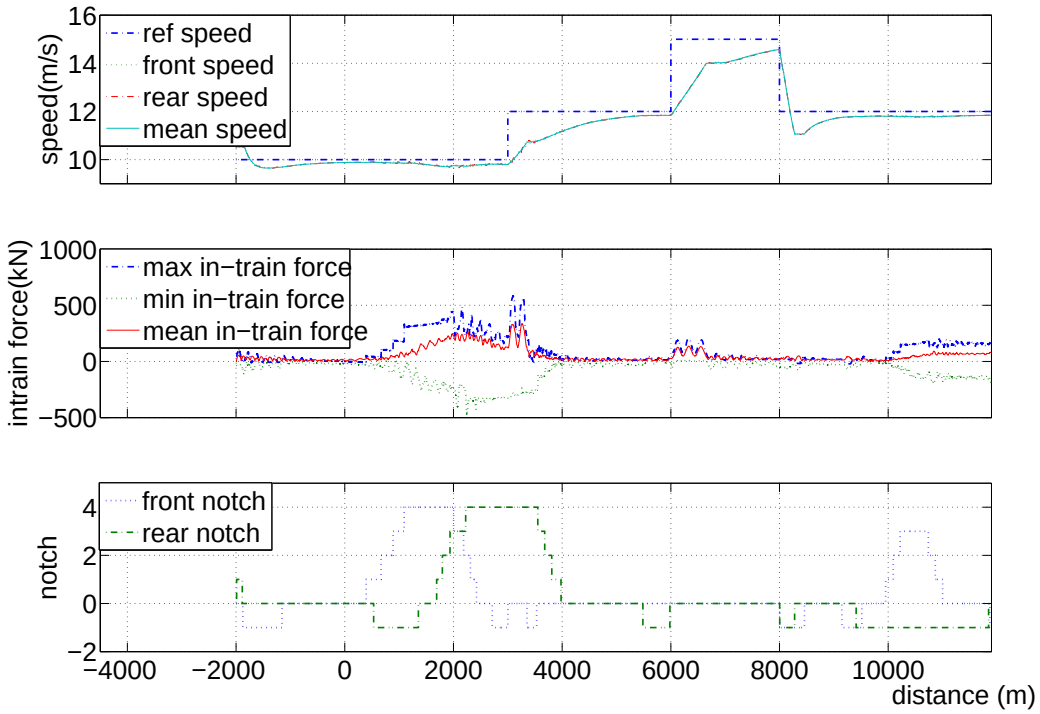

Figure 5.6: FTC (sensor accuracy of $1 \pm 5\%$)

is faulty with a gain fault +5%). All sensors in the former case have accuracies of 100% while those in the latter have accuracies of $1 \pm 5\%$.

Comparing Fig. 5.3 with Fig. 5.4, one can see that the random error has very little effect on the speed regulators without fault-tolerant capacity when there is no fault with the sensors. Comparing Fig. 5.5 with Fig. 5.6, it can be seen that the random error makes the performance a little worse with the fault-tolerant controller even though no fault occurs. The effects are, however, very small. The performance index is referred to in Table 5.1. From a comparison of Fig. 5.7 with Fig. 5.8, one sees that the random errors of sensors have little impact on the performance of the fault-tolerant controllers when a fault occurs with the second sensor. From a comparison of the last two pairs, it is concluded that random errors have effects on the performance of the fault-tolerant controllers, but the effects are limited. The result is still acceptable. In the following simulation of this study, one therefore seldom considers the random errors of the sensors. From the above discussion, it is clear the results are not affected.

A discussion of the effects of the FTC on the performance of a speed regulator is as below.

The figures from Fig. 5.3 to Fig. 5.9 are compared. Fig. 5.9 is the simulation result of a faulty system (the second sensor is faulty with a gain fault +5%) with all sensors having accuracies of $1 \pm 5\%$. The controller in this simulation is a non-FTC.

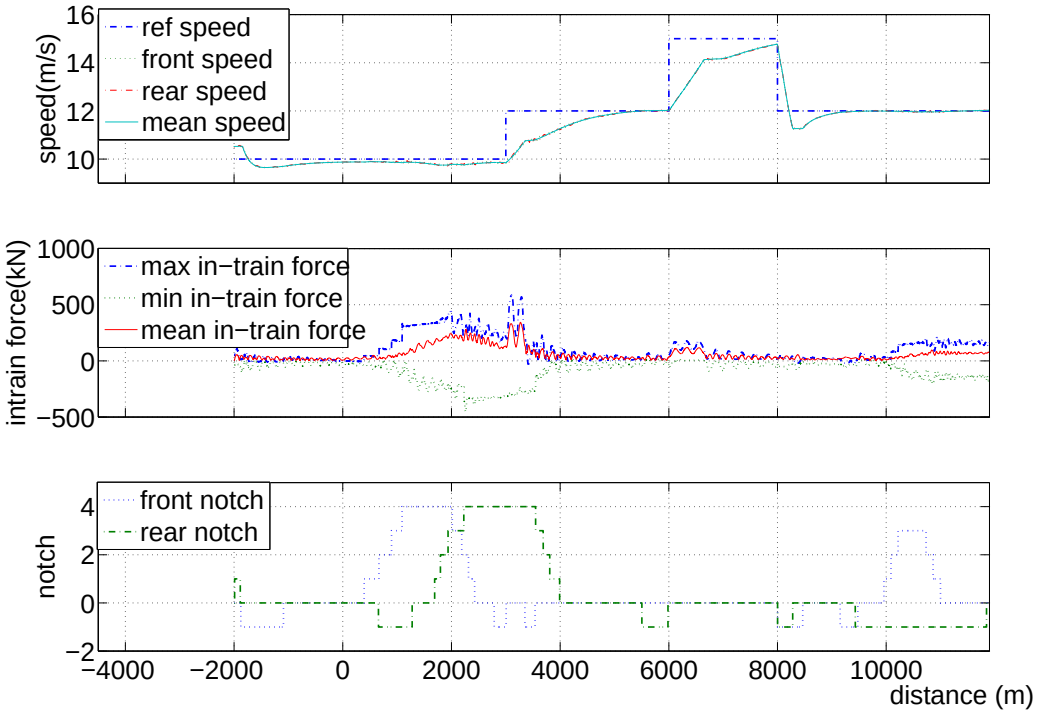

Figure 5.7: FTC (sensor accuracy of $1 + 0\%$ and second sensor gain fault of $+5\%$)

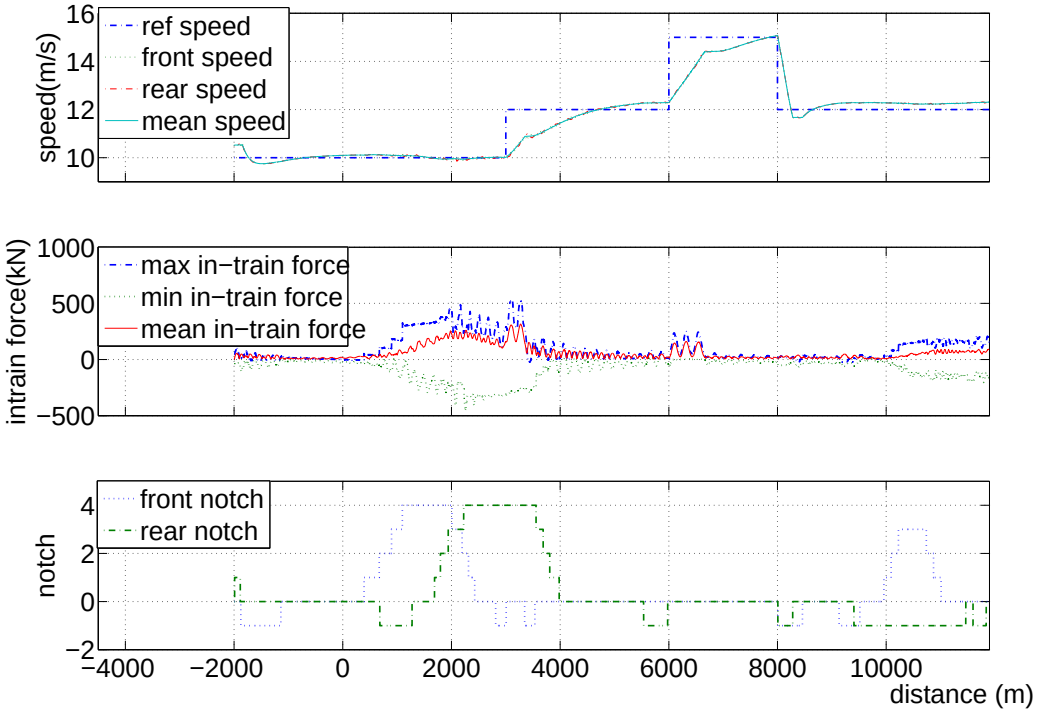

Figure 5.8: FTC (sensor accuracy of $1 \pm 5\%$ and second sensor gain fault of $+5\%$)

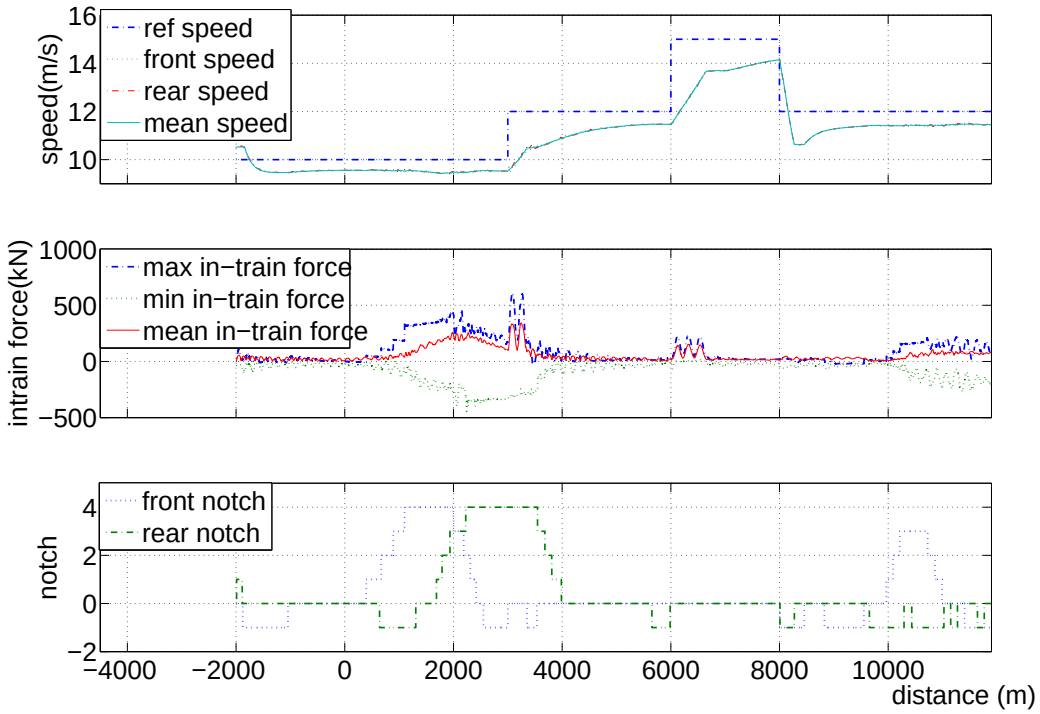

Figure 5.9: Non-FTC (sensor accuracy of $1 \pm 5\%$ and 2^{nd} sensor gain fault of $+5\%$)

One first compares Fig. 5.3 with Fig. 5.5, in which the sensors have accuracies of 100% and the system is faultless. The former is controlled with a non-FTC while the latter is controlled with an FTC. From these two figures, one can see that the performance is visually very similar although from Table 5.1 the last one appears to be slightly worse.

Then Fig. 5.4 is compared with Fig. 5.6, in which the sensors have accuracies of $1 \pm 5\%$ and the system is faultless. The former is controlled with a non-FTC while the latter is controlled with an FTC. The speed performance of the latter is a little worse than that of the former, and even the latter has a steady speed error. This is because the random errors of the sensors have an effect on the performance of an FTC. Even so, the FTC does not explicitly worsen the performance of the speed regulator. The result is still acceptable.

The advantage of an FTC can be seen when a fault occurs. Fig. 5.9 and Fig. 5.8 represent simulation of a faulty system (all sensors with accuracies of $1 \pm 5\%$ and the second one has a gain fault of $+5\%$) with a non-FTC and with an FTC, respectively. It is seen that the speed performance of the latter is obviously better than that of the former. That is the contribution of the FTC. From the above comparison, one can conclude that

1) When no fault occurs and all sensors have accuracies of 100%, the speed perfor-

mance of an FTC is very similar to that of a non-FTC.

2) When no fault occurs and all sensors have accuracies of $1 \pm 5\%$, the speed performance of an FTC is a little worse than that of a non-FTC. However, the result is still thought as a good result.

3) When a small fault (the second sensor has a gain fault of $+5\%$) occurs and all sensors have accuracies of $1 \pm 5\%$, the speed performance of an FTC is much better than that of a non-FTC.

From the above, it is concluded that the FTC for the sensors' faults is suitable.

In the above simulations, only the FTC for the second sensor fault is given. In the following, one can see the FTC applied in the faults of the third and fourth sensors, and in the concurrent faults of the second and fourth ones. Since the accuracy of a sensor does not explicitly affect the performance of the controller, without a special description, the sensor accuracy is assumed to be 100% in the rest of this thesis.

Fig. 5.10 shows an FTC with the third sensor having a gain fault of $+7\%$ from the beginning. Fig. 5.11 shows an FTC with the fourth sensor having a gain fault of -20% from the beginning. Fig. 5.12 shows an FTC with the fourth sensor having a gain fault of $+20\%$ from the beginning.

A kind of concurrent fault (the second sensor has a gain fault of $+43\%$ and the fourth one has a gain fault of $+12\%$ from the beginning) is shown in Fig. 5.13 with an FTC. Another kind of concurrent fault (the second sensor has a gain fault of $+30\%$ from the distance of $2,000$ m and the fourth one has a gain fault of -30% from the distance of $4,000$ m) is shown in Fig. 5.14 with an FTC.

The comparison of these figures in performance is shown in Table 5.1. The statistical items are the same as those in the Table 4.1.

From an analysis of the figures and a comparison with Table 5.1, one can conclude that the application of FTC of sensor faults in the speed regulation explicitly improves performance in the case of fault occurrence and does not explicitly worsen performance in the case of a faultless train.

5.6.2 Simulation of locomotive faults

In the previous parts, fault detection and isolation of locomotive faults are assumed to be done by other approaches and only fault-tolerant control is considered in this thesis. The fault signal is assumed to be given when a fault occurs.

In the train setting of simulation, there are two groups of locomotives at the front

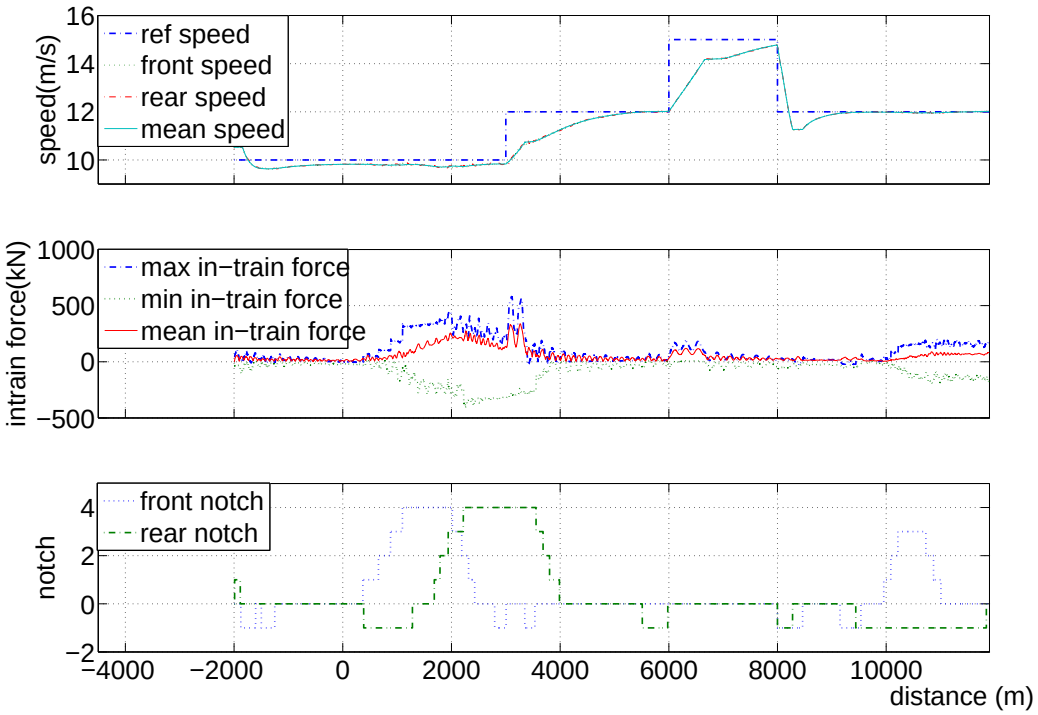

Figure 5.10: FTC (third sensor with a gain fault of +7%)

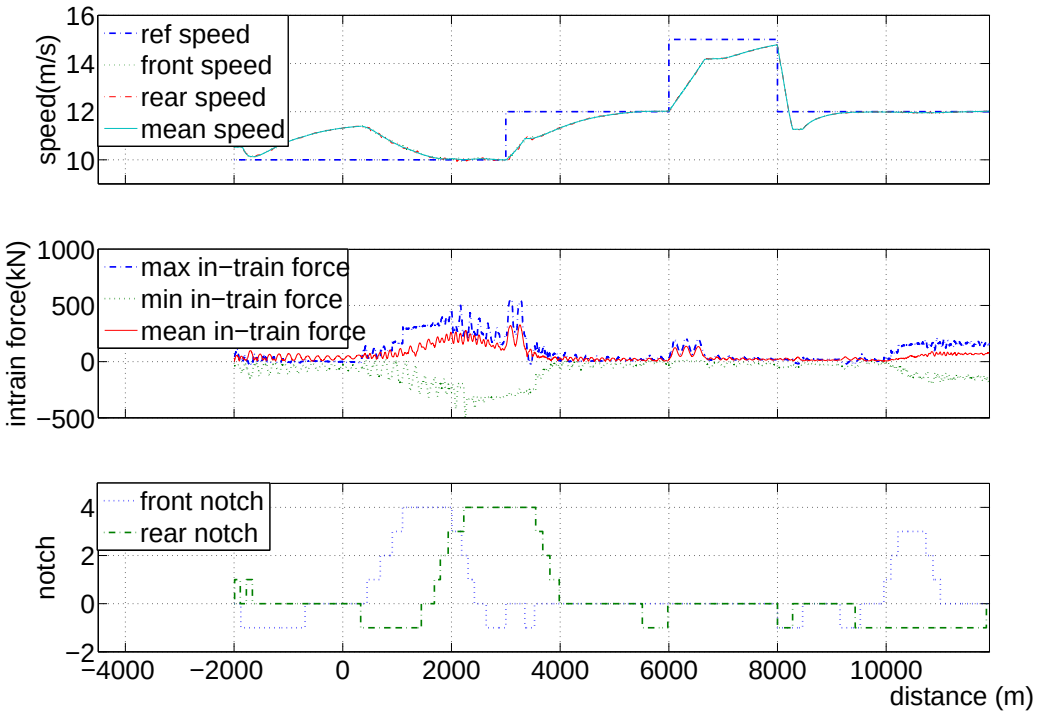

Figure 5.11: FTC (fourth sensor with a gain fault of −20%)

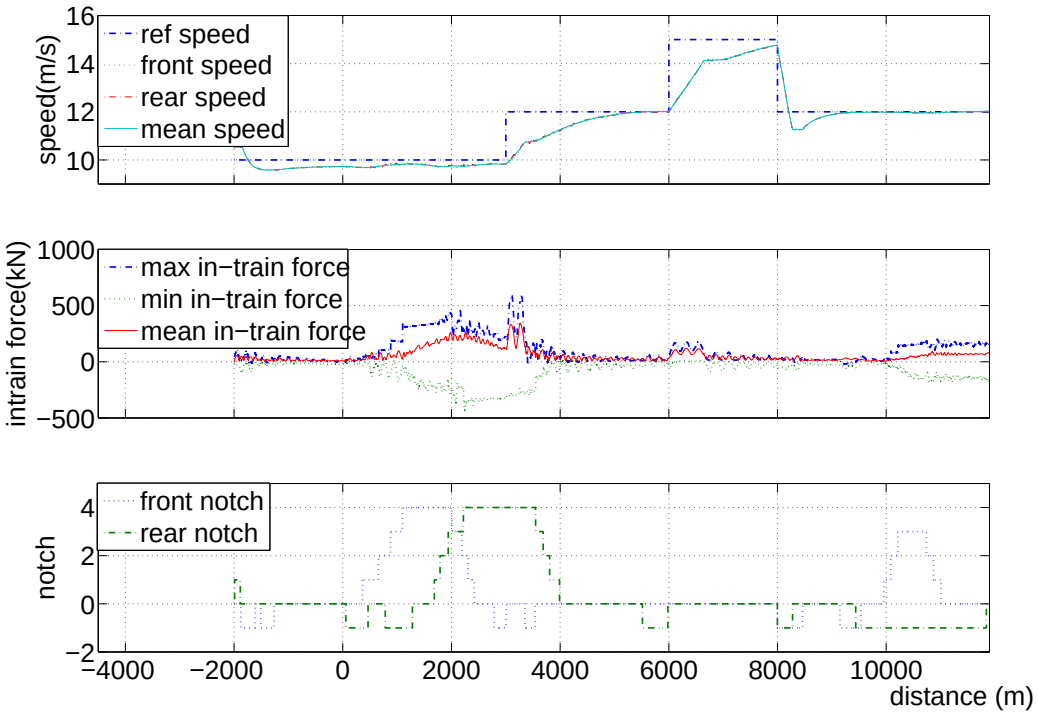

Figure 5.12: FTC (fourth sensor with a gain fault of +20%)

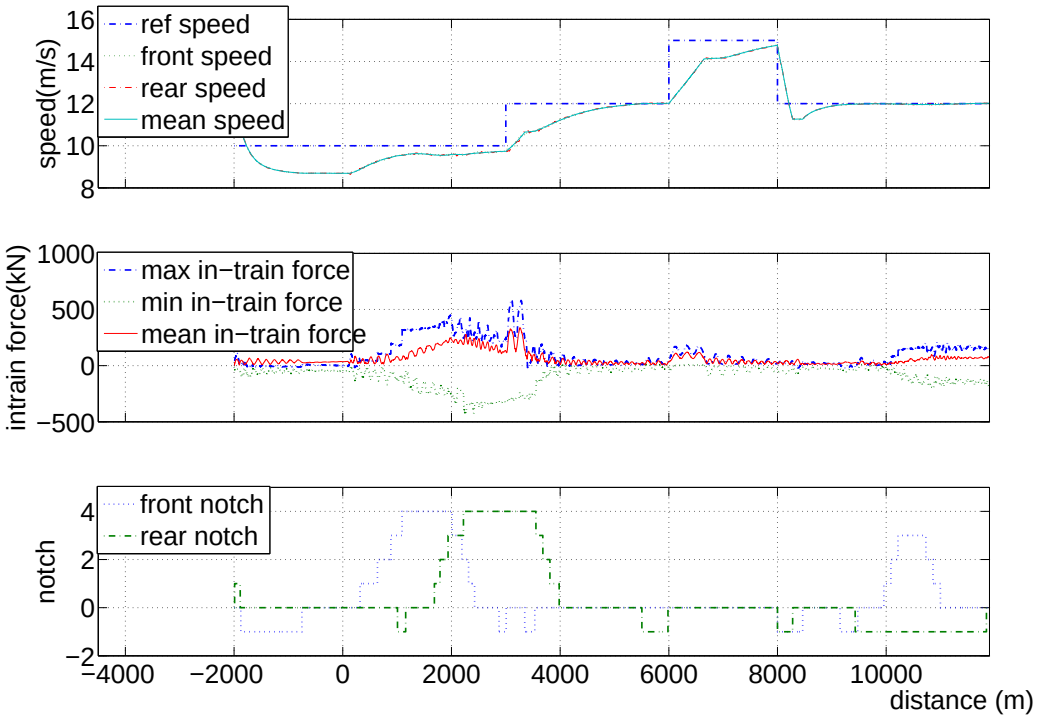

Figure 5.13: FTC (concurrent faults)

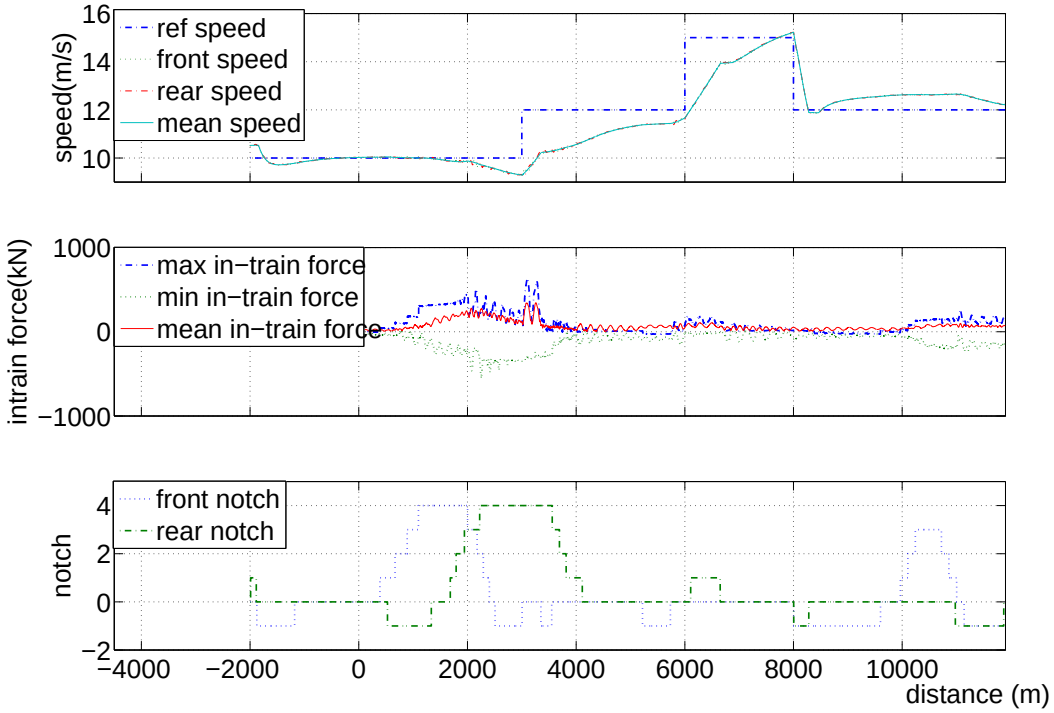

Figure 5.14: FTC (concurrent faults)

Table 5.1: Comparison of non-FTC and FTC of sensor faults

	$\lvert\delta\bar{v}\rvert$(m/s)			$\overline{\lvert f_{in}\rvert}$(kN)			E
	max	mean	std	max	mean	std	(MJ)
Fig. 5.3	2.9813	0.3277	0.5321	331.1579	58.5970	63.0519	12,400
Fig. 5.4	2.9102	0.3163	0.5129	323.3944	56.4624	63.8505	12,200
Fig. 5.9	3.5348	0.7831	0.5225	343.8927	57.7336	63.6908	13,100
Fig. 5.8	3.0783	0.3329	0.4672	316.3416	59.3843	65.0268	12,600
Fig. 5.7	2.9780	0.3718	0.5181	343.3660	59.7467	63.4535	12,900
Fig. 5.5	2.9812	0.3324	0.5288	331.1538	59.5132	63.5522	12,800
Fig. 5.6	3.1587	0.4667	0.5230	338.3691	55.7556	65.5126	13,200
Fig. 5.10	2.9825	0.3902	0.5132	338.7165	58.7065	64.1423	13,000
Fig. 5.11	2.9782	0.5067	0.5788	28.4991	60.5036	63.3990	12,600
Fig. 5.12	2.9810	0.4066	0.5102	343.1219	58.9628	64.1343	13,100
Fig. 5.13	2.9840	0.6170	0.5842	336.3811	63.6549	62.9222	13,400
Fig. 5.14	3.3412	0.6047	0.6593	345.4785	65.6464	62.0612	13,500

and at the rear, respectively. Every group is composed of two locomotives. In simulation of an FTC, one assumes that the fault is that one locomotive in a locomotive group does not work. When the two locomotive in a group do not work, distributed power control cannot apply, which is not discussed in this study. So, in the simulation, it is assumed that the fault is detected 60 second after it happens and the controller is then redesigned. There are three types of faults:

1) Front-loco-fault: one locomotive of the front locomotive group does not work;

2) Rear-loco-fault: one locomotive of the rear locomotive group does not work;

3) Both-loco-fault: one locomotive of the front locomotive group and one of the rear group do not work;

Fig. 5.15 and Fig. 5.16 are simulation results of Front-loco-fault with an FTC and a non-FTC, respectively. One of the locomotives at the front does not work from the distance $1,500m$.

Fig. 5.17 and Fig. 5.18 are simulation results of rear-loco-fault with an FTC and a non-FTC, respectively. One of the locomotives at the rear does not work from the distance $1,500m$.

Fig. 5.19 and Fig. 5.20 are simulation results of Both-loco-fault with an FTC and a non-FTC, respectively. One locomotive at the front and one at the rear do not work from the distance $1,500m$.

From comparing Fig. 5.15 and Fig. 5.16, it can be seen that the performance of an FTC is better than that of a non-FTC during the period when the train is passing over a hill. (In these figures, the track profile is the same as that of previous simulation and is not shown.) That can also be seen from the front locomotive effort. When the effort of the front locomotive group is zero, then there is no difference between the FTC and non-FTC. When the front locomotive group uses traction power, the speed performance of the FTC is better.

The above conclusion is also clear from a comparison of Fig. 5.17 with Fig. 5.18 and Fig. 5.19 with Fig. 5.20. The performance comparison of these figures is shown in Table 5.2.

The advantage of an FTC in the locomotive fault does not seem obvious in the above simulation. This is because the locomotive groups make no effort (unpowered) during most of the travel period. When the locomotive groups make efforts, the advantage is obvious.

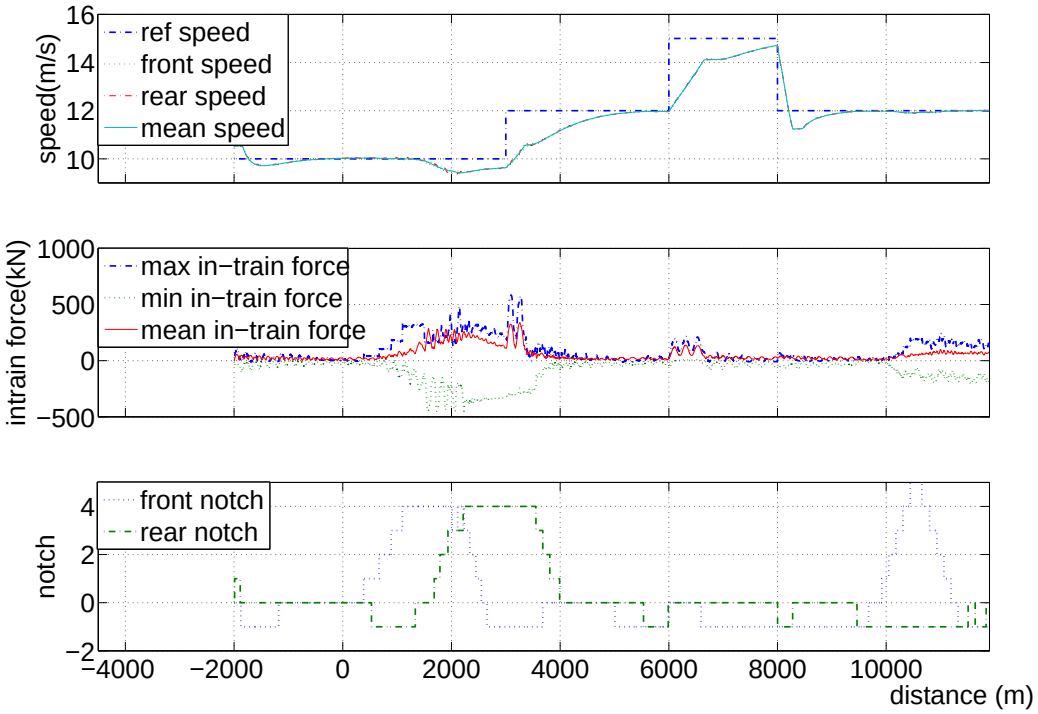

Figure 5.15: Front-loco-fault with an FTC

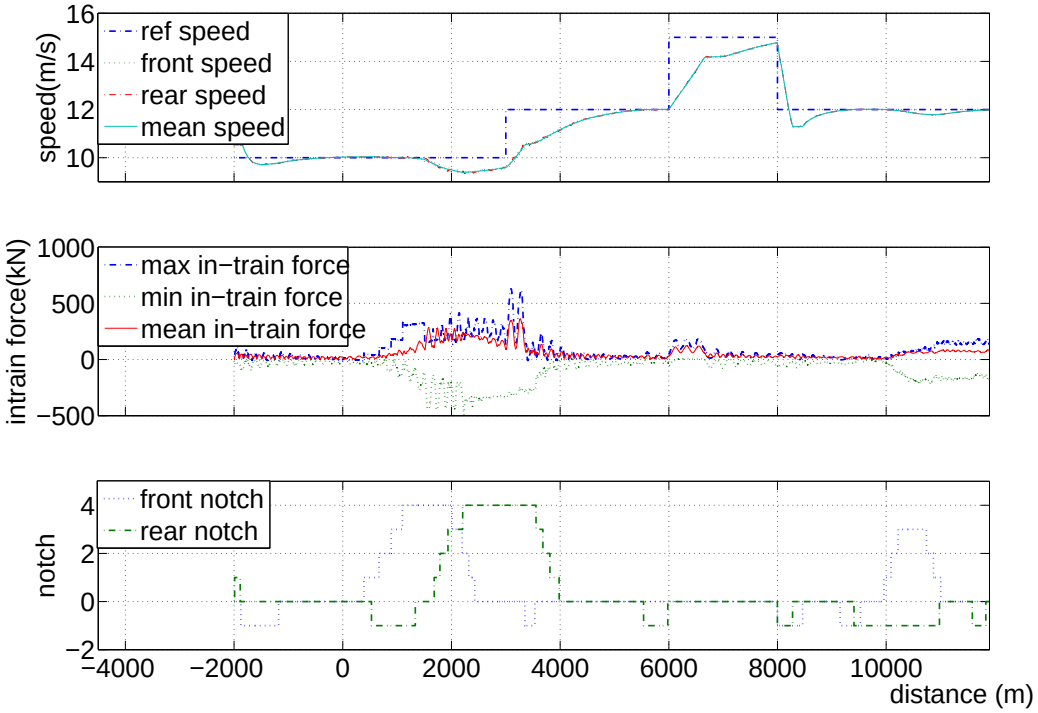

Figure 5.16: Front-loco-fault with a non-FTC

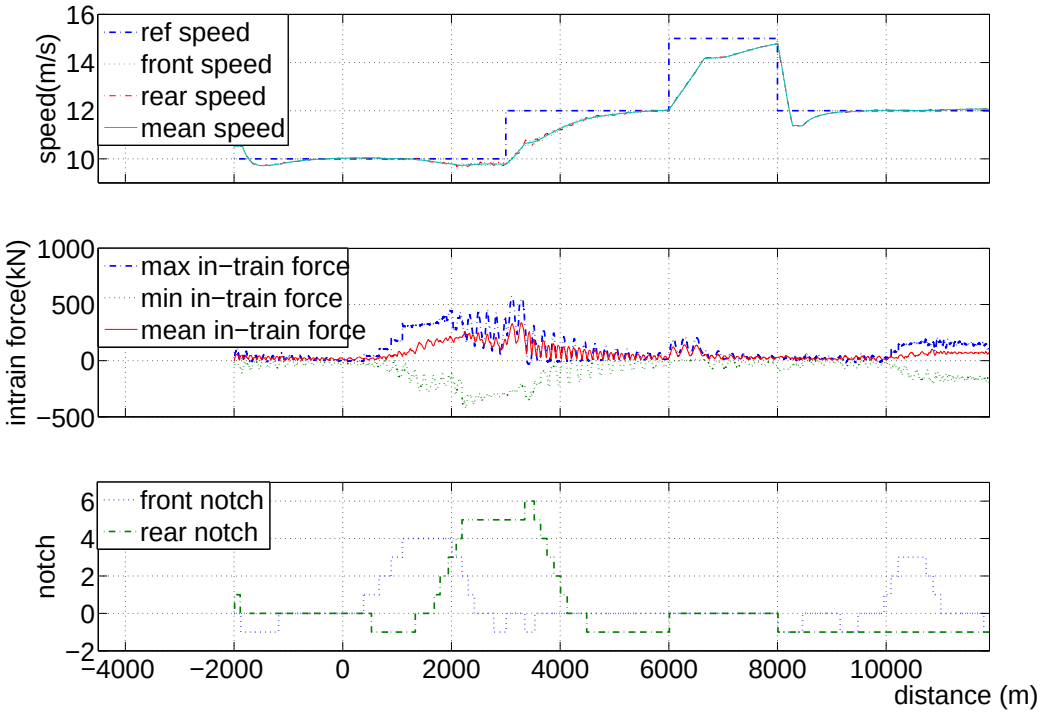

Figure 5.17: Rear-loco-fault with an FTC

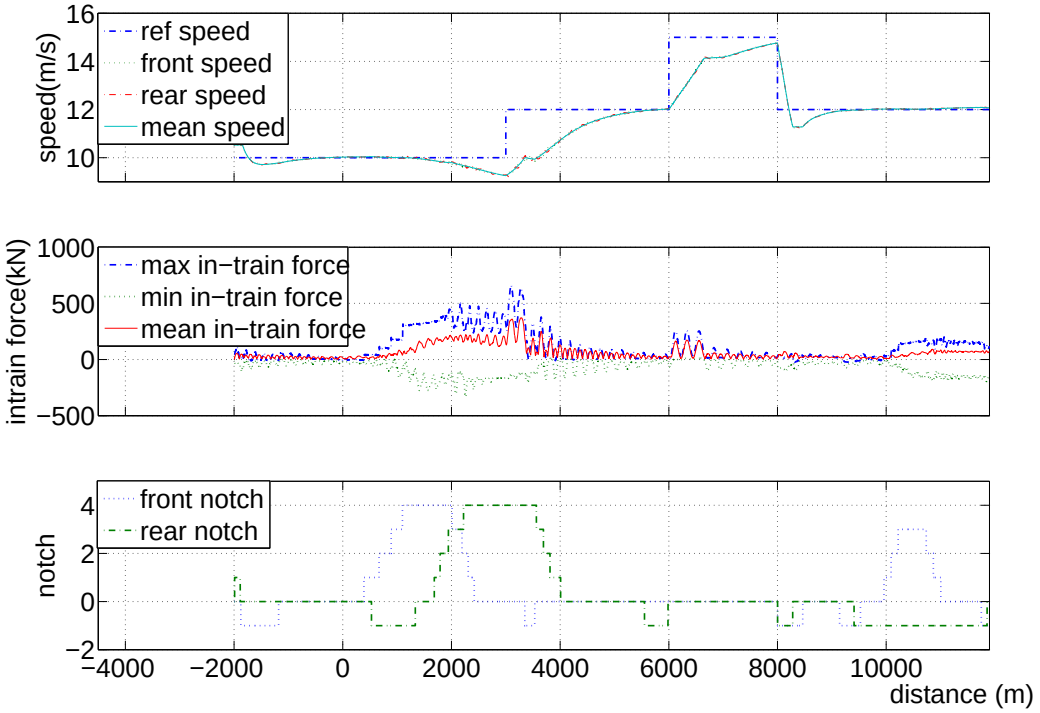

Figure 5.18: Rear-loco-fault with a non-FTC

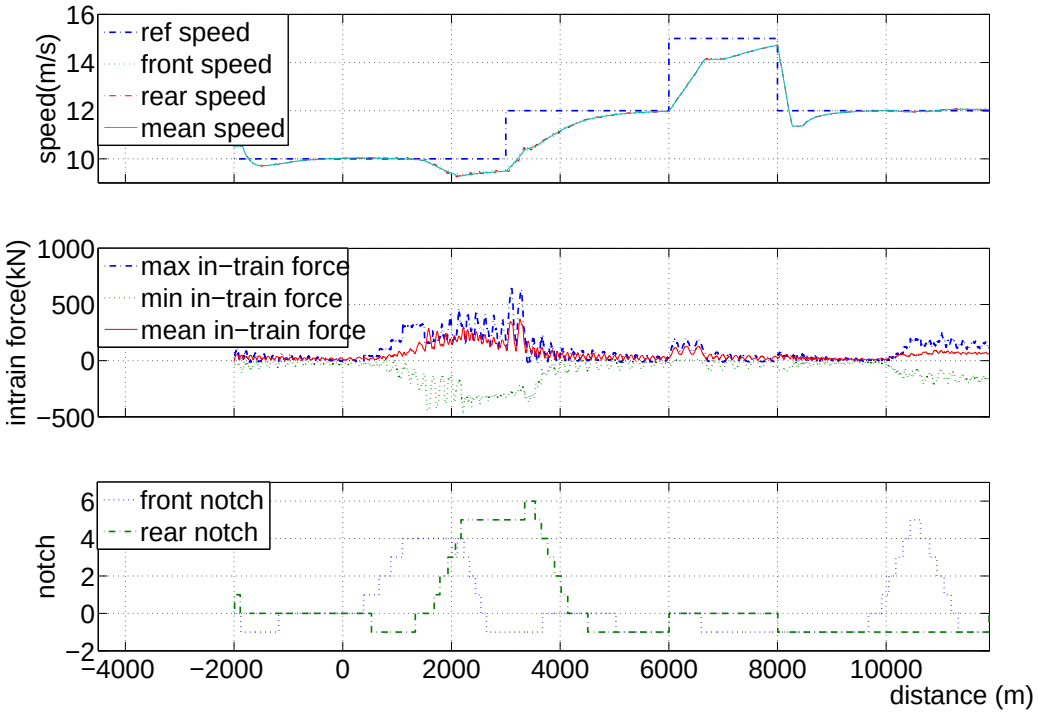

Figure 5.19: Both-loco-fault with an FTC

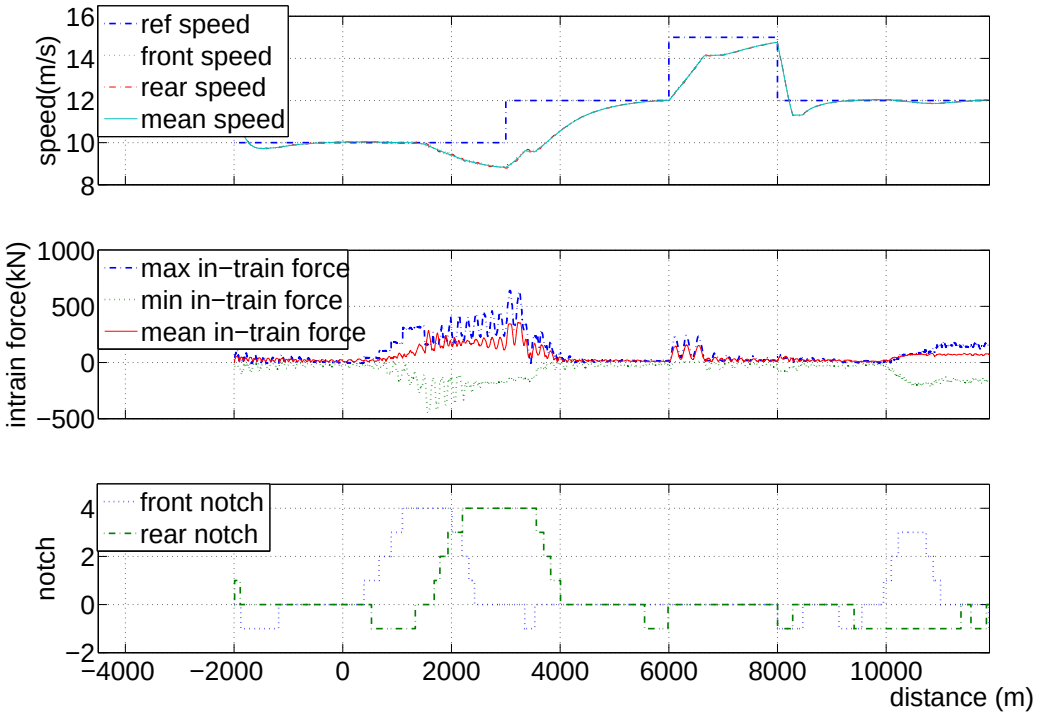

Figure 5.20: Both-loco-fault with a non-FTC

Table 5.2: Comparison of non-FTC and FTC of locomotive faults

	$\lvert\delta\bar{v}\rvert$(m/s)			$\overline{\lvert f_{in}\rvert}$(kN)			E
	max	mean	std	max	mean	std	(MJ)
Fig. 5.15	3.0302	0.4068	0.56	338.40	56.57	65.32	11,600
Fig. 5.16	2.9863	0.4061	0.55	361.80	60.19	65.19	10,800
Fig. 5.17	2.9773	0.3498	0.54	339.61	64.53	63.98	12,200
Fig. 5.18	2.9786	0.4505	0.65	372.29	64.31	65.98	9,680
Fig. 5.19	3.0244	0.4180	0.57	370.39	60.00	64.87	11,400
Fig. 5.20	3.1717	0.5349	0.73	355.97	58.80	66.31	7,800

5.6.3 Simulation of wagon faults

In previous sections, an approach of calculation of the steady-state speed difference as an FDI of the wagons' brake fault was proposed. In simulation, all faults occur from the distance $1,500$ m. The simulation results are shown below.

Fig. 5.21 depicts the simulation of an FTC of the wagon braking system with a faultless system. The corresponding simulation of a non-FTC is the same as Fig. 4.2. In comparing these two figures, one can see that the FTC does not explicitly worsen the performance of the speed regulator.

Fig. 5.22 and Fig. 5.23 represent the simulation results of an FTC and a non-FTC when the braking system makes only 97% of the expected braking efforts. This fault is very small. From a comparison of the FTC and the non-FTC, the difference between them is very small. Also from comparing Fig. 5.22 with Fig. 5.21, one knows such a small fault does not affect the performance of the speed regulator.

When a more serious fault occurs (the braking system makes 70% of the expected braking efforts), the difference between the FTC and the non-FTC is obvious, which can be seen from a comparison of Fig. 5.24 with Fig. 5.25. The former is with an FTC and the latter with a non-FTC.

When only part of the braking efforts are faulty, the performance of an FTC is also better than that of a non-FTC, although the FTC is designed for the whole braking system, which can be seen from a comparison of Fig. 5.26 with Fig. 5.27. In Fig. 5.26 and Fig. 5.27, the outputs of wagons numbered from 2 to 31 are 70% of the expected. The performance comparison is shown in Table 5.3.

From the above comparison, one can draw the following conclusions:

1) A small fault in the braking system has very little effect on the performance of the speed regulator.

2) The application of an FTC together with a speed regulator does not explicitly

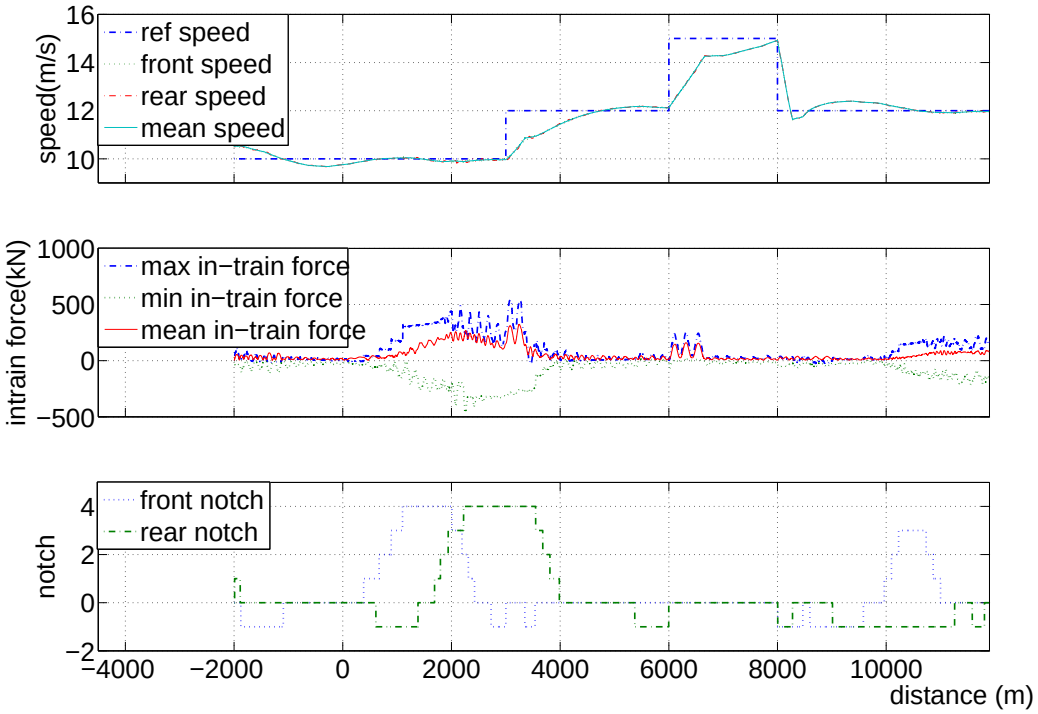

Figure 5.21: Faultless train with an FTC of braking system

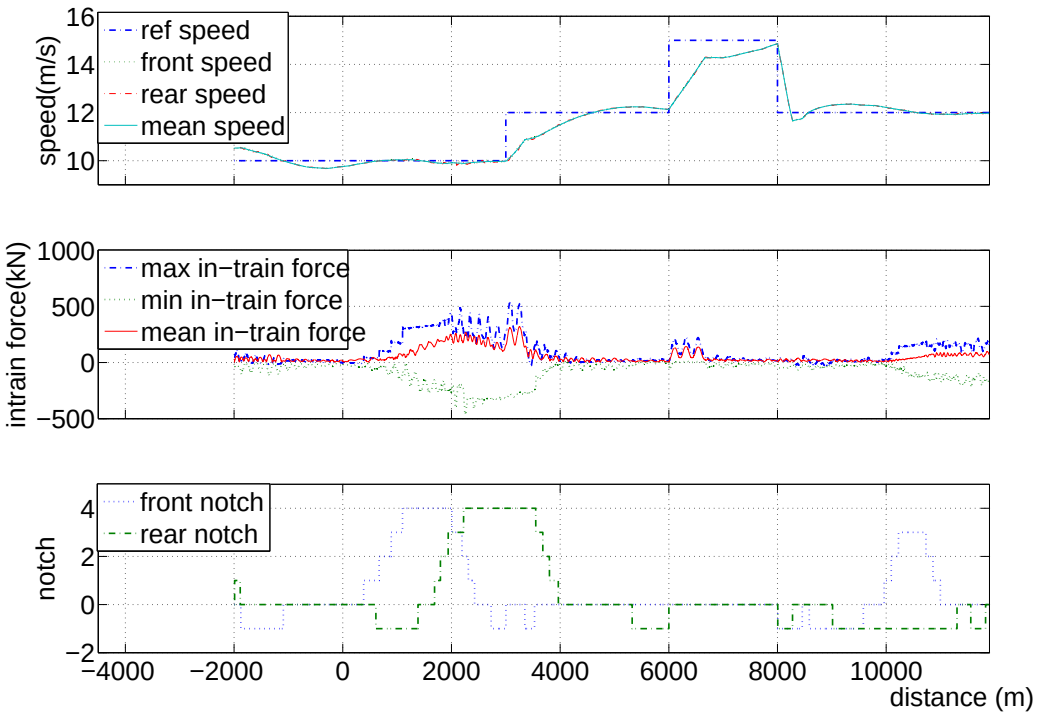

Figure 5.22: Small fault in an FTC of braking system

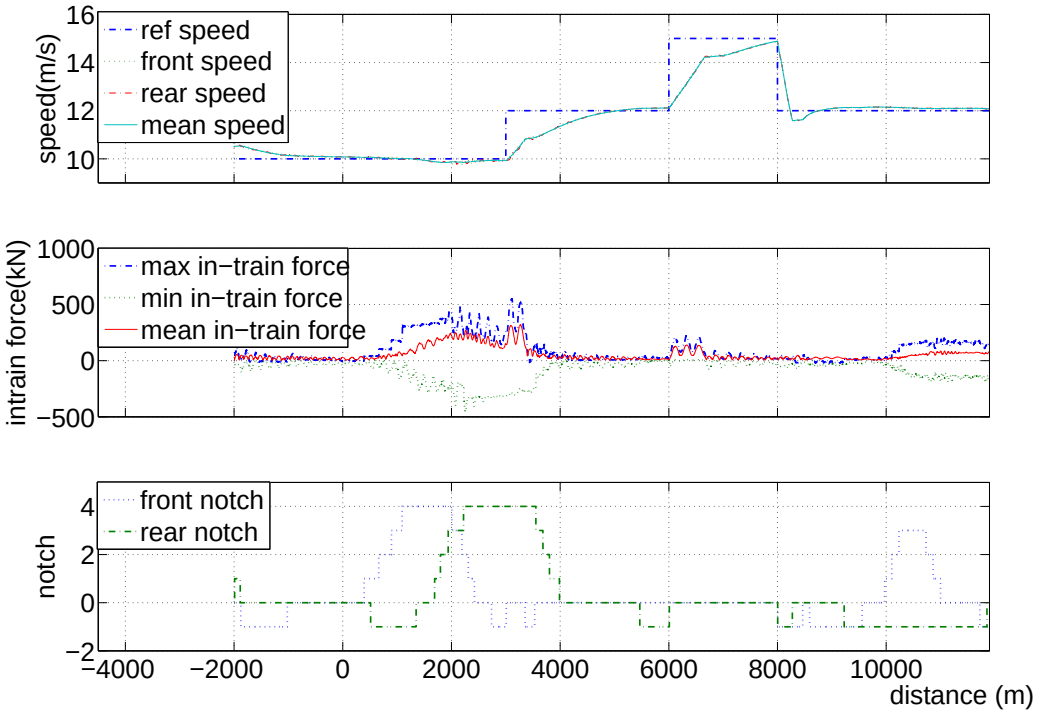

Figure 5.23: Small fault in a non-FTC

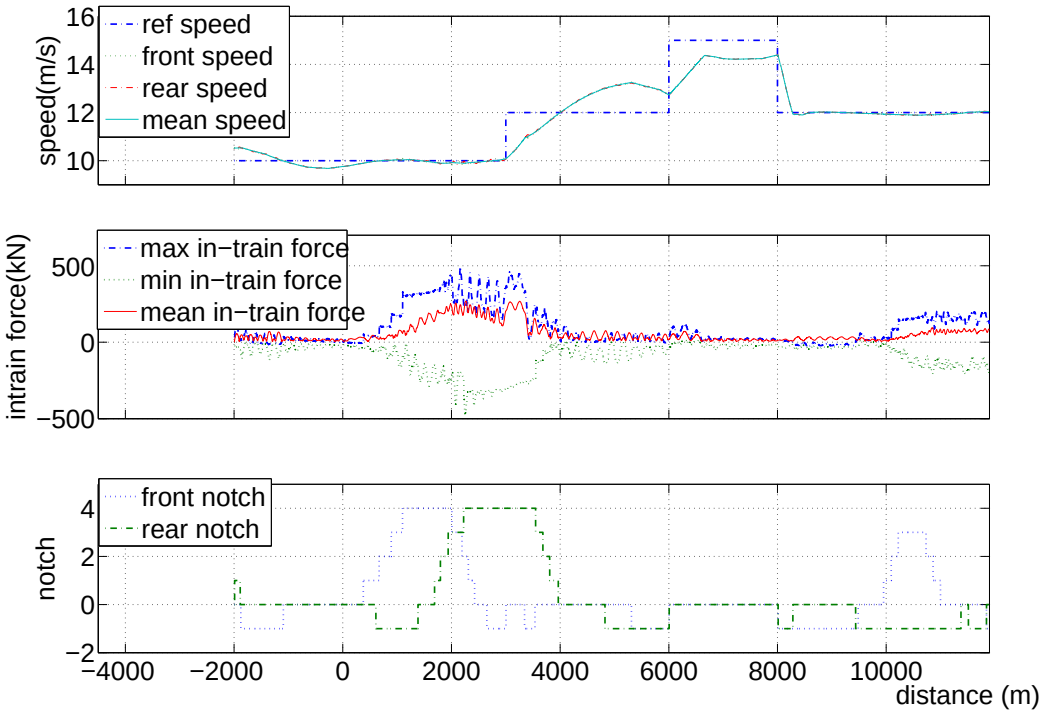

Figure 5.24: Big fault in an FTC of braking system

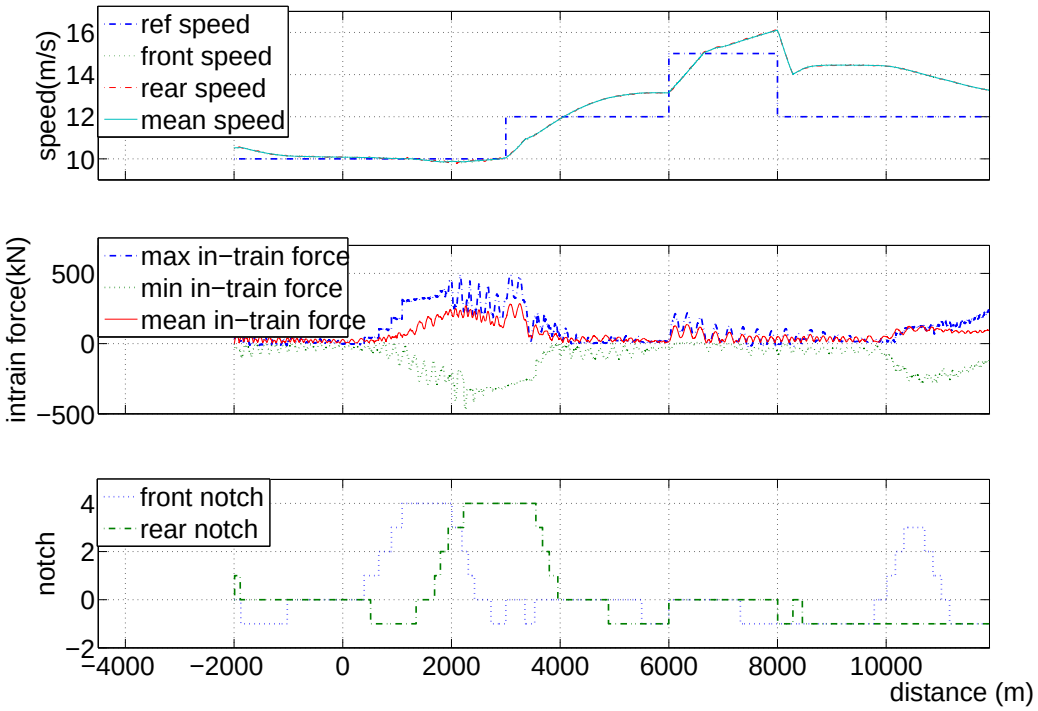

Figure 5.25: Big fault in a non-FTC

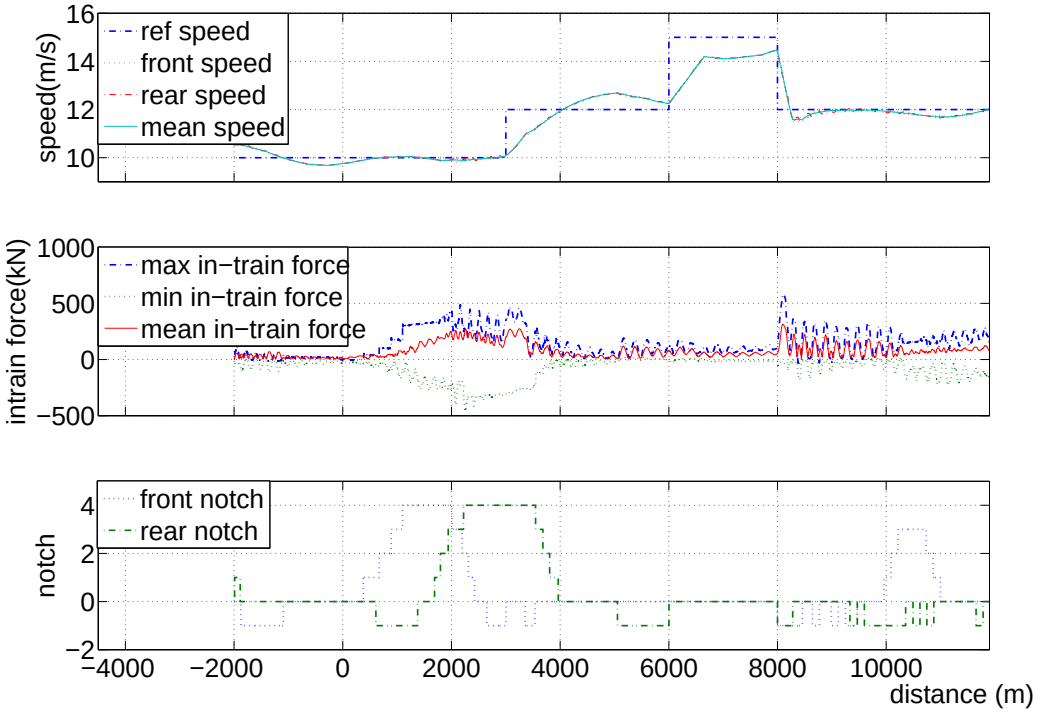

Figure 5.26: Partial fault in an FTC of braking system

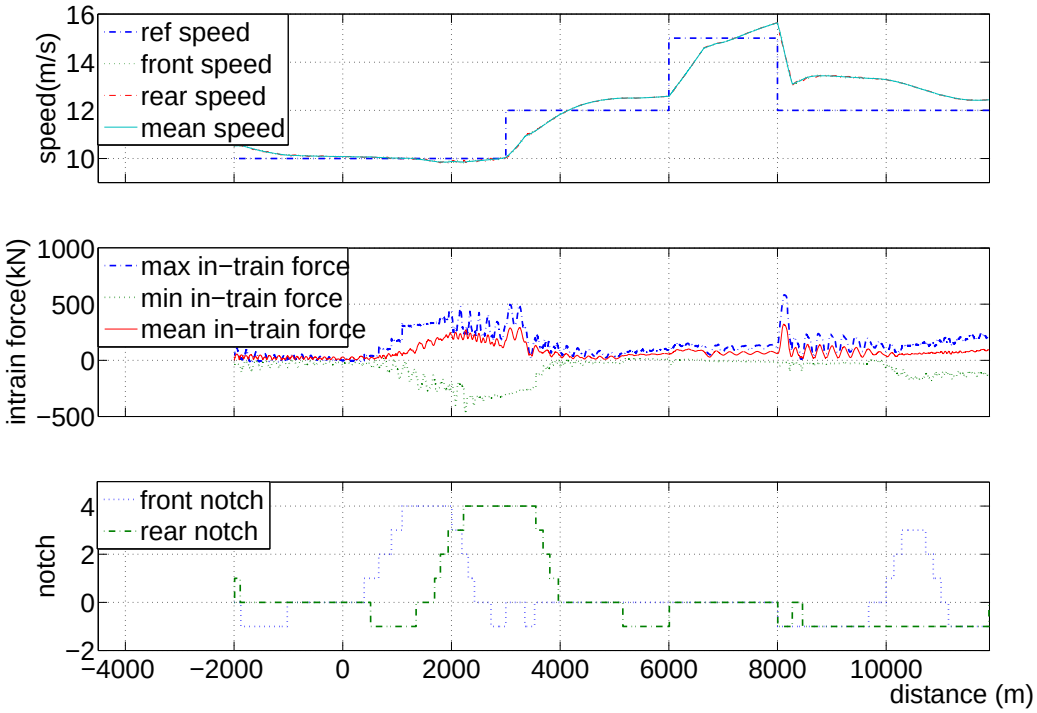

Figure 5.27: Partial fault in a non-FTC

Table 5.3: Comparison of non-FTC and FTC of wagon faults

	$\lvert\delta\bar{v}\rvert$(m/s)			$\overline{\lvert f_{in}\rvert}$(kN)			E
	max	mean	std	max	mean	std	(MJ)
Fig. 5.21	2.9227	0.3480	0.49	323.89	56.64	63.99	12,300
Fig. 4.2	2.9863	0.4061	0.55	361.80	60.19	65.19	10,800
Fig. 5.22	2.8723	0.3458	0.48	321.31	55.86	63.70	12,300
Fig. 5.23	2.8913	0.3299	0.50	321.64	56.79	63.51	12,299
Fig. 5.26	2.7629	0.3728	0.47	315.71	78.30	66.15	12,256
Fig. 5.27	3.6407	0.5251	0.56	322.02	75.93	63.79	11,957

worsen the performance of the speed regulator when the system is faultless.

3) When a small fault occurs, there is little difference between the application of an FTC and a non-FTC.

4) The application of an FTC can improve the performance when a big fault of the braking system occurs.

5) Even if a fault occurs in part of the braking system, which is different from the assumed fault in (5.25) (fault with the whole braking system), the application of an FTC can improve the performance of the speed regulator.

5.7 Conclusion

In this chapter, the fault-tolerant control of the handling of heavy haul trains is discussed. The discussion is based on the redesign of the speed regulator with measurements proposed in chapter 4.

The FDIs for the gain faults of the sensors and the braking system are respectively studied, while the FDI of the locomotive fault is not studied in this thesis, but can be done following some other approaches, such as one proposed in [69]. The FDI of sensor faults is based on a geometric approach proposed in [61]. The FDI of a braking system is based on observation of the steady-state speed. From the difference of the steady speed between the fault system and the faultless system, one can get the fault information.

These two kinds of FDIs are studied separately, but need to be studied further together. In the opinion of the researcher, it is possible to apply them together, because the FDI of a sensor fault is based on the difference between the measured speed of a sensor and the estimated speed of the observer while the FDI of a braking fault is based on the difference between the measured speeds (steady-state speeds) and the reference speed. In the former, a necessary condition for the diagnosis of a fault is that there are differences among the measured speeds while in the latter, a necessary condition for a diagnosis of a fault is that there are nearly no differences among the measured speeds (because a steady state is assumed). This is, however, just a theoretical discussion. In fact, because of the accuracy of the sensor and the ideal assumption of a steady state, the judgement of the difference among the measured speeds depends on a threshold. This is a difficult problem. The setting of a threshold affects the performance of the two FDIs, which is not discussed in this chapter.

In simulation, tests were conducted on the suitability of the two FDIs and the redesign of speed regulators according to the fault signals from the FDIs of sensor faults and braking system faults, and the FDI (not included in this study) of locomotive faults.

Simulation shows that the random errors of the speed sensors have very little impact on the train's performance. It is also shown that the proposed fault-tolerant controller does not explicitly worsen the performance of the speed regulator in the case of a faultless system, while it obviously improves the performance of the speed regulator in the case of a faulty system. It should be pointed out that the approach in this chapter cannot guarantee performance in the case of the occurrence of a serious fault.

Chapter 6

Conclusions

6.1 Summary

The objective of the study is to find optimal driving methodologies for an implementation of the desired speed profile with energy consumption and in-train forces considered.

Firstly, three control strategies are proposed in this study for train handling.Keeping in mind the characteristics of traditional pneumatic braking systems and ECP braking systems, a simulation study of optimal open loop controllers is undertaken. The result shows that ECP braking systems demonstrate superb performance compared with pneumatic braking systems, especially together with iDP control.

Then, the study mainly deals with the control of a heavy haul train equipped with an ECP braking system. It is shown that there are redundancies in designing an open loop controller. An optimization procedure is applied to schedule cruise control by taking in-train forces and energy consumption into initial design consideration. Optimal open loop scheduling presents a better starting point for a closed-loop controller design. A type of LQR controller with state feedback is simulated to verify the above result.

However, the closed-loop control law is designed based on the full state feedback, which is not practical, since not all the states can be measured.

An observer could be designed to supplement the LQR controller if partial states are measured. This is, however, not the approach taken in this study. Instead, the application of output regulation of nonlinear systems with measured output feedback to the control of heavy haul trains is considered. Optimal scheduling of the open loop controller is still based on "trading off" the equilibria. Thus the balance between energy consumption and in-train forces is still maintained. For closed-loop control, speed regulation is imposed. This approach to design is practically feasible and manageable,

and by its nature, is also easily integrable with human drivers. Instead of a linear system theory, a nonlinear system theory is adopted so that without a linear approximation philosophy, control is closer to reality. Another advantage of the approach is the assumption that only the locomotives' speeds are available for measurement.

In this study, the existing result of output regulation of nonlinear systems is also extended. The output regulation problem of nonlinear systems with measured output feedback is formulated in this study and solved for the local version and global version. For its application to train control, some application issues of the output regulation of nonlinear systems with measured output feedback to train handling are discussed. Based on the proposed theory, a speed regulator for train control is designed. Simulation result shows its applicability.

Lastly, this study concentrates on the fault-tolerant capacity of the speed regulator. Two kinds of fault modes are considered. Fault detection and identification for sensor faults and braking system faults are examined. Controller redesign is also given. Simulation results show that the FTC speed regulator proposed in this thesis has a fault-tolerant capacity to corresponding faults.

6.2 Assessment

It is should be pointed out that a speed profile is assumed first in the study. This assumption is a prerequisite for the study. The optimization between energy consumption and in-train force are only done at a point of the track on the assumption that the train is running at the reference speed. Firstly, this optimization is only local and is not global (considering the dynamics of the train). Secondly, this optimization does not consider the optimization of the speed profile, which is rather a problem of a "golden run" in terms of travelling speed.

The cruise phase of train handling is studied, as well as the speed acceleration/ deceleration phases. The start phase and stop phase of train handling are not studied because the models of the train within those phases are different from those in this thesis and more aspects related to safe handling need to be considered. However, considering a train is running at cruise phase or acceleration/deceleration phases most of the travel period, the study of this thesis is significant.

The fault-tolerant control in chapter 5 is currently proposed for sensor gain fault, locomotive actuator fault and braking system fault, respectively. The FDI of locomotive faults is not discussed, which is also a study subject in the literature. The FDIs of sensor faults and wagon faults are discussed separately. As pointed out at the end of chapter 5, it is possible to study them or combine the two approaches to them. However, this combination is not finished because of difficulties in tuning the thresholds related to them. Nevertheless, this study is a good start to such an FTC problem.

The simulation in this study is undertaken on a short track (12 km long). It is enough for the test of a driving profile, which can be seen from the good speed tracking performance on such a track. However when the objective is to test the optimization combination of a driving profile and a reference speed profile, a longer track might be necessary. On the other hand, the track is largely downhill, which is the case with the COALink of Spoornet when the train is loaded. When the unloaded train travels back inland, because of the larger ratio of traction effort to mass, it is relatively easy to drive, which is not simulated in this thesis. Even on such a largely downhill track, the loaded train runs well when it passes over some hills on the track with a carefully designed speed profile.

6.3 Future work

To extend the research in this thesis further, the following directions are noted:

1) The optimization problem of the speed profile. Various papers [6, 7, 8, 9] have studied such a problem, with energy consumption considered. The problem considering the optimization of energy consumption and in-train forces is still open in an extremely long train.

2) The optimal scheduling problem with the dynamics of the train. Optimal scheduling in this thesis is done in ignorance of the dynamics of the train. Methods considering the dynamics of the system, such as model predictive control (MPC), might be able to improve the performance of optimal scheduling.

3) A uniform FDI design problem for the faults of sensors and actuators. The tuning criterion of the parameters of the FDIs for sensor faults and braking system faults needs to be studied further, as well as the FDI of the locomotive faults.

4) The optimization problem of the train composition structure. On the basis of this study, the researcher is of the opinion that the train structure (composition and sequence of locomotives and wagons) has a significant impact on the performance, besides the controller. The optimization of the train composition structure needs to be considered in future studies. However, the logistics of restructuring the train impose a much bigger constraint than any other technical ones.

Reference

[1] R. C. Kull, "WABTEC ECP system update," *IEEE Vehicular Technology Society Land Transportation Division and ASME Rail Transportaion Division Joint Railroad Conference*, April 2001, Toronto, pp. 129–134.

[2] M. J. Hawthorne, "Real world benefits from electronic train control technologies," *Proceedings of Heavy Haul Conference*, Dallas, May 2003.

[3] Air Brake Association, *Management of Train Operation and Train Handling*, 1972. 9.

[4] J. Cheng and P. Howlett, "Application of critical velocities to minimization of fuel consumption in the control of trains," *Automatica*, Vol. 28, 1992, pp. 165–169.

[5] J. Cheng and P. Howlett, "A note on the calculation of optimal strategies for the minimization of fuel consumption in the control of trains," *IEEE Transactions on Automatic Control*, Vol. 38, 1993, pp. 1730–1734.

[6] P. G. Howlett, I. P. Milroy and P. J. Pudney, "Energy-efficient train control," *Control Engineering Practice*, Vol. 2, No. 2, 1994, pp. 193–200.

[7] P. Howlett, "Optimal strategies for the control of a train," *Automatica*, Vol. 32, No. 4, April 1996, pp. 519–532.

[8] P. G. Howlett, "The optimal control of a train," *Annals of Operations Research*, Vol. 98, 2000, pp. 65–87.

[9] E. Khmelnitsky, "On an optimal control problem of train operation," *IEEE Transactions on Automatic Control*, Vol. 45, 2000, pp. 1257–1266.

[10] R. Liu and I. M. Golovitcher, "Energy-efficient operation of rail vehicles," *Transportation Research Part A: Policy and Practice*, Vol. 37, 2003, pp. 917–932.

[11] P. Gruber and M. Bayoumi, "Suboptimal control strategies for multilocomotive powered trains," *IEEE Transactions on Automatic Control*, Vol. 27, No. 3, 1982, pp. 536–546.

[12] C. Yang and Y. Sun, "Robust cruise control of high speed train with hardening/softening nonlinear coupler," *Proceedings of American Control Conference*, Vol. 3, 2–4 June 1999, pp. 2200–2204.

[13] C. Yang and Y. Sun, "Mixed H_2/H_∞ cuise controller design for high speed train," *International Journal of Control*, Vol. 74, No. 9, 2001, pp. 905–920.

[14] A. Astolfi and L. Menini, "Input/output decoupling problem for high speed trains," *Proceedings of the American Control Conference*, Anchorage, May 2002, pp. 549–554.

[15] M. Chou and X. Xia, "Optimal cruise control of heavy haul train equipped with electronic controlled pneumatic brake systems," *16th IFAC World Congress*, Prague, July, 2005.

[16] M. Chou and X. Xia, "Optimal cruise control of heavy-haul trains equipped with electronic controlled pneumatic brake systems," *Control Engineering Practice*, (2006), doi:10.1016/j.conengprac.2006.09.007.

[17] M. Chou, X. Xia and C. Kayser, "Modelling and model validation of heavy-haul trains equipped with electronic controlled pneumatic brake systems", *Control Engineering Practice*, (2006), doi:10.1016/j.conengprac.2006.09.006.

[18] G. Rao, "Modellbildung und Regelung für lange güterzüge unter verwendung unendlichdimensionaler modelle," *Master's Thesis: Technische Unversität Dresden* (in Germany).

[19] J. Rudolph, *Flatness Based Control of Distributed Parameter Systems*, Shaker Verlag, 2003.

[20] X. Zhuan and X. Xia, "Cruise control scheduling of heavy haul trains," *IEEE Transactions on Control System Technology*, Vol. 14, No. 4, 2006, pp. 757–766.

[21] X. Zhuan and X. Xia, "Optimal scheduling and control of heavy haul trains equipped with electronically controlled pneumatic braking systems," *IEEE Transactions on Control System Technology*, 2006 (accepted).

[22] R. S. Raghunathan, H. D. Kim and T. Setoguchi, "Aerodynamics of high-speed railway train," *Progress in Aerospace Sciences*, Vol. 38, No. 6–7, 2002, pp. 469–514.

[23] J. A. Scetz, "Aerodynamics of high-speed trains," *Annu. Rev. Fluid Mech*, 2001, pp. 371–414.

[24] V. K. Garg and R. V. Dukkipati, *Dynamics of Railway Vehicle System*, xiii ed. Toronto: Academic Press, 1984.

[25] Railway Technical Web Pages, 2006, http://www.railway-technical.com/index.html. Last accessed on 10 October 2006.

[26] P. E. Gill, W. Murray and M. H. Wright, *Practical Optimization*, London: Academic Press, 1981.

[27] G. C. Goodwin, S. F. Graebe and M. E. Salgado, *Control System Design*, New Jersey: Prentice Hall, 2001.

[28] T. Kailath, *Linear Systems*, Englewood Cliffs, NJ: Prentice Hall, 1980.

[29] J.-J. E. Slotine and W. Li, *Applied Nonlinear Control*, New Jersey: Prentice Hall, 1991.

[30] B. A. Francis and W. M. Wonham, "The internal model principle of control theory," *Automatica*, Vol. 12, 1976, pp. 457–465.

[31] B. A. Francis, "The linear multivariable regulator problem," *SIAM J. Control Optim.*, Vol. 15, 1977, pp. 486–505.

[32] W. M. Wonham, *Linear Multivariable Control: A Geometric Approach*, 2nd ed., NewYork: Srpringer-Verlag, 1979.

[33] J. S. A. Hepburn and W. M. Wonham, "Error feedback and internal models on differentiable manifolds," *IEEE Transaction on Automatic Control*, Vol. AC-29, 1984, pp. 397–403.

[34] V. Anantharam and C. A. Desoer, "Tracking and disturbance rejection of MIMO nonlinear systems a PI or PS controller," *Proceedings of IEEE Conference on Decsion and Control*, Vol. 24, 1985, pp. 1367–1368.

[35] M. D. Di Benedetto, "Synthesis of an internal model for nonlinear output regulation," *International Journal of Control*, Vol. 45, 1987, pp. 1023–1034.

[36] J. Huang and W. J. Rugh, "On a nonlinear multivariable servomechanism problem," *Automatica*, Vol. 26, No. 6, 1990, pp. 963–972.

[37] A. Isidori and C. I. Byrnes, "Output regulation of nonlinear systems," *IEEE Transactions on Automatic Control*, Vol. 35, No. 2, 1990, pp. 131–140.

[38] D. Cheng, T. J. Tarn and S. K. Spurgeon, "On the design of output regulators for nonlinear system," *Systems and Control Letter*, Vol. 43, 2001, pp. 167–179.

[39] Y. Zheng, C. Zhang and R. J. Evans, "A differential vector space approach to nonlinear system regulation," *IEEE Transactions on Automatic Control*, Vol. 45, No. 11, 2000, pp. 1997–2010.

[40] L. Marconi and A. Isidori, "Mixed internal model-based and feedforward control for robust tracking in nonlinear systems," *Automatica*, Vol. 36, 2000, pp. 993–1000.

[41] L. Marconi, A. Isidori and A. Serrani, "Non-resonance conditions for uniform observability in the problem of nonlinear output regulation," *Systems and Control Letters*, Vol. 53, 2004, pp. 281–298.

[42] C. I. Byrnes, F. D. Priscoli, A. Isidori and W. Kang, "Structurally stable output regulation of nonlinear systems," *Automatica*, Vol. 33, 1997, pp. 369–385.

[43] J. Huang and Z. Chen,"A general framework for tackling the output regulation problem," *IEEE Transactions on Automatic Control*, Vol. 49, No. 12, 2004, pp. 2203–2218.

[44] Z. Chen and J. Huang, "A general formulation and solvability of the global robust output regulation problem," *IEEE Transactions on Automatic Control*, Vol. 50, No. 4, 2005, pp. 448–462.

[45] A. Isidori, *Nonlinear Control Systems I*, third edition, Springer-Verlag, 1997.

[46] A. Isidori, *Nonlinear Control Systems II*, third edition, Springer-Verlag, 1997.

[47] Z. Chen and J. Huang, "Robust output regulation with nonlinear exosystems," *Automatica*, Vol. 41, 2005, pp. 1447–1454.

[48] P. M. Frank, "Fault diagnosis in dynamic systems using analytical and knowledge-based redundancy – a survey and some new results," *Automatica*, Vol. 26, No. 3, 1990, pp. 459–474.

[49] P. M. Frank, "On-line fault detection in uncertain nonlinear systems using diagnostic observers: a survey," *Int. J. Syst. Sci.*, Vol. 25, No. 12, 1994, pp. 2129–2154.

[50] R. J. Patton, "Fault-tolerant control: The 1997 situation (survey)," *Proceedings of IFAC Symposium on Fault Detection, Supervision and Safety for Technical Processes*, 1997, pp. 1029–1052.

[51] R. Isermann, "Fault diagnosis of machines via parameter estimation and knowledge processing – tutorial paper," *Automatica*, Vol. 29, No. 4, 1993, pp. 815–835.

[52] E. Alcorta García and P. M. Frank, "Deterministic nonlinear observer-based approaches to fault diagnosis: a survey," *Control Engineering Practice*, Vol. 5, No. 5, 1997, pp. 663–670.

[53] M. Blanke, R. Izadi-Zamanabadi, S. A. Bøgh and C. P. Lunau, "Fault-tolerant control systems – a holistic view," *Control Engineering Practice*, Vol. 5, No. 5, 1997, pp. 693–702.

[54] R. Isermann, "Supervision, fault-detection and fault-diagnosis methods An introduction," *Control Engineering Practice*, Vol. 5, No. 5, 1997, pp. 639–652.

[55] R. Isermann, "Model-based fault-detection and diagnosis – status and applications," *Annual Reviews in Control*, Vol. 29, No. 1, 2005, pp. 71–85.

[56] M.-A. Massoumnia, G. C. Verghese and A. S. Willsky, "Failure detection and identification," *IEEE Transactions on Automatic Control*, Vol. 34, No. 3, 1989, pp. 316 –321.

[57] M. Basseville, "Information criteria for residual generation and fault detection and isolation," *Automatica*, Vol. 33, No. 5, 1997, pp. 783-803.

[58] H. Hammouri, P. Kabore and M. Kinnaert, "A geometric approach to fault detection and isolation for bilinear systems," *IEEE Transactions on Automatic Control*, Vol. 46, No. 9, 2001, pp. 1451–1455.

[59] Q. Zhang, M. Basseville and A. Benveniste, "Fault detection and isolation in nonlinear dynamic systems: a combined input-output and local approach," *Automatica*, Vol. 34, No. 11, 1998, pp. 1359–1373.

[60] H. Hammouri, M. Kinnaert and E. H. El Yaagoubi, "Observer-based approach to fault detection and isolation for nonlinear systems," *IEEE Transactions on Automatic Control*, Vol. 44, No. 10, 1999, pp. 1879–1884.

[61] C. De Persis and A. Isidori, "A geometric approach to nonlinear fault detection and isolation," *IEEE Transactions on Automatic Control*, Vol. 46, No. 6, pp. 853–865.

[62] C. De Persis and A. Isidori, "On the observability codistributions of a nonlinear system," *Systems and Control Letters*, Vol. 40, pp. 297–304, 2000.

[63] Z. Qu, C. M. Ihlefeld, Y. Jin and A. Saengdeejing, "Robust fault-tolerant self-recovering control of nonlinear uncertain systems," *Automatica*, Vol. 39, No. 10, 2003, pp. 1763–1771.

[64] X. Zhang, T. Parisini and M. M. Polycarpou, "Adaptive fault-tolerant control of nonlinear uncertain systems – an information-based diagnostic approach," *IEEE Transactions on Automatic Control*, Vol. 49, No. 9, 2004, pp. 1259–1274.

[65] A. Xu and Q. Zhang, "Nonlinear system fault diagnosis based on adaptive estimation," *Automatica*, Vol. 20, 2004, pp. 1181–1193.

[66] R. Mattone and A. D. Luca, "Relaxed fault detection and isolation: an application to a nonlinear case study," *Automatica*, Vol. 42, No. 1, 2006, pp. 109–116.

[67] A. Schwarte, F. Kimmich and R. Isermann, "Model-based fault detection and diagnosis for diesel engines," MTZ Worldwide, Vol. 63(7–8), pp. 612–620.

[68] F. Kimmich, A. Schwarte and R. Isermann, "Fault detection for modern diesel engines using signal- and process model-based methods," *Control Engineering Practice*, Vol. 13, No. 2, 2005, pp. 189–203.

[69] S. Daley, D. A. Newton, S. M. Bennett and R. J. Patton, "Methods for fault diagnosis in rail vehicle traction and braking systems," *IEE Colloquium on Qualitative and Quantitative Modelling Methods for Fault Diagnosis*, London, April 1995, pp. 5/1–5/13.

[70] S. M. Bennett, R. J. Patton and S. Daley, "Sensor fault-tolerant control of a rail traction drive," *Control Engineering Practice*, Vol. 7, No. 2, 1999, pp. 217–225.

[71] C. Bonivento, A. Isidori, L. Marconi and A. Paoli, "Implicit fault-tolerant control: application to induction motors," *Automatica*, Vol. 40, No. 3, 2004, pp. 355–371.

[72] A. Serrani, A. Isidori and L. Marconi, "Semi-global nonlinear output regulation with adaptive internal model," *IEEE Transactions on Automatic Control*, Vol. 46, No. 8, 2001, pp. 1178–1194.

[73] F. Delli Priscoli, L. Marconi and A. Isidori, "A new approach to adaptive nonlinear regulation," *SIAM Journal on Control and Optimization*, Vol. 45, No. 3, 2006, pp. 829–855.

[74] L.S. Jennings, M.E. Fisher, K.L. Teo and C.J. Goh, "MISER3: Solving Optimal Control Problems - An Update," *Advances in Engineering Software*, Vol. 13, 1991, pp. 190–196.